https://dspace.org/

Morphological Sex Estimation from Low-Dose X-Ray Scans – An Exploratory Study

Morele, Boikano Molalelo

2025
University of the Witwatersrand, Johannesburg
https://hdl.handle.net/10539/49791
Morele, Boikano Molalelo. (2025). Morphological Sex Estimation from Low-Dose X-Ray Scans – An Exploratory Study [Master's dissertation, University of the Witwatersrand, Johannesburg]. WIReDSpace. https://hdl.handle.net/10539/49791

Downloaded from a DSpace repository. https://dspace.org/

MORPHOLOGICAL SEX ESTIMATION FROM LOW DOSE X-RAY SCANS – AN EXPLORATORY STUDY

Boikano Molalelo Morele



UNIVERSITY OF THE
WITWATERSRAND,
JOHANNESBURG

A dissertation submitted to the Faculty of Health Sciences, University of the Witwatersrand, Johannesburg, in fulfilment of the requirements for the degree of Master of Science in Medicine (Dissertation)

Johannesburg, 2025

CANDIDATES DECLARATION

I Boikano Molalelo Morele declare that this dissertation is my own, unaided work. It is being submitted for the Degree of Master of Science in Medicine (Dissertation) at the University of the Witwatersrand, Johannesburg. It has not been submitted before for any degree or examination at any other University.



_____

(Signature of candidate)

29 day of September 2025 in Johannesburg

PRESENTATION ARISING FROM THIS STUDY

2025: An abstract has been accepted for an oral presentation for the 50th conference of the Anatomical Society of Southern Africa (ASSA) to be held in Muldersdrift, South Africa.

Title: Morphological sex estimation of the cranium and pelvis from low dose x-ray scans – An exploratory study.

POTENTIAL PUBLICATIONS ARISING FROM THIS DISSERTATION

Morele, B.M, Lottering, T.L., Brits, D. Suggested title: Morphological sex estimation of the cranium and pelvis from low dose x-ray scans – An exploratory study. In preparation.

Morele, B.M, Lottering, T.L., Brits, D. Suggested title. Morphological sex estimation of postcranial skeletal traits from low dose x-ray scans – An exploratory study. In preparation.

ABSTRACT

Technological advancements in forensic imaging have promoted the use of radiographs for skeletal sex estimation, minimising the need to macerate human remains. Radiographs have been shown to yield sex classification accuracies similar to those achieved through dry bone analyses method. This study investigated the observability, repeatability, and sex classification accuracy of skull and postcranial traits for morphological sex estimation using Lodox® Statscan™ radiographs of white European adult individuals (n = 150 scans; 72 males, 78 females). The skull and eight postcranial elements, in association with 32 morphological traits, were assessed for observability and scorability, followed by sex classification, to assess accuracy. The skeletal elements were observed first, followed by the observations of associated skeletal traits, given the observability of respective skeletal elements from Lodox scans. Nominal and ordinal traits were scored on two-point nominal and five-point ordinal scales, respectively. Intra- and inter-observer repeatability were assessed using Cohen's Kappa statistics. Eight skeletal elements were observed in over 88% of scans, with cranium and pelvic bones each achieving 99% observability. High observability and scorability frequencies were noted for four skull traits (80-93% and 76-93%, respectively), eight pelvic traits (87-97% and 82-93%, respectively), and select traits of the scapula and distal humerus (78-82% and 72% and 80%, respectively), with varying repeatability agreements. Sex classification accuracies ranged from moderate (53-81% for skull and pelvic traits) to low (15-54% for non-pelvic traits). Sex accuracies of the non-pelvic postcranial traits were low (15-54%). Lodox scans demonstrated limited trait observability and moderate sex classification, proving less effective than dry bone analysis. Limitations included interference from soft tissue, distortion, superimposition, and reliance on anteroposterior scans. Alternative metric sex estimation approaches are recommended, leveraging the observable traits identified despite Lodox® Statscan™ limitations.

ACKNOWLEDGEMENTS

I am deeply grateful to the numerous individuals whose support and guidance were essential to the completion of this Master's dissertation. I wish to extend my sincere gratitude to my supervisors, Associate Professor Desiré Brits and Miss Tamara Lottering, for their invaluable expertise, insightful feedback, and unwavering encouragement throughout this research journey. Their patience and dedication have been instrumental in shaping this dissertation. I am deeply indebted to the individuals who donated their remains to the Department of Anatomical Sciences Body Donor program for health sciences teaching and furtherance of medical sciences research. I am also grateful to my friends for their constructive criticism and moral support. Most importantly, I extend my profound appreciation and gratitude to my family for their unwavering love, understanding, and patience. Their constant encouragement and belief in me have been my greatest source of strength.

Funding from the National Research Foundation (NRF) towards the collection of Lodox® Statscan™ images granted to Associate Professor Desiré Brits (Grant UID: 118149) is hereby also acknowledged. Opinions expressed and conclusion arrived at, are those of the authors and not necessarily to be attributed to the NRF.

TABLE OF CONTENTS

CANDIDATES DECLARATION ii

PRESENTATION ARISING FROM THIS STUDY iii

POTENTIAL PUBLICATIONS ARISING FROM THIS DISSERTATION iii

ABSTRACT iv

ACKNOWLEDGEMENTS v

TABLE OF CONTENTS vi

LIST OF FIGURES x

LIST OF TABLES xii

NOMENCLATURE xii

CHAPTER 1: INTRODUCTION AND BACKGROUND 1

1.1. Introduction 1

1.2. Background on Skeletal Sex Estimation 1

1.2.1. Biological sex and sexually dimorphic skeletal elements 1

1.2.2. Sex estimation methodological approaches 2

1.3. Imaging in Forensic Anthropology 4

CHAPTER 2: LITERATURE REVIEW 6

2.1. An Overview of Morphological Skull Traits for Sex Estimation 6

2.2. An Overview of Morphological Postcranial Traits for Sex Estimation 10

2.2.1. Scapula morphology 10

2.2.2. Clavicular rhomboid fossa presence 11

2.2.3. Distal humerus morphology 12

2.2.4. Rib costal cartilage morphology 14

2.2.5. Pelvis morphology 15

2.2.6. Other postcranial morphological traits of interest 20

2.3. Modern Medical Imaging Modalities in Forensic Anthropological Sex Estimation 23

2.3.1. Computed Tomography 24

2.3.2. X-ray radiography 25

2.4. The Lodox® Systems in South Africa 27
2.5. Study Aim and Objectives 29
CHAPTER 3: METHODS AND MATERIALS 30
3.1. Study Sample 30
3.1.1. Ethical clearance 30
3.1.2. Inclusion and exclusion criteria 30
3.1.3. Study sample 30
3.1.4. Lodox® Statscan™ scans 31
3.2. Study Method 32
3.2.1. Lodox scan analysis 32
3.2.2. Skeletal elements observations 32
3.2.3. Skeletal traits assessed 35
3.2.4. Skeletal trait scoring procedures 35
3.3. Statistical Analysis 51
3.3.1. Repeatability assessment and analysis 51
3.3.2. Data analysis 52
CHAPTER 4: RESULTS 54
4.1. Descriptive Statistics 54
4.2. Observable Skeletal Elements 54
4.3. Observable and Scorable Skeletal Traits 55
4.3.1. Skull traits 56
4.3.1.1. Observability 56
4.3.1.2. Scorability 58
4.3.2. Postcranial traits 60
4.3.2.1. Observability 60
4.3.2.2. Scorability 62
4.4. Skeletal Traits Sex Classification Accuracies 67
4.4.1. Sex classification accuracies per study sample 67

4.4.1.1. Skull traits 67
4.4.1.2. Postcranial traits 70
4.4.2. Sex classification accuracies per scorable skeletal traits 75
4.4.2.1. Skull traits 75
4.4.2.2. Postcranial traits 77
4.4.3. Sex classification accuracies per skeletal element 83
4.4.4. Skeletal traits with over 75% sex classification accuracy 85
CHAPTER 5: DISCUSSION 91
5.1. Observability and Scorability of Skeletal Elements and Traits 92
5.1.1. Skeletal elements observability 92
5.1.2. Skeletal traits observability 93
5.1.2.1. Skull traits 94
5.1.2.2. Postcranial traits 96
5.1.3. Skeletal traits scorability 98
5.1.4. Overall interpretation 100
5.2. Repeatability of Observed Skeletal Elements and Traits 101
5.2.1. Repeatability of observed skeletal elements 102
5.2.2. Repeatability of observed skeletal traits 103
5.2.3. Repeatability of scored skeletal traits 106
5.2.3.1. Skull traits 106
5.2.3.2. Pelvic traits 107
5.2.3.3. Non-pelvic postcranial traits 108
5.2.4. Overall interpretation 109
5.3. Sex Classification Accuracies 113
5.3.1. Skull traits 113
5.3.2. Postcranial traits 116
5.4. Lodox Scans Limitations for Morphological Skeletal Sex Estimation 120
5.5. Study Limitations and Recommendations for Future Research 122

5.5.1. Limitations 122
5.5.2. Recommendations for future research 124
CHAPTER 6: CONCLUSION 125
REFERENCES 129
APPENDICES 152
Appendix 1: Ethical clearance for Cadaveric Collection of the Department of Anatomical Sciences, School of Biomedical Sciences, University of the Witwatersrand, Johannesburg. . 152
Appendix 2: Declaration on plagiarism and research misconduct 153
Appendix 3: Turn-it-in Report 153

LIST OF FIGURES

Figure 3.1: Examples of skeletal tissue and associated soft tissues visible from Lodox scans. Also evident is a tilted head on the top left scan. a = muscle tissue; b = bone; c = lung; d = breasts; e = internal prosthesis; f = male external reproductive organ; g = rib costal cartilages. 33

Figure 3.2: Skeletal elements assessed in the current study. a = cranium; b = mandible; c = clavicle; d = scapula; e = distal humerus and proximal ulna; f = pelvic girdle; g = sacrum; h = proximal femur; i = distal femur. See Figure 3.1 for the lower ribs' costal cartilages. 34

Figure 4.1: Visual representation to indicate skeletal element(s) with the most/least observable and/or scorable skeletal traits, on average frequencies. None-observable and/or -scorable skeletal traits were excluded from calculations of average frequencies. 56

Figure 4.2: Example of skull traits with higher frequency (>89%) of observability from Lodox scans. a = parietal eminence; b = orbit morphology; c = mental eminence; d = overall skull morphology. 57

Figure 4.3: Image examples of postcranial traits with high frequency of observability (>80%) from Lodox scans. Images: Top left = scapula; top right = distal humerus; bottom images = pelvis. a = infraspinous fossa lateral border; b = olecranon fossa shape; c = ilium morphology; d = pelvic brim; e = obturator foramen shape; f = subpubic shape; g = overall pelvis morphology; h = acetabulum position; i = ventral arc; j = subpubic contour.....62

Figure 4.4: Visual representation of average sex classification accuracy of skeletal elements with scorable skeletal traits. 84

Figure 4.5: Visual representation of average sex classification accuracy of skeletal elements with scorable skeletal traits. Non-scorable elements and traits were excluded from these calculations. 85

Figure 4.6: Visual representation of skeletal traits with at least over 75% correct sex classification accuracy either for males or females, or both sexes. 87

Figure 5.1: Lodox scans that represent 1% non-observability of the cranium (A) and pelvis (B). Evident in image A is a cross-sectionally dissected cranium, creating a view that shows the interior cranial base. Also, evident in image B is an example of low patient contrast, extensive soft tissue presence throughout the individual's body and a bent knee, indicating an individual not scanned in a standard anatomical position. Siding: Left is towards the right.....93

Figure 5.2: An example of a Lodox scan of an individual not scanned in a standard anatomical position, exhibiting image distortion and superimposed anatomical structures on the cranial, thoracic and pelvic regions. Left hand side is towards the right.....98

Figure 5.3: An example of a Lodox scan of an individual exhibiting image distortion, superimposed anatomical structures, and/or soft tissue interference in the thoracic, elbow, and pelvic regions,

in addition to not being scanned in a standardised anatomical position. Both hands are partially pronated. a = internal prosthesis. 105
Figure 5.4: Examples of Lodox scans showing soft tissues of external reproductive organs. Image A is a Lodox scan of a male individual and image B is a Lodox scan of a female individual. a = male penis; b = breast. Left hand side is towards the right..... 124

LIST OF TABLES

Table 2.1 : Discrimination of sex based on Krogman and İşcan's (1962) cranioscopy descriptions. 7

Table 2.2 : Discrimination of sex based on Krogman and İşcan (1962) pelvis morphological traits. 16

Table 3.1 : Age distributions (in years) for Lodox scans of male and female individuals with documented ages-at-death. 31

Table 3.2 : Image illustrations of skeletal traits assessed for morphological sex estimation from Lodox scans 36

Table 3.3 : Sexually dimorphic traits of the skull and associated assessment scores used in the present study. 40

Table 3.4 : Sexually dimorphic postcranial traits and associated assessment scores used in the current study. 44

Table 3.5 : Cohen's Kappa strengths of agreements and associated coefficients, adapted from Viera & Garret (2005). 52

Table 4.1 : Counts and frequencies (in brackets) of observable skeletal elements from assessed Lodox scans (n = 150) with associated intra- and inter-observer Cohen's Kappa agreement scores (K). 55

Table 4.2 : Tabulated counts and frequencies (in brackets) of the observable and scorable morphological skull traits, and their respective intra- and inter-observer Cohen's Kappa coefficients (K). 59

Table 4.3 : Skull traits observability and scorability differences between the total study sample (n = 150 scans) and a subset of observable and scorable trait. 60

Table 4.4 : Tabulated counts of the observable and scorable morphological postcranial traits, associated frequencies in brackets, and their respective intra- and inter-observer Cohen's Kappa coefficients (K). 64

Table 4.5 : Postcranial traits observability and scorability differences between the total study sample (n = 150 scans) and a subset of observable and scorable trait. Non-observable skeletal traits are excluded. 67

Table 4.6 : Predicted sex classification counts and accuracy rates (in brackets) of skull traits morphological scored for sex estimation from 150 assessed Lodox scans. 69

Table 4.7 : Predicted sex classification counts and accuracy rates (in brackets) of postcranial traits morphologically scored for sex estimation from 150 assessed Lodox scans. 72

Table 4.8 : Predicted sex classification counts and accuracy rates (in brackets) for sex estimation of morphologically observable and scorable skull traits from Lodox scans. 76

Table 4.9 : Predicted sex classification counts and accuracy rates (in brackets) for sex estimation of morphologically observable and scorable postcranial traits from certain Lodox scans. ... 80
Table 4.10 : Lodox® Statscan™ images illustrating male and female skulls and associated morphological skeletal traits. ... 88
Table 4.11 : Lodox® Statscan™ images illustrating male and female pelves and associated morphological skeletal traits. ... 89

NOMENCLATURE

2D – Two-dimensions/dimensional

3D – Three-dimensions/dimensional

CT – Computed Tomography

DFA – Discriminant Function Analysis

DNA – Deoxyribonucleic Acid

EOP – External Occipital Protuberance

FDA – Flexible Discriminant Analysis

Femoral NSA – Femoral Neck Shaft Angle

FPS – Forensic Pathology Services

LDA – Linear Discriminant Analyses

LR – Logistic Regression

Lodox – Low Dose X-ray

MRI – Magnetic Resonance Imaging

OID – Object-to-Image Distance

Q angle – Quadriceps angle

RFM – Random Forest Models

SID – Source-to-Image Distance

X-ray – X radiation

CHAPTER 1: INTRODUCTION AND BACKGROUND

1.1. Introduction

When skeletonised human remains are recovered in a medico-legal context, forensic anthropologists are often tasked to assist with the documentation of such remains through the estimation of biological profile which mainly involves the estimation of biological sex, age-at-death, population affinity, and stature (Christensen *et al.,* 2014a; Klales, 2020a; Pilli *et al.,* 2023). Forensic anthropologists may also assess (if present) the pathology, trauma, and taphonomic changes associated with unidentified skeletal human remains (Christensen *et al.,* 2014b). A biological profile is mainly achieved by using techniques based on biological anthropology to obtain details about the deceased individual and the circumstances surrounding their death (Christensen *et al.,* 2014b).

Biological sex estimation is a crucial parameter of the biological profile and one of the most crucial steps when conducting forensic anthropological analysis of human remains recovered in a medico-legal context (Spradley & Jantz, 2011; Krishan *et al*., 2016; Klales, 2021). This is because the accurate estimation of biological sex can effectively eliminate about 50% of the population from further consideration during the identification of human remains (Christensen *et al.,* 2014c; Berg, 2017). Moreover, the estimation of the other biological profile parameters relies on the accurate estimation of biological sex (Christensen *et al.,* 2014c), making it an invaluable parameter in medico-legal investigations.

1.2. Background on Skeletal Sex Estimation

1.2.1. Biological sex and sexually dimorphic skeletal elements

The terms "gender" and "sex" are often used interchangeably in everyday conversation; however, they have distinct meanings, particularly in a scientific context like forensic anthropology (Berg, 2017; Garofalo *et al.,* 2020). Gender is a social construct encompassing ascribed and perceived individual roles, behaviours, expressions, and identities (Berg, 2017). In contrast, sex refers to biological traits, typically categorized as male or female, based on sex chromosomes, hormones, and associated anatomical features (Berg, 2017; Garofalo *et al.,* 2020). These features include reproductive organs and skeletal variations, particularly those related to reproduction, which arise from differences in sex chromosomal arrangement and hormonal production (Frayer & Wolpoff, 1985; Leong, 2006; Berg, 2017; Garofalo *et al.,* 2020; Stull *et al.,* 2020). As such, humans are sexually dimorphic, with morphological variations between sexes expressed through sex-specific phenotypical differences and skeletal features that are primarily influenced by sex chromosomes, hormones, and evolutionary pressures related to reproduction and locomotion (Khosla *et al.,* 2001;

Leong, 2006; Stull *et al.,* 2020). Moreover, hormonal influences that drive the development secondary sexual characteristics post-puberty also affects skeletal development, leading to distinctions in bone size, shape, and density between males and females, subsequently forming the basis for skeletal sex estimation (Khosla *et al.,* 2001; Leong, 2006; Berg. 2017; Stull *et al.,* 2020). Skeletal sex estimation is easier to conduct in adults and late adolescents compared to subadult individuals (Berg. 2017; Stull *et al.,* 2020). The purpose of skeletal sex estimation it is to estimate the individual's biological sex assigned at birth and not the individual's gender (Wilson *et al.,* 2008; Berg. 2017; Garofalo *et al.,* 2020; Stull *et al.,* 2020). Therefore, while societal use of "gender" and "sex" interchangeably may lessen the distinction between the two concepts, the biological definition of sex is what is relevant for skeletal sex estimation and potential skeletal identification.

The human pelvis exhibits sexually dimorphic traits and has long been documented to be the best skeletal indicator of sex (Phenice, 1969; Klales, 2020a; Stull *et al.,* 2020). The observable differences primarily arise from selective pressures on males and females due to bipedal locomotion and parturition (Washburn, 1960; Christensen *et al.,* 2014c; Uy & Laudicina, 2021). The skull also exhibits significant sexual dimorphism that can assist with sex estimation in humans (İşcan & Steyn, 2013; Christensen *et al.,* 2014c). The degree of sexual dimorphism is primarily population-specific, attributed to genetic, temporal (i.e., abiotic and biotic factors), and secular variations that occur between and within populations (Frayer & Wolpoff, 1985; Bharati *et al.,* 2001; Bharati *et al.,* 2005; Dillon, 2014; Lewis & Garvin, 2016; Kenyhercz *et al.,* 2017). In the absence of the skull and pelvis for morphological sex estimation, especially in cases of remains associated with skeletal trauma, fragmentation, or scattering due to certain taphonomic agents, various postcranial elements have been found to display significant sexual dimorphism (Patyal & Bhatia, 2022; Stock, 2020). For example, the clavicle (Prado *et al.,* 2009; Ishwarkumar *et al.,* 2016), scapula (Scholtz *et al.,* 2010; Maranho *et al.,* 2023), humerus (López-Lázaro *et al.,* 2020; Tallman & Blanton, 2020), and the elbow (Airan & Dwivedi, 2018), resulting in the development of additional morphological methods suitable for sex estimation.

1.2.2. Sex estimation methodological approaches

Skeletal sex estimation primarily involves the estimation of biological sex into binary sex categories (male and female) through analyses of sexually dimorphic traits of the skull, pelvis, and various postcranial traits using metric, non-metric (morphological) or a combination of both metric and morphological (i.e., morphometric) anthropological approaches (Vance & Steyn, 2013; Krüger *et al.,* 2015; Berg, 2017; American Academy of Forensic Sciences Standards Board, 2019; Stock, 2020; Pilli *et al.,* 2023). The accuracy of such methods range from 50% to 95% (Rowbotham &

Blau, 2020), and therefore the best skeletal sex estimation results can be obtained when using a combination of these methods, depending on the available skeletal elements (Klales, 2013).

Metric methods are typically based on standardised dry bone measurements from defined osteometric landmarks that quantitatively assess the size differences between males and females (Christensen *et al.*, 2014c; Langley *et al.,* 2016; Klale *et al.,* 2020). These methods are less subjective, provide quantifiable accuracy rates, and can be applied to incomplete or fragmented remains to estimate skeletal sex (Christensen *et al.*, 2014c; Berg, 2017; Klales *et al.,* 2020). Unlike morphological methods, which primarily rely on the description of the degree of sexual dimorphism associated with a skeletal element, metric methods can potentially detect subtle sexual dimorphism even in minimally dimorphic skeletal elements, based on the bone's dimensions (Christensen *et al.,* 2014c; Rowbotham & Blau, 2020). However, metric methods often require skeletal analyses based on published statistical models that are mostly population-specific (as sexual dimorphism varies across populations) and require the utilisation of specialized equipment and or computer software programs to yield accurate classifications (Buikstra &Ubelaker, 1994; Ousley & Jantz, 2012; McKeown & Schmidt, 2013; Berg, 2017; Klales *et al.,* 2020).

In contrast, non-metric methods are typically based on the subjective visual assessment of morphological traits that exhibit sexual dimorphism (Bidmos *et al.,* 2010; Berg, 2017; Klales *et al.,* 2020). These traits are then compared to standards that are based on composite visual images/illustrations and descriptions and are often evaluated based on a nominal and/or ordinal scoring system to yield accurate sex classification (Bidmos *et al.,* 2010; Berg, 2017; Klales, 2020a). Despite limitations such as observer subjectivity and reduced applicability to subadult or fragmented remains, non-metric methods are time- and cost-effective, do not require specialized equipment, and are suitable for preliminary assessments of skeletal remains in various settings (Bidmos *et al.,* 2010; Stull *et al.,* 2020; Leskovar *et al.,* 2023). Furthermore, they can be highly accurate with complete and well-preserved remains, and they are supported by extensive documentation and a long history of use in biological anthropology (Bidmos *et al.,* 2010; İşcan & Steyn, 2013; Christensen *et al.*, 2014c; Berg, 2017; Klales, 2020a). High sex classification accuracy is often achieved using a combination of metric and non-metric methods (i.e., morphometric). This involves quantifying morphological traits with multivariate statistical techniques, usually linear distances, angles, and ratios between anatomical landmarks, thus enabling both the visualisation and statistical quantification of macroscopic and subtle morphological measurements as well as the assessments of patterns of variation amongst anatomical features (Adams *et al.,* 2004; Mitteroecker & Gunz, 2009; Vance *et al.,* 2011; Djorojevic *et al.,* 2014; Krishan *et al.,* 2016). Despite the increasing use of metric and

morphometric methods in anthropological analyses, morphological sex estimation methods remain a valuable tool and should be continuously improved and integrated with the latest technological advancements to enhance biological profile estimation.

1.3. Imaging in Forensic Anthropology

Photography plays a crucial role in forensic anthropological cases, allowing the photo-documentation of the scene and human remains, thus offering a visual record of the scene, human remains, and associated physical evidence (Rohatgi & Kapoor, 2014; Garvin & Stock, 2016). The field of forensic anthropology has seen a gradual integration of radiological imaging modalities to assist in and enhance the estimation of biological profile of skeletal remains, alongside already established anthropological methods and techniques (Franklin *et al.,* 2016; Garvin & Stock, 2016; Mamabolo *et al.,* 2020; Rowbotham *et al.,* 2020; Zhang, 2022). Technological advances in forensic imaging have favoured the incorporation of radiographs in forensic anthropology to mainly document human remains recovered in medico-legal context, associated pathology and trauma, and any individualizing characteristics (e.g., bone healing and internal prosthesis) (Buikstra & Ubelaker, 1994; Garvin & Stock, 2016; Viner, 2018; Zhang, 2022; LODOX®, 2024). Radiographic modalities, such as Computed Tomography (CT), Magnetic Resonance Imaging (MRI), and conventional x-rays, are increasingly utilised in forensic anthropological analysis to aid with the biological profile estimation (Franklin *et al*., 2016; Garvin & Stock, 2016; Krishan *et al.,* 2016; Brits *et al.,* 2017; Brits *et al.,* 2018; Rowbotham & Blau, 2020; Zhang, 2022).

Traditional forensic anthropological analyses often require maceration of human remains for skeletal assessments, which is labour-intensive, can potentially cause damage to the structural integrity of bones, including DNA degradation (Triaca *et al.,* 2022), and frequently contravene with various cultural and religious beliefs (Lembert & Walker, 2019; Zhang, 2022). As such, using radiographic modalities and radiographs can further reduce the need to macerate human remains, providing an alternative approach for non-invasive forensic anthropological analyses (Viner, 2018). Additionally, given that radiation exposure is not a concern in postmortem examination or skeletal analyses, high-resolution imaging, which requires high radiation exposure to the subject, can be utilised to obtain the best image quality for better visualisation (DeMaio *et al.,* 2019; Zhang, 2022). Thus, forensic anthropologists can utilise high-resolution radiographic images for comparison across various skeletal regions, assessing bone morphology to aid with skeletal sex estimation, including estimations of other biological profile parameters (Aly *et al.,* 2016; Garvin & Stock, 2016; Rowbotham & Blau, 2020; Zhang, 2022). The principle of skeletal sex estimation from radiographic images is considered similar to that applied when utilising dry bone, whereby traits of skeletal elements known to be sexually dimorphic are examined and assessed on

radiographs using known and validated morphological and/or metric sex estimation methods (Rowbotham, 2016; Rowbotham & Blau, 2020).

Although CT scans have been favoured globally and are considered as the golden standard for virtual skeletal analyses, they are expensive to set-up and maintain, require trained professional operators and are not readily available in medico-legal facilities, especially in developing countries (e.g., South Africa) (Mamabolo *et al.,* 2020; Zhang, 2022). In contrast, Low Dose X-ray Systems (commonly known as Lodox®) are frequently found in South African Forensic Pathology Services (FPS) (Boffard *et al.,* 2006; Reid *et al.,* 2020; Morele *et al.,* 2024). Moreover, Lodox® Systems are installed in over 20 South African FPS facilities, and more than 50 forensic pathology centres worldwide, particularly those associated with resource constraints such as financial disadvantages, high workload/caseload, and limited access to advanced radiographic modalities (Boffard *et al.,* 2006; Reid *et al.,* 2020; LODOX®, 2023a; Segar, 2023; Morele *et al.,* 2024).

The Lodox® Systems, particularly the Lodox® Statscan™, are primarily used to scan for metal artifacts (e.g., firearm projectiles) and detect skeletal injuries in FPS facilities, prior to postmortem examinations (du Plessis *et al.,* 2020; Spies *et al.,* 2021; LODOX®, 2023b; Morele *et al.,* 2024), and in hospital trauma centres with patients associated with multiple skeletal injuries (Boffard *et al.,* 2006; Amirlak *et al.,* 2009; Deyle *et al.,* 2010; Dempers *et al.*, 2018; Thambura, 2023). The Lodox® Systems produces high-quality, full-body two-dimensional (2D) digital images of skeletal structures in anterior-posterior, lateral, or oblique planes, with minimal distortion, spatial resolution of 1.04 to 5 line-pairs per millimetre, and 14-bit contrast resolution (Beningfield *et al.,* 2003; Boffard *et al.*, 2006; Chen *et al.,* 2010; Stull *et al.*, 2013b; Mamabolo *et al.*, 2020). Little is however known about the application of Lodox® Systems in forensic anthropology cases compared to their use in postmortem examinations of unnatural death cases (Knobel *et al.,* 2006; Stull, 2013a; Quarrie, 2015; du Plessis *et al.,* 2020; Spies *et al.,* 2021; Morele *et al.,* 2024). As such, the current study was aimed at investigating the capability of Lodox® Systems to visualise skeletal elements and morphological skeletal traits for radiographic adult sex estimation.

CHAPTER 2: LITERATURE REVIEW

A multitude of methods and procedures have been developed and are utilised for accurate and reliable sex estimation using various regions of the human skeleton (Bainbridge & Tarazaga, 1956; McCornick *et al.*, 1985; Buikstra & Ubelaker, 1994; Walker, 2008; Raveendranath *et al.*, 2009; Scholtz *et al.,* 2010; Vance *et al.,* 2011; Klales *et al.,* 2012; İşcan & Steyn, 2013; Ishwarkumar, 2016; Rogers, 2021; Gupta *et al.,* 2022). A survey by Klales (2013) about the 'Practices in Physical Anthropology for Sex Estimation in Unidentified, Adult Individuals' showed that most biological anthropologists prefer combining morphological and metric methods for skeletal sex estimation. Specifically, when using morphological methods, numerous biological anthropologists preferred the pelvis for morphological sex estimation, followed by the skull and then the long bones (Klales, 2013). Regarding the pelvic morphology, the methods developed by Phenice (1969) (54% first choice) and Buikstra and Ubelaker (1994) (43% second choice) were the most favoured for accurate pelvic sex estimation. For skull morphology, the most preferred methods were those of Buikstra and Ubelaker (1994) (59% first choice) and Walker (2008) (42% second choice). Regarding long bone morphology, at least 33% of biological anthropologists preferred this approach for sex estimation (Klales, 2013). The overall bone robusticity was the most preferred method (63% first choice), while morphological traits of the distal humerus, described by Rogers (1999), were the second most preferred method (52% second choice) for sex estimation based on long bone morphology (Klales, 2013). To improve sex classification accuracy, these morphological sex estimation methods have been tested and validated on specific populations, including South African populations (Vance *et al.,* 2011; Kenyhercz *et al.,* 2012; Stull *et al.,* 2013a; Krüger *et al.,* 2015; Ishwarkumar *et al.,* 2016; Kenyhercz *et al.,* 2017; Gupta *et al.* 2022). This chapter reviews the literature on morphological sex estimation of the skull and various postcranial elements, including studies and skeletal traits relevant to South African populations and various global geographic populations. The current study also explores the application of modern radiographical modalities in forensic anthropological sex estimation.

2.1. An Overview of Morphological Skull Traits for Sex Estimation

In forensic anthropological casework, the cranium is commonly the most recovered skeletal element due to its durability, therefore the most studied bone and a valuable skeletal element for anthropological analyses (İşcan & Steyn, 2013; Indra & Lösch, 2021). Generally, male cranial morphology is often characterized by larger, more rugged, and robust features, whereas female cranial morphology is often smaller, more gracile, and smoother. (İşcan & Steyn, 2013; Berg, 2017). Earlier work from Krogman and İşcan (1962) highlighted several general morphological differences between the male and female crania, based on a binary nominal scoring system from a

multitude of morphological traits (Table 2.1). Numerous sex estimation studies have shown the value of using the skull in morphological sex estimation, achieving accuracies of 85% to 95% when using traditional morphological traits (Williams & Rogers, 2006; Walker, 2008; Krüger *et al.*, 2015; Gupta *et al.,* 2022). This makes the skull an invaluable skeletal element for morphological sex estimation.

Table 2.1: Discrimination of sex based on Krogman and İşcan's (1962) cranioscopy descriptions.

Skull Trait	Male	Female
General skull size	Large	Small
Architecture	Rugged	Smooth
Supraorbital ridges	Medium to large	Small to medium
Mastoid processes	Medium to large	Small to medium
Occipital area	Muscle lines and protuberance marked	Ill-defined muscle lines and protuberance
Occipital condyles	Large	Small
Frontal eminences	Small	Large
Parietal eminence	Small	Large
Orbital bones	Squared, lower, relatively smaller, with rounded margins	Rounded, higher, relatively larger, with sharp margins
Forehead slope	Steeper, less rounded	Rounded, full, infantile
Zygomatic bones	Heavier, more laterally arched	Lighter, more compressed
Mandible	Larger, higher symphysis, broader ascending ramus	Smaller, with smaller corporal and ramal dimensions
Palate	Larger, broader, tends to U-shape	Small, tends to parabolic shape
Teeth	Large, lower M1 more often 5 cusped	Small, molars often 4 cusped

de Villiers (1968) conducted morphological sex estimation based on 14 morphological skull traits (including five of the traits suggested by Krogman and İşcan (1962)) of black South African individuals. These skull traits all exhibited significant sexual dimorphism and subsequently served as a pioneer study for morphological sex estimation of the skull of Black South Africans. Williams and Rogers (2006) evaluated the accuracy and precision of morphological sex estimation using 21 morphological skull traits, assessed on 50 adult crania of individuals of European (white) ancestry. Overall, a 96% accuracy was obtained using 20 traits in combination, with at least 14 morphological traits having accuracies ranging from 58% to 92% for combined sexes, 64% to 100% for males, and 24% to 96% for females. However, only six skull traits were identified as high-quality traits due to high intra-observer agreements and achieving over 80% classification accuracies. These six traits were the mastoid process, supraorbital ridge, skull morphology, zygomatic morphology, nasal aperture, and mandible-gonial angle. The study concluded that these traits should be of primary focus when utilising skull morphology for sex estimation. Sangvichien and colleagues (2008) also conducted a sex estimation study based on the 14 morphological traits of the skull (described by Krogman and İşcan (1962) (Table 2.1)) of individuals from central Thailand. The method resulted in a 95.5% accuracy for males and 82.9% accuracy for females, with a combined (male + female) accuracy of 91%. However, the study's findings did not specify the sex classification accuracy associated with each skull trait assessed, in addition to using a non-equally distributed study sample (males: n = 66; females: n = 35).

Buikstra and Ubelaker (1994) developed skeletal sex estimation standards that emphasise the use of five morphological traits of the skull (mastoid process, glabella, supraorbital margin, nuchal crest, and mental eminence) for reliable skull morphological sex estimation. Each skull trait was morphologically assessed and scored on a five-point ordinal scale, with robust, masculine features at the higher end of the scale (Buikstra and Ubelaker, 1994). However, the provided descriptions were vague, and the scoring system was primarily developed for individuals of European ancestry instead of considering the wide range of variations associated with the morphology of the skull. Subsequently, Walker (2008) modified the method by improving the trait descriptions and computing population-specific sex estimation logistic regression discriminant functions for individuals of European American, Native American, African American, and English descents, thus allowing practitioners to utilise one of the provided, population-specific formulae to insert assessed trait scores and obtain a final sex estimate. The logistic regression discriminant analysis achieved an 88% correct sex classification accuracy when all five skull traits were assessed, with a 0.1% sex bias. The Walker's (2008) method has been tested and validated in numerous distinct populations, deriving population-specific discriminant function formulae that achieve similar sex classification accuracies (Krüger *et al.*, 2015; Jilala *et al.,* 2021; Garvin, 2020; Rogers *et al.,* 2024).

Therefore, the Walker (2008) method (in conjunction with Buikstra and Ubelaker (1994) sex estimation standards) has been regarded as the most preferred morphological method for sex estimation using the skull, by most biological anthropologists (Klales, 2013). Subsequently, Klales and Cole (2018) added photos of real bone specimens of each skull trait score described by Walker (2008) including providing descriptions for the scores between the extreme trait scores (i.e., 2-4) to improve the interpretation and assessment of these scores.

Krüger and colleagues (2015) tested the reliability and accuracy of the Walker (2008) method on a South African skull sample (245 skulls) and generated South African-specific logistic regression formulae. The utilisation of Walker's (2008) logistic regression formulae yielded correct sex classification that were 80% or higher for combinations of the mastoid process, glabella, and mental eminence traits (White males = 94-97%, White females = 57-62%, Black males = 84-92%, and Black females = 83-90%). Modified South African logistic regression formulae were generated, providing 83% to 93% correct sex classification accuracies (combined sex classification: 81-84% for Black South Africans and 80-93% for White South Africans), thus validating the method for applicability to South African Black and White population groups. Jilala and colleagues (2021) tested the Walker (2008) method on a sample of 50 male and 36 female skulls of contemporary Tanzanian individuals (Black Africans) for morphological skull sex estimation. The combined (male + female) correct sex classification accuracies ranged from 66% (nuchal crest) to 87% (mastoid process) with the correct sex classification accuracy being higher for females (83-88%) than males (47-88%), for all assessed traits. With accuracy rates similar to the original Walker (2008) findings, the authors recommended further validation of the method for modern Tanzanian samples. The use of a contemporary sample highlights its potential for skeletal sex estimation in the Tanzanian population.

A study by Gupta and colleagues (2022) evaluated multiple cranial and mandibular morphological traits for sex estimation on a South African skeletal sample. Overall mandibular morphology had the highest sex classification accuracy (combined sex = 83%, males = 92%, and females = 68%), followed by overall cranium morphology (combined sex = 81%, males = 88%, and females = 69%), glabella morphology (combined sex = 81%, males = 86%, and females = 74%), and gonial angle (combined sex = 80%, males = 90%, and females = 86%). In contrast, other assessed skull traits had sex classification accuracies of less than 80%. Malek and colleagues (2023) assessed the crania of Southern African Holocene San and Khoekhoe populations using the Buikstra and Ubelaker (1994) standards, in conjunction with the scoring method by Walker (2008) and compared them with pelvic sex estimates (based on the Phenice (1969) method) to assess agreements. Of the cranial traits assessed, the morphology of the mastoid process and shape of the

mandible showed the strongest agreements with sex estimates of the pelvis, with accuracies of 73% and 72% respectively, indicating the greatest degree of sexual dimorphism. In contrast, the morphologies of the mental eminence and nuchal crest yielded the lowest agreements with pelvic estimates (both 53%).

2.2. An Overview of Morphological Postcranial Traits for Sex Estimation

Numerous studies have attempted sex estimation from almost every single skeletal element that could be used in cases where the skull is not available for anthropological analysis (e.g., Bainbridge & Tarazaga, 1956; McCormick & Stewart, 1983; Rogers, 1999; Scholtz *et al.,* 2010). Most of the derived methods are age and population-dependent, applicable in conjunction with metric measurements and discriminant function formulae to yield accurate sex estimations (İşcan & Steyn, 2013; Klales, 2020a). The following sections provide literature on some of the postcranial skeletal elements and traits that have been investigated and established for morphological sex estimation, with the potential to be assessed radiographically.

2.2.1. Scapula morphology

The scapula bone has been studied extensively to investigate its shape and size for sex estimation. A multitude of the available literature highlights the prioritization of metric and morphometric methods, which combine metric and non-metric approaches to quantify shape differences, often in conjunction with population-specific logistic regression formulae and measurements of various scapular parameters for sex estimation (e.g., maximum length, breadth, spine, glenoid cavity) (İşcan & Steyn, 2013; Oliveira Costa *et al.,* 2016; Koukiasa *et al.,* 2017; Curate *et al.,* 2024; Smal, 2020). There has been an increase in the use of geometric morphometric approaches to provide mathematical descriptions of the scapula morphology based on geometric landmarks that retain shape information, therefore used to assess sexual dimorphism of the scapula and estimate sex (Snow, 2004; Scholtz *et al.,* 2010; Maranho *et al.,* 2022; Maranho *et al.,* 2023). In contrast, there is limited literature on studies that utilise traditional morphological approaches to investigate and assess sex differences in the morphology of the scapula (Bainbridge & Taragaza, 1956; Scholtz *et al.,*2010).

Various scapular bony features have been reported to display sexual dimorphism in their presence and/or expressions (Bainbridge & Taragaza, 1956; Scholtz *et al.,* 2010). For instance, the depth of the suprascapular notch has been reported to vary between males and females, with males reported to exhibit a very deep notch, approaching a full circle, while females exhibit shallow-like notch (Bainbridge & Taragaza, 1956; Christensen *et al.,* 2014c). Bainbridge and Taragaza (1956) identified three morphological sexually dimorphic traits of the scapula among a collection of 17th-18th-century skeletons of European ancestry (i.e., suprascapular notch presence/absence,

supraspinous fossa curvature, and infraspinous fossa border curvature). A study by Scholtz and colleagues (2010) investigated the sexual dimorphism associated with the three borders (lateral, medial, and superior) of the scapula using geometric morphometric analysis (males: n = 45; females: n = 45). The study found that female scapulae were associated with straighter/steep-sloped lateral and medial infraspinous fossa borders and a convexly curved supraspinous fossa border compared to male scapulae. Additionally, the use of the three scapular borders in combination achieved significant sex classification accuracies (males = 95% and females = 91%), with the supraspinous superior border displaying the most variation between males and females. Similarly, Maranho *et al.* (2022) evaluated scapula sexual dimorphism based on a geometric morphometric approach from two Portuguese reference skeletal collections (males: n = 100; females: n = 111): the 21st Century Identified Skeletal Collection and the Coimbra Identified Skeletal Collection. The study reported significant differences between male and female scapulae (males = 67% and females = 68%), with males exhibiting larger scapulae with more curved medial and lateral infraspinous borders compared to female scapulae. Moreover, a discriminant function analysis of combined shape and size variables increased the overall sex classification accuracy of the scapula to 80% (males = 76% and females = 82%).

Overall, the use of geometric morphometric methods for scapula sex estimation allows for the quantification of two- or three-dimensional homologous structures of the scapula that can be analysed and assessed morphologically for morphological sex estimation (Scholtz *et al.,* 2010; Maranho *et al.,* 2022). Further evaluation of sexually dimorphic morphological features of the scapulae, especially those identified through geometric morphometric analyses, using radiographs for potential morphological sex estimation is warranted.

2.2.2. Clavicular rhomboid fossa presence

Traditional approaches to morphological sex estimation have not extensively incorporated the clavicle's morphological features. The majority of the available literature focuses mostly on metric methods for clavicular sex estimation that can achieve more than 70% sex classification accuracy (Spradley & Jantz, 2011; Cleary, 2012; Scott *et al.,* 2018; Demir *et al.,* 2022). A multitude of studies have investigated the relationship between the presence of the rhomboid fossa (i.e., costoclavicular tuberosity) and sex across skeletal collections of various global populations, with varying findings (Jit & Kaur, 1986; Rogers, 2000; Singh & Singh, 2009; Ishwarkumar *et al.*, 2016). Jit and Kaur (1986) investigated the presence of the rhomboid fossa in the clavicle of 789 North Indians adults, however, found no sex differences in the presence or absence of the trait, as it was bilaterally present in 58% and 54% of the male and female individuals, respectively. Furthermore, Ishwarkumar and colleagues (2016) investigated the incidence of the rhomboid fossa (in

conjunction with other morphometric parameters of the clavicle) in a South African sample (males: 66; females: 34; age range = 25 to 95 years of age). Ishwarkumar and colleagues (2016) corroborated Jit and Kaur's (1986) findings, reporting no statistically significant correlation between the trait and sex, given its presence in 97% of male and 85% of female clavicles.

Rogers and colleagues (2000) derived a clavicle-based sex estimation method based on the absence or presence of the rhomboid fossa (also known as costoclavicular tubercle). The study was based on a skeletal collection comprising predominately white Americans (males: n = 195; females: n = 106; age range = 10 to 92 years) from the William F. McCormick collection, University of Tennessee, Knoxville. The method found that rhomboid fossae were more frequently present in males between 20 and 30 years, with an 81% posterior probability of the individual being male if found on the right clavicle (59% for females), and a 92% posterior probability of the individual being male if found the on left clavicle (58% for females). Similarly, Prado and colleagues (2009) investigated the presence of the rhomboid fossa in a Brazilian population (males: n = 107; females: n = 102; age range = 19 to 85 years) and found statistically significant sex differences, as the traits was absent in 97% of female clavicles and present in 64% of male clavicles. Overall, there appears to be no consensus among the available literature regarding the rhomboid fossa being a sexually dimorphic trait, particularly across different global populations. However, those who report sex differences in the trait advocate for it to be used as an indicator of sex, and suitable for morphological sex estimation in medico-legal investigation (Rogers, 2000; Prado *et al.,* 2009). Nevertheless, further investigation of associated sex differences of the trait is required.

2.2.3. Distal humerus morphology

Amongst postcranial skeletal elements (in the absence of the pelvis), the humerus has been found to differ significantly, morphologically between sexes (Rogers, 1999; Falys *et al.,* 2005; Vance *et al.,* 2011; Tallman & Blanton, 2020). Rogers (1999) identified four morphological traits on the distal and posterior humerus that display sexual dimorphism (i.e., medial epicondyle angle, olecranon fossa shape, trochlear symmetry, and trochlear constriction) based on a sample of white Americans from the Documented Skeletal Collection at the University of New Mexico (n = 35) and the William M. Bass Donated Skeletal Collection at the University of Tennessee, Knoxville (n = 93). Male distal humeri exhibit a flat medial epicondyle angle, a triangular-shaped olecranon fossa, as well as an asymmetrical and less constricted trochlea. In contrast, female distal humeri exhibit a posteriorly angulated medial epicondyle, an oval-shaped olecranon fossa, as well as a more symmetrical and constricted trochlea. As a result, each trait was scored as either “male-like” or “female-like”, with the traits having a sex classification accuracy range from 69% to 88% individually, and a 91% combined sex classification accuracy. Subsequent validation indicate that

the methods perform moderately well, achieving over 70% overall sex classification accuracies, particularly when all four traits are assessed (Falys *et al.,* 2005; Vance *et al.,* 2011; Tallman & Blanton, 2020).

Falys and colleagues (2005) evaluated Rogers' (1999) distal humerus sex estimation method using the St. Bride's Documented skeletal collection comprising of individuals of British European ancestry (males: n = 184; females: n = 167). The individual traits had a significant sex classification accuracy ranging from 69% (trochlea constriction) to 81% (olecranon fossa shape), with a combination of all traits providing a 79% sex classification accuracy. Vance *et al.* (2011) tested and validated Rogers' (1999) distal humerus method on a skeletal collection of black and white South African individuals from the Pretoria Bone Collection, University of Pretoria (males: n = 420; females: n = 188). However, Vance and colleagues (2011) modified Rogers' (1999) method by excluding trochlea constriction (due to the ambiguous definition) and implemented a five-point ordinal scoring scale for the remaining distal humerus traits. Additionally, schematic diagrams for each of the assessed traits were generated to complement the ordinal scoring system. The combined three traits provided a 75.5% sex classification accuracy for black and white South Africans (males = 74% and females = 77%), which was lower than Rogers' (1999) 91% sex classification accuracy but still acceptable for forensic casework.

Similarly, Vance and Steyn (2013) reported 78% and 79% male and female sex classification accuracies (respectively) when geometric morphometric analysis of the three distal humeri traits from Vance and colleagues (2011) was assessed (males: n = 66; females: n = 55). Furthermore, Tallman and Blanton (2020) derived five-point ordinal scores for each of Rogers' (1999) distal humerus morphological traits from skeletal collections of modern Thai individuals (males: n = 418; females: n = 198). The assessment of distal humerus traits was also conducted according to the schematic diagrams and descriptions provided by Vance and colleagues (2011). Tallman and Blanton (2020) also provided real bone specimen photos of each posterior distal humerus trait to visualize intricate details of associated traits' morphologies, including subtle morphological features that may be critical for accurate sex classification. The achieved sex classification accuracies ranged between 13.9% (trochlear constriction for females) and 81.4% (medial epicondyle angle for males). However, all of the traits exhibited male biases, ranging from 29% to 64%. Similar to Vance and colleagues (2011), the trochlear constriction performed inadequately due to its ambiguous definition and description. Nevertheless, these studies highlight that population differences exist in the morphology of the distal humerus and those distal humerus traits are significantly suitable for morphological sex estimation in forensic anthropological

casework, when other elements are absent. As such, further assessment of these distal humerus morphological traits from radiographs for potential morphological sex estimation is warranted.

2.2.4. Rib costal cartilage morphology

The skeletal elements of the anterior thoracic cage are often associated with subtle morphological variations or anomalies that may be informative in the sex and age-at-death estimation of human remains (Macaluso Jr. & Lucena, 2014a). Moreover, the components of the anterior thoracic cage are frequently preserved and recovered in decomposing and skeletonised remains, thus deemed invaluable for biological profile estimation of unidentified skeletal remains (McCormick *et al.,* 1985; Damiata *et al.,* 2013; Keyes *et al.,* 2020). As such, rib costal cartilages have been studied extensively for morphological sex estimation (with literature dating back to the 1950s) by analyzing calcification/ossification patterns within the costal cartilages of male and female individuals (Fischer, 1955 as cited in Patyal & Bhatia, 2022; Elkeles, 1966; McCormick & Stewart, 1983; McCormick *et al.,* 1985; Rejtarová *et al.,* 2004; Patyal & Bhatia, 2022). Contrary to most morphological traits, costal cartilage ossification patterns are mainly visible on radiographic images, especially once they begin to calcify, around the ages of 35 years or older (McCormick *et al.,* 1985; Ontell *et al.,* 1997; Rejtarová *et al.,* 2004; Patyal & Bhatia, 2022). A multitude of studies have reported significant sex differences in costal cartilage ossification patterns, with females exhibiting a more centrally placed ossification pattern and males exhibiting a more peripheral, marginal ossification pattern (e.g., McCormick *et al.,* 1985; Rejtarová *et al.,* 2004; Christensen *et al.,* 2014c; Patyal & Bhatia, 2022). Similar to most sex estimation methods, the accuracy of the use of costal ossification patterns for morphological sex estimation is variable amongst and/or between population groups and are also age-dependent as they are mainly visible on radiographic images once they begin to calcify (McCormick *et al.,* 1985; Ontell *et al.,* 1997; Rejtarová *et al.,* 2004; Christensen *et al.,* 2014c; Patyal & Bhatia, 2022). As such, population affinity and age parameters should be considered when attempting morphological sex estimation using costal cartilages ossification patterns. Nevertheless, this method has been shown to be invaluable for morphological sex estimation, especially in medico-legal cases whereby the thoracic cage is recovered (McCormick *et al.,* 1985; Rejtarová *et al.,* 2004; Patyal & Bhatia, 2022).

Elkeles (1966) observed sex differences in the ossification patterns of the ventral costal cartilages from radiographs of 2606 patients of European ancestry (males: n = 1329; females: n = 1277) with an age-at-death range of 30 to 80 years. The study found that the ossification pattern in males were characterized by linear-like bands confined to the perichondrium (i.e., peripheral) whereas in females they were curved-like bands of dense granular ossification patterns. Moreover, the degree of ossification was five times higher in female individuals than in males aged between 30 and 50

years. Later, McCormick and Stewart (1983) investigated sex estimation based on costal cartilage ossification patterns from adult chest x-ray plates of individuals of European (males: n = 396; females: n = 268), African (males: n = 204; females: n = 122) and Hispanic descent (males: n = 94; females: n = 43). A 92% sex classification accuracy was achieved. Females exhibit centrally placed globules of ossification patterns, whereas males had predominantly heavy peripheral ossification patterns. Rejtarová *et al.* (2004) also evaluated sex differences in the costal cartilage ossification patterns from x-rays of 537 male and 507 female individuals of European descent (Czech Republic). Similar to prior studies, peripheral ossification patterns (93% classification accuracy) were associated with male individuals, whereas centrally placed, globular/lingual ossification patterns (77% classification accuracy) were associated with females. In addition, Patyal and Bhatia (2022) conducted similar investigations of sex estimation from costal cartilage ossification patterns. The study utilised posterior-anterior x-ray radiographs of North Indians (n = 450) and achieved similar observations as prior studies (i.e., peripheral ossification patterns in males and centrally-placed, globular ossification patterns in females). However, compared to prior studies conducted on distinct population groups, Patyal and Bhatia (2022) achieved significantly high classification accuracies for sex estimation based on rib costal cartilage ossification patterns, reporting 99% classification accuracy for males and a 100% classification accuracy for females.

The above-mentioned studies reported the costal cartilage ossification patterns of the lower ribs (8^{th} -12^{th}) to exhibit the most sexual dimorphism, which is positively correlated with increasing age (Elkeles, 1966; McCormick *et al.,* 1985; Rejtarová *et al.,* 2004; Patyal & Bhatia, 2022). Unfortunately, no subsequent African-based studies in the available literature have investigated this phenomenon. As such, further investigation based on a sample of individuals of African descent is needed as the available literature statistically emphasises the existence of morphological sex differences in the ossification patterns of human costal cartilage that is highly predictive of sex estimation across distinctive populations.

2.2.5. Pelvis morphology

The pelvis is widely regarded as the most sexually dimorphic element of the human skeleton, studied extensively for sex estimation, and thus considered the best skeletal element for biological sex estimation of human remains (Krogman & İşcan, 1962; Phenice, 1969; Buikstra & Ubelaker, 1994; Austin & King, 2016; Klales, 2020a; Garvin *et al.,* 2021; Braun *et al.,* 2023). Similar to the skull, Krogman and İşcan (1962) highlighted general morphological differences between the male and female pelvic bone from a multitude of morphological traits that can be assessed and scored based on a binary nominal scale (Table 2.2). Like the skull, there is a likelihood of a large degree of overlap in the traits, with the existence of an infinite number of morphological variations

between the ultra-masculine and ultra-feminine pelvic traits (İşcan & Steyn, 2013). Subsequent studies have tested and sought to determine the accuracy of the traditional morphological traits outlined in Table 2.2, including improving and validating them across distinct geographic populations, highlighting their significance in forensic anthropological cases (Patriquin *et al.,* 2003; Walker, 2005; Listi & Bassett, 2006; Blanchard, 2010; Klales *et al.,* 2012; Gupta *et al.,* 2022; Rojas González *et al.,* 2024).

Table 2.2: Discrimination of sex based on Krogman and İşcan (1962) pelvis morphological traits.

Pelvis Trait	Male	Female
Pelvis as a whole	Massive, rugged	Smaller, gracile
Pubic symphysis	Higher	Lower
Subpubic angle	V-shaped (<90^{o})	U-shaped/broader divergent (>90^{o})
Pubic bone shape	Triangular	Rectangular
Ventral arc	Absent	Present; well defined
Obturator foramen shape	Large, ovoid	Small, triangular
Acetabulum	Large, directed laterally	Small, directed antero-laterally
Greater sciatic notch	Smaller, narrow, deep	Large, broad, shallower
Sacroiliac joint	Slightly everted	Strongly everted
Auricular surface	Raised	Flat
Postauricular space	Narrow	Wide
Preauricular sulcus	Absent, not frequent	More frequent, better developed
Postauricular sulcus	Absent. Not frequent	More frequent, sharper auricular surface edge
Ilium	High, vertically aligned	Lower, laterally divergent
Iliac tuberosity	Large, not pointed	Small or absent, pointed
Sacrum	Longer, narrower, with more evenly distributed curvature	Shorter, broader, with a tendency of marked curvature at S1-2 and S2-5
Pelvic brim/inlet	Heart-shaped	Round, elliptical
True pelvis or cavity	Relatively small	Oblique, shallow, spacious

Patriquin and colleagues (2003) assessed five morphological pelvic traits from the Krogman and İşcan (1962) trait list using a sample of black and white South African contemporary skeletal remains (i.e., pubic bone shape, subpubic concavity, ischiopubic ramus form, ischial tuberosity

orientation, and greater sciatic notch morphology). The study results indicated that the pubic bone shape was the most reliable trait for accurate pelvic sex estimation in both sexes and population groups. The pubic bone shape and subpubic concavity were the most discriminating traits in white South Africans, with an 88% combined sex classification accuracy, while the greater sciatic notch form was the most discriminating traits in black South Africans with 87.5% classification accuracy, followed by the pubic bone shape (combined accuracy = 84.5%). Furthermore, Steyn and colleagues (2004) analysed the morphology of the greater sciatic notch using geometric morphometric analyses on a skeletal sample of black and white South African individuals (males: n = 57; females: n = 58). Black males (91%) were found to be characterised by a narrow configuration, while there were no significant distinctions between the sciatic notch shapes of white males (67%) and females (91%), and black females (84%), characterized by a predominantly wide configuration.

A subsequent, similar study by Pretorius and colleagues (2005), utilised a sample of black South African individuals (males: n = 29; females: n = 31) and reported slightly improved accuracies, with a 90.3% combined sex accuracy (male = 93.1% and female = 87.1%). Similar accuracies have also been reported by Walker (2005) using traditional morphological assessment of the greater sciatic notch morphology based on a skeletal sample of white and black Americans, and geometric morphometric analyses by Gonzalez *et al.* (2009) and Gómez-Valdés *et al.* (2012) based on skeletal samples of white European and contemporary Mexican individuals, respectively. Similarly, the subpubic angle has been studied extensively with regards to discriminating between sexes and reported to yield significant sex classification accuracies across distinct population groups (Small *et al.,* 2012; Stull *et al.,* 2013a; Gupta *et al.,* 2022). For instance, a study by Small and colleagues (2012) quantified the subpubic angle from a sample of Black and White South African human pelves. The subpubic angle was found to have an 86% average sex classification accuracy for both population groups. Similarly, a study by Gupta *et al.* (2022) evaluated four morphological traits on the pelvis, including subpubic angle, for sex estimation on a skeletal sample of black South Africans (n = 161) from the Raymond A. Dart Collection of Modern Human Collection, University of the Witwatersrand. The authors reported 93% and 95% sex classification accuracies for male and female subpubic angles (respectively), followed by the greater sciatic notch form (males = 87% and females = 66%), arc compose (males = 88% and females = 71%), and iliac crest (males = 73% and females = 65%). Overall, the above-mentioned study findings tentatively highlight that numerous traits of the pelvis, including those outlined by Krogman and İşcan (1962) (Table 2.2), are invaluable for accurate morphological sex estimation of the pelvis, including South African population groups. Numerous studies have found that three pubic bone traits (subpubic contour, ventral arc, and ischiopubic ramus form) can accurately and reliably estimate pelvic morphological

sex. These traits consistently demonstrate accuracy rates of up to 95%, across distinct population groups, leading to their recommendation as standards methods (e.g., Phenice, 1969; Buikstra and Ubelaker. 1994; Klales, 2013; Klales & Cole, 2018)

Phenice (1969) developed a morphological method for sexing the pelvic bone (os coxae) using a sample of Black African (males: n = 20; females: n = 27) and white European (males: 160; females: 43) individuals. The author reported significant sexual dimorphism in the morphologies of the ventral arc, subpubic contour and ischiopubic ramus. Sex estimation using these traits in combination provided 95.56% male accuracy (black Africans = 95%; white European = 95.62%) and 96.84% female accuracy (black Africans = 94.23%; white Europeans = 100%). Subsequent studies have tested and validated the Phenice (1969) method across distinct population groups, reporting significantly similar sex classification accuracies (e.g., Ubelaker & Volk, 2002; Kenyhercz, 2012; Salim, 2012; Kenyhercz *et al.,* 2017; Jager & Eliopoulos, 2023; Rojas González *et al.,* 2024).

For instance, Buikstra and Ubelaker (1994) presented: Standards for Data Collection from Human Remains, and emphasised the use of Phenice's (1969) three traits, in combination with the presence of a preauricular sulcus and the morphology of the greater sciatic notch for reliable morphological sex estimation of the pelvis. That same year, Rogers and Saunders (1994) assessed the accuracy and reliability of 17 morphological traits of the pelvis, including Phenice's (1969) traits and traits outlined in Table 2.2, using skeletal remains of 49 19th-century Canadian individuals. The authors reported combined sex classification accuracies ranging from 6.1% (sacral segments) to 94% (sacrum shape). However, the overall effectiveness of a trait for reliable sex estimation was ranked based on an effective score that was a combination of sex accuracy and precision (intra-observer error) scores. Unfortunately, no attempt was made to balance the validity and reliability of the scores, thus, some traits achieved high overall effective ranking even with relatively low accuracy or precision scores. As a result, not all traits suggested by Buikstra and Ubelaker (1994) were in the top ten list of most effective pelvic traits for sex estimation.

For instance, both the greater sciatic notch (combined accuracy = 85.6%; ranked 12^{th} in precision) and the medial ischiopubic ramus (combined accuracy = 80%; ranked 10^{th} in precision) were ranked 12^{th} and 15^{th} in overall effective pelvic morphological sex estimation, respectively, even though they have been emphasised as standard traits for pelvic sex estimation by Buikstra and Ubelaker (1994). Nevertheless, their findings were in agreement with the ventral arc being the most effective trait for pelvic sex estimation (ranked 1^{st}) even though it was the fifth most accurate pelvic trait (86.9% combined accuracy; ranked 1^{st} in precision). Overall, while taking into consideration degree of precision and correct sex accuracy associated with assessing a particular

trait, the authors suggested six traits as the most effective as sex discriminators due to due high precision (<5% intra-observer errors) and greater than 83% combined classification accuracies (i.e., ventral arc, obturator foramen shape, true pelvis shape, sacrum shape, subpubic concavity and pubis shape). Despite this ranking, the survey by Klales (2013) indicated an overwhelming preference for pelvic traits by biological anthropologists, particularly those recommended by Phenice (1969) and Buikstra and Ubelaker (1994), for reliable morphological skeletal sex estimation.

Klales and colleagues (2012) as well as Klales and Cole (2018) revised the Phenice (1969) method to use five-point ordinal scoring scale, to account for intermediate and/or ambiguous features and provided real bone specimen photos of each pelvis trait, respectively, with gracile, feminine features at the lower end of the scale. Using logistic regression formulae by Klales and colleagues (2012), the combination of the traits achieved a 95.5% accuracy (males = 99% and females = 92%) for experienced observers and 85.5% for inexperienced observers (males = 87% and females = 84%), with the ventral arc (88.5% combined sex) and subpubic concavity (86.6% combined sex) achieving the highest trait combination accuracy of 93.5% (males = 95.4% and females = 91.6%) amongst Phenice's (1969) traits. Overall, the Phenice (1969) method, in conjunction with the Klales *et al.* (2012) and Klales and Cole (2018) methods, is considered the most preferred morphological method for pelvic sex estimation by most biological anthropologists (Klales, 2013) and has been validated in distinct population groups, including South African population groups (Kenyhercz, 2012; Stull *et al.,* 2013a; Kenyhercz *et al.,* 2017).

Kenyhercz (2012) evaluated and validated the accuracy of the pelvis sex estimation method by Klales *et al.* (2012), including the associated logistic regression formulae, on a sample of modern South Africans (males: n = 61; females: n = 44) from the Pretoria Bone Collection, University of Pretoria. The Klales *et al.* (2012) method indicated significant success when applied to a modern South African sample, with classification accuracies ranging from 90.6% (k-nearest neighbour analysis) to 99.2% (ordinal logistic regression analysis) combined accuracies, depending on the method of analysis. Although the accuracies associated with the assessed pelvic traits were not indicated, the ventral arc was highlighted as the most sexually dimorphic pelvic trait, followed by the subpubic concavity, and the ischiopubic ramus medial aspect. Similarly, Stull and colleagues (2013a) tested and validated the Klales *et al.* (2012) method on a South African sample in conjunction with five statistical analyses (discriminant function analysis (DFA), flexible discriminant analysis (FDA), logistic regression (LG), classification trees, and random forest models (RFM)). The average classification accuracies ranged from 92% to 99% for the respective statistical methods (i.e., classification tree = 92%, RFM = 96%, DFA & FDA = 96.5%, and LG =

99.2%). Moreover, the Klales *et al.* (2012) method was subsequently validated and recalibrated by Kenyhercz (2017) across four distinct population groups (i.e., black and white North Americans, black and white South Africans, Thai, and Hispanic border crossers). The achieved accuracies were relatively greater than those of the original study (Klales *et al.,* 2012), with validation accuracies ranging from 87.5% (Hispanic border crossers) to 95.6% (North Americans) and combined correct recalibration accuracies ranging from 89.6% (Hispanic border crossers) to 98% (South African Blacks), with an average global recalibration accuracy of 95.9%. These high accuracies are indicative of the significant sexual dimorphisms associated with the human pubic bone and also indicate that the Klales *et al.* (2012) method can be applied in diverse worldwide populations for accurate morphological sex estimation without the need for population specific equations. Consequently, the method has since been applied to South African forensic anthropological case analyses for sex estimation of skeletal remains, thus further assessment of the Klales *et al.* (2012) methods from radiographs of South Africans is warranted to determine if similar accuracies can be achieved.

Overall, pelvic morphology has been considered the most reliable sex estimation method for South African forensic casework of unknown human remains, particularly by examining the pubis due to exhibiting a significant degree of sexual dimorphism. Further investigation of the applicability of x-ray radiographs to sufficiently visualise pelvic traits for morphological sex estimation, based on current South African validated morphological pelvic sex estimation methods is warranted.

2.2.6. Other postcranial morphological traits of interest

The morphology of the female pelvis has been reported to be associated with adaptations of other long bones, namely, the elbow (olecranon-coronoid angle also known as the elbow carrying angle), hip (femoral neck shaft angle), and knee angles (quadriceps angle also known as Q angle) (Livingston, 1998; Airan & Dwivedi, 2018; Stock, 2020). However, there is limited literature on studies investigating morphological sex differences of such traits, and those studies that are available, are based mainly on assessments for clinical significance and application in bone fracture repair surgeries, rather than forensic anthropological analysis (Horton & Hall, 1989; Purkait, 2001; Raveendranath *et al.,* 2009; Rogers *et al.,* 2021; Skouras *et al.,* 2022). For instance, the femoral neck shaft angle (NSA) (i.e., the angle between the axis of the femoral neck and femoral long axis) is regarded as one of the frequently measured anatomical features of the hip as it is invaluable for the assessment of hip anatomy and surgical operations (Haddad *et al.,* 2013; Boese *et al.,* 2016). In general, varying ranges of the femoral NSA have been reported as standard references, with mean ranges between 120° to 150°, when measured from pelvic radiographs (Boese *et al.,* 2016). Moreover, various clinically based studies such as those by Elbuken *et al.*

(2012), Haddad *et al.* (2013), and Fischer *et al.* (2020) have reported small but significant sex differences in the femoral NSA, while studies by Gilligan *et al.* (2013) and Rogers *et al.,* 2021) had reported the opposite.

For those that reported significant sex differences, there seem to be no consensus on whether the femoral NSA is wider or narrower in females and males, and this could be attributed to no consensus in the method of measurement and hip alignment (Boese *et al.,* 2016). Study findings by Elbuken *et al.* (2012) and Haddad *et al.* (2013) reported the femoral NSA to be significantly larger in males (mean = 129.63° and 133.14° ± 5.54°, respectively) compared to females (mean = 129.14° and 132.98° ± 5.90°, respectively). In contrast, study findings by Fischer *et al.* (2020) and Rogers *et al.* (2021) have reported the NSA to be significantly wider in females (mean = 127.4° ± 6.6° and 133.61° ± 5.17°, respectively) than in males (mean = 126.5° ± 6.8° and 131.56° ± 4.74°, respectively), with Rogers *et al.* (2021) reporting an 87.7% combined sex accuracy in variation of the femoral NSA (males = 86.8% and females = 88%). As such, further assessment of the femoral NSA from x-ray radiographs is required, especially on a South African based sample, to investigate associated sex differences and determine if they could be applicable in forensic anthropological analysis.

Purkait (2001) devised a sex estimation method using three measurements of the ulna (including olecranon-coronoid angle) from 160 dry adult ulnae (100 males and 60 females) of individuals of Indian ancestry. The olecranon-coronoid angle was measured by placing the bone on its medial surface on an osteometric board, with the styloid process in contact with the lateral wall of the board. A thread was adjusted to align parallel to the line connecting the upper lip and the beak of the olecranon process, measured at the intersection of the lateral wall of the board (base) and the extended thread using a protractor (Purkait, 2001). The study findings indicated the olecranon-coronoid angle as the single best parameter for sex estimation, yielding 85% classification accuracy, and being broader/wider in male ulnae (mean = 22.26° ± 3.47°; 89% classification accuracy) and narrow in female ulnae (mean = 14.73° ± 4.46°; 78% classification accuracy). Airan and Dwivedi (2018) conducted a cross-sectional study of 400 individuals of Indian descent (males: n = 201; females: n = 199) to investigate sex differences in the elbow carrying angle radiographically (i.e., acute angle formed between median axis of the arm and that of the extended, supinated humerus) and found that angle was wider in females (mean = 12.31° ± 2.53) compared to males (mean = 8.71° ± 2.54°). It was inferred that the elbow carrying angle could be considered as a secondary sexual characteristic due to significant differences between the male and female elbow carrying angles (Airan & Dwivedi, 2018), thus, it could be applicable in forensic

anthropological analysis and sex estimation of unknown remains, particularly for fragmentary skeletal remains.

The available literature indicates that there are significant sex differences in the average degrees of the Q angle (i.e., the articulation angle of the femur with the tibia at the knee) between sexes and various population groups (e.g., Arabians, Black Nigerians, and North Indians), ranging from 10^0 to 15^0 in males, and 15^0 to 20^0 in females (Omololu *et al.,* 2009; Raveendranath *et al.,* 2011; Khasawneh *et al.,* 2019; Shantanu *et al.,* 2023). The observed sex differences in Q angle likely result from variations in the relative positions of the anterior superior iliac spine (ASIS), patella, and tibial tuberosity, leading to distinct ranges of the Q angles between sexes (Shantanu *et al.,* 2023; Gant *et al.,* 2024). Specifically, the wider female pelvis increases the distance between the ASIS and patella, effectively causing the knees to angle inward. This increased angle shifts the weight and force laterally at the knee, particularly onto the tibial tuberosity, which is positioned more laterally in females compared to males (Shantanu *et al.,* 2023; Gant *et al.,* 2024). Horton and Hall (1989) investigated the relationship between the Q angle and sex based on a sample of 100 American individuals equally distributed by sex and reported the Q angle to be narrow in male individuals (11.2 ± 3°) compared to female individuals (15.8° ± 4.5°). Similarly, Raveendranath *et al.* (2009) and Shantanu *et al.* (2023) measured and assessed the Q angles of individuals of Indian ancestry, equally distributed by sex, to determine if there are significant sex differences between male and female Q angles. Like Horton and Hall (1989), Raveendranath *et al.* (2009), and Shantanu *et al.* (2023) also reported significant sex differences in Q angles, with the mean values higher in females ($14.48^0 \pm 2.02^0$ and $13.68^0 \pm 1.87^0$, respectively) compared to males ($10.98^0 \pm 1.75^0$ and $11.14^0 \pm 1.9^0$, respectively). These findings agree that the Q angle is sex-specific and contributes to efficient locomotion, since it influences knee joint biomechanics, lower limb alignment, and weight distribution, and it enables proper patellar tracking within the femoral groove which is essential for smooth movement during activities like walking, running, and jumping (Shantanu *et al.,* 2023; Gant *et al.,* 2024).

While extensive research exists on skeletal sex estimation using traditional morphological traits and in combination with various methodological approaches (metric and morphometric methods), the application of modern medical imaging modalities, particularly Lodox® Systems, remains underexplored for morphological sex estimation. This is a significant gap, considering the advantages of Lodox® Systems imaging in visualising skeletal tissue in addition to its widespread global availability in forensic pathology centres for assistance in postmortem examinations, human identification, and skeletal trauma and pathology assessments (Viner, 2018; du Plessis *et al.,* 2020; Reid *et al.,* 2020; Venketsamy, 2022; LODOX®, 2024; Morele *et al.,* 2024). Moreover, given the

high sex estimation accuracy of the aforementioned skull and postcranial traits, further investigation into the ability to visualize these traits on x-ray radiographs for morphological sex estimation is warranted. Such investigations should prioritize the use of Lodox® Systems x-ray modalities (e.g., Lodox® Statscan™ and Lodox® eXero-dr™), given their widespread installation in South African FPS facilities (Evangelopoulos *et al.,* 2009; du Plessis *et al.,* 2020; Reid *et al.,* 2020; LODOX®, 2024; Morele *et al.,* 2024).

2.3. Modern Medical Imaging Modalities in Forensic Anthropological Sex Estimation

Forensic radiology involves obtaining, interpreting, and reporting of radiological images for medico-legal investigations, which may include cases presented in a courtroom (Elifritz *et al.,* 2014). Majority of imaging modalities used in clinical medicine are generally applicable to medico-legal investigation cases as well, including traditional radiography (x-rays), ultrasound, CT and MRI scanners (Elifritz *et al.,* 2014; Garvin & Stock, 2016; Viner, 2018; Mamabolo *et al.,* 2020). However, traditional radiography is the oldest and remains the most commonly utilised imaging modality (Elifritz *et al.,* 2014; Viner, 2018); although postmortem CT and postmortem MRI are increasingly being used in forensic practices, including in forensic anthropological analyses (Elifritz *et al.,* 2014; Garvin & Stock, 2016; Viner, 2018; Brits *et al.,* 2018; Zhang, 2022). Radiological images allow for non-invasive assessment of human remains, in-situ with soft tissue intact, through virtual reconstruction and digital evaluation of the scanned remains, providing detailed information that can be utilised in medico-legal investigations (Elifritz *et al.,* 2014; Garvin & Stock, 2016; Viner, 2018; Mamabolo *et al.,* 2020). This allows for anatomically detailed descriptions of human remains, regardless of the preservation state of the soft tissues, including anatomical descriptions that can potentially facilitate the assessment of the biological profile, pathology, and trauma (Garvin & Stock, 2016; Teodoru-Raghina *et al.,* 2017; Varzandeh *et al*., 2019; Zhang, 2022). Radiographs present certain challenges, primarily due to their limited 2D view (Garvin & Stock, 2016; Mamabolo *et al.*, 2020). This limitation results in the distortion, overlap and superimposition of bony features, which can obscure or underestimate the true extent and 3D morphology of bony features (Williams *et al.,* 2007; Stull *et al.,* 2013b; DeMaio *et al.,* 2019; Biehler-Gomez et al., 2019; Mays, 2022). Nevertheless, radiographs remain essential for visualising detailed internal anatomical features in a non-invasive manner, providing information critical to understanding the limitations of direct dry-bone analyses (Mamabolo *et al.,* 2020; Garnett & Lewis, 2022; Mays, 2022).

Regarding x-ray radiographs, particularly Lodox® Systems radiographs, there is limited research in the literature about the utilisation thereof for biological sex estimation, particularly from

morphological traits, as compared to CT modalities. The available literature is mostly populated by studies that have quantitatively (i.e., metric & morphometric) assessed the application of Lodox® Systems and three-dimensional (3D) CT scans for sex estimation in distinct population groups, particularly on the cranium (e.g., Mehta *et al.,* 2015; Teodoru-Raghina *et al.,* 2017; Bertsatos *et al.,* 2020; Gillet *et al.,* 2020; Meral *et al.,* 2022), scapula (e.g., Giurazza *et al.,* 2013), pelvis (e.g., Decker *et al.,* 2011; Franklin *et al.,* 2014; Abdallah *et al.,* 2021; Setiawati *et al.,* 2023), and upper and lower limbs (e.g., Stull, 2013b; Hishmat *et al.,* 2015;; Stull *et al.,* 2017; Maijanen *et al.,* 2021; Maijanen *et al.,* 2024).

2.3.1. Computed Tomography

Studies that have utilised 3D CT scans for morphological sex estimation have also reported similar accuracies as the standard methods used on dry bones, mainly the skull (Ramsthaler *et al.,* 2010; Dereli *et al.,* 2018; Bertsatos *et al.,* 2020; Kelley, 2022; Bareša *et al.,* 2024) and pelvic morphological traits (Ali *et al.,* 2020; Zhang, 2024). For instance, Ramsthaler and colleagues (2010) examined the validity and reliability of morphological sex estimation using volume-rendered cranial CT (CCT) scans of 50 individuals of central European descent (males: n = 31; females: n = 19), assessing 17 morphological skull traits, including Krogman and İşcan's (1962) skull traits (Table 2.1). The study reported a 96% correct sex classification accuracy, with the supraorbital ridge having the highest accuracy (combined accuracy = 85%, males = 85.5% and females = 84%), followed by the glabella morphology (combined sex = 81%, males = 82% and females = 78%).

A study by Dereli *et al.* (2018) also demonstrated the applicability of 3D modeling of volumetric CCT scans for morphological sex estimation (males: n = 49; females: n = 36) based on the five morphological skull traits and the five-point ordinal scale by Buikstra and Ubelaker (1994) and Walker (2008). Over 98% and 83% correct sex classification accuracies for males and females were reported, respectively, with the glabella being the most effective morphological trait for sex estimation. Ali and colleagues (2020) examined sexual dimorphism of the subpubic angle from reconstructed 3D multidetector CT scans of 50 males and 50 females from a contemporary Malaysian population. The overall sex classification accuracy for the subpubic angle was 94%, with the angle being significantly wider (i.e., obtuse) in females (87.4° ± 6.5°) than in males (i.e., sharp) (68.6° ± 7.6°). The available literature shows the feasibility of conducting morphological sex estimation from radiographs, particularly 3D CT scans, achieving nearly similar accuracy rates as dry bone analyses. Specifically, sex estimation for the skull (Kelley, 2022; Bareša *et al.,* 2024) and pelvis (Ali *et al.,* 2020; Zhang, 2024) typically ranges from 80% to 95% accuracy. While 3D CT scans offer a promising avenue for sex estimation, further research is needed to explore the

potential of x-ray radiographs for morphological skeletal sex estimation, considering that x-ray modalities are less expensive, easier to operate, can produce radiographs in quick successions, and are readily accessible in medico-legal facilities, particularly in developing countries (Garvin & Stock, 2016; Mamabolo *et al.,* 2020; Zhang, 2022; LODOX®, 2024).

2.3.2. X-ray radiography

In conventional radiography, x-rays pass through an individual (e.g., patient) and are recorded on a film or digital plate (i.e., receiver), thus generating an x-ray radiograph (Thrall, 2012; Rowbotham & Blau, 2020). Areas of black on the image represent radiolucent regions whereby many x-rays passed through the individual and reached the receiver, while areas of white represent radiopaque regions whereby the individual absorbed or blocked many x-ray beams. Various shades of grey between these extremes exist due to differences in tissue composition which is influenced by the effective atomic number, physical density and the degree of x-ray beam penetration and absorption by body tissues (e.g., bone, fat, and soft tissues like muscles and organs) (Thrall, 2012; Rowbotham & Blau, 2020). Bone tissue is comprised mostly of calcium and phosphorus, which consist of high atomic masses; thus, bone tissue is relatively dense compared to soft tissues and therefore highly radiopaque (Thrall, 2012; Rowbotham & Blau, 2020). As such, highly dense bony elements and regions are characterized by bright white or different shades of white colour (i.e., indicate higher mineral content and radiopaque) whereas less dense bone regions including soft tissues will appear as different shades of grey (Berger, 2002; Thrall, 2012; Mamabolo *et al.,* 2020; Rowbotham & Blau, 2020).

The existing literature on forensic anthropology demonstrates the broad utility of x-ray radiographs in estimating other parameters of the biological profile, such as stature (Macaluso Jr. & Lucena, 2014b; Pomeroy *et al.,* 2018; Venketsamy, 2022) and age-at-death estimations (Carneiro *et al.,* 2013; Stull, 2013b; Lakha, 2015; Poongodi *et al.,* 2015; Stull & Armelli*,* 2020) in addition to metric and morphometric skeletal sex estimation (Poongodi *et al.,* 2015; González-Colmenares *et al.,* 2019; Varzandeh *et al.,* 2019; Maijanen *et al.,* 2021). Maijanen and colleagues (2021) investigated sex estimation based on knee breadth dimensions from Lodox® Statscan™ radiographs of 1645 individuals from the Northern Finland Birth Cohort of 1966 (males: n = 759; females: n = 895). Combined sex classification accuracies ranging from 90.1% (femoral bi-epicondylar breadth) to 93% (tibial plateau lateromedial breadth) based on a knee dimension logistic regression model were achieved. Although relatively high classification accuracies were achieved from the assessment of x-ray radiographs, the study design was based on osteometric measurements and logistic regressions, and more research based on morphological assessments is needed. Furthermore, Abdallah and colleagues (2021) investigated sex estimation accuracies of

morphometric measurements of five pelvic parameters from anteroposterior pelvic x-ray scans (i.e., ilium height, inter-acetabular distance, acetabulum diameter, pelvic breadth, and pelvic inlet breadth) (males: n = 78; females: n = 78). The study reported significant sex differences in some of the assessed parameters, however, unlike CT scan-based studies, relatively low sex classification accuracies were reported, with a maximum of 68% sex classification accuracy (i.e., ilium height). The relatively low classification accuracies can likely be attributed to the limitations of 2D x-ray radiographs in visualising overlapping or morphologically complex skeletal structures, which often hinders the accurate assessment of morphological features (Dorion, 1983; Stull *et al.,* 2013a). In contrast, 3D CT scans offer greater precision and are better suited for analyzing intricate anatomical structures (Saitou *et al.,* 2011; Stull *et al.,* 2014; Braun *et al.,* 2022), thus can achieve classification accuracies similar to those achieved by dry bone analysis methods. Nevertheless, studies such as these highlight the potential applicability of x-ray radiographs for biological profile estimation including skeletal sex estimations, even though they are primarily limited to metric sex estimation approaches.

While x-ray radiographs offer a potential avenue for metric sex estimation, current research and applications on morphological sex estimation is primarily limited to a set of features, including rib costal cartilage ossification patterns (detailed in 2.2.3. Rib costal cartilage morphology section), the olecranon-coronoid angle, femoral NSA, and Q angle (discussed in 2.2.6. Other postcranial morphological traits of interest section) (McCormick *et al.,* 1985; Purkait, 2001; Rejtarová *et al.,* 2004; Raveendranath *et al.,* 2011; Airan & Dwivedi, 2018; Khasawneh *et al.,* 2019; Fischer *et al.,* 2020; Rogers *et al.,* 2021; Patyal & Bhatia, 2022). For example, Patyal and Bhatia (2022) investigated costal cartilage ossification patterns for sex estimation from 450 posterior-anterior x-ray radiographs of North Indians, reporting a 99% classification accuracy for males (peripheral ossification patterns) and 100% classification accuracy for females, who exhibited a central-type, globular ossification pattern. Moreover, Rogers and colleagues (2021) have investigated sex differences of the femoral NSA from anteroposterior adult pelvic x-ray radiographs and reported it to be significantly wider in females (88% accuracy) and narrower in males (86.8% accuracy). Unfortunately, this approach neglects the most sexually dimorphic skeletal traits, such as Walker's (2008) cranial traits and Klales's *et al.* (2012) pelvic traits, hindering the full potential of x-ray radiographs for morphological sex estimation. Therefore, further exploration of various x-ray modalities is necessary to effectively visualize the most sexually dimorphic skeletal traits from radiographs, with consideration for their potential use in sex estimation.

Despite the high morphological sex classification accuracy achievable with CT scans, their application in South African forensic anthropology is hindered by their limited availability in

medico-legal forensic pathology facilities. In contrast, x-ray modalities, particularly Lodox® Systems (e.g., Lodox® Statscan™ and Lodox® eXero-dr™), are commonly found in South African medico-legal FPS facilities for usage as a screening imaging tool in unnatural death cases, prior to the conduct of postmortem examinations (Quarrie, 2015; Grabherr *et al.,* 2017; du Plessis *et al.,* 2020; Reid *et al.,* 2020; Morele *et al.,* 2024; LODOX®, 2024). However, the utilisation of Lodox® Systems modalities for forensic anthropological analyses have mainly been limited to the estimation of age-at-death (Stull, 2013b; Lakha, 2015; Stull & Armelli*,* 2020), stature (Venketsamy, 2022), and subadult metric sex estimation (Stull, 2013b; Stull *et al.,* 2017).

Stull and colleagues (2017) investigated the potential of long bone diaphyseal dimensions (humerus, radius, ulna, femur, and tibia) for sex estimation in subadults (birth-12 years) using Lodox® Statscan™ radiographs of modern South African children. Using logistic regression, FDA, and Linear Discriminant Analysis (LDA), they found single-bone classification accuracies ranging from 57% (ulna, LDA) to 75% (femur, FDA), per logistic regression model. However, when combining bone measurements, bootstrap accuracies for each model ranged from 75% (LDA) to 93% (FDA) combined sex classification accuracies. Therefore, considering the prevalence of Lodox® Statscan™ modalities in South African FPS facilities and the proven accuracy of using Lodox scans for metric skeletal sex estimation, further investigation into the potential of Lodox® Statscan™ radiographs for morphological sex estimation within a South African population is warranted.

2.4. The Lodox® Systems in South Africa

Due to the overlapping nature of internal body structures such as skeletal elements, organs, and various soft tissues, x-ray projection of these structures compresses them onto a single plane, thus creating a 2D image with superimposed, overlapping elements/structures (Dorion, 1983). Additionally, x-ray images are prone to distortion, leading to misrepresentations of internal body structure size and shape. These distortions are largely caused by errors in x-ray beam angulation, patient positioning, and image receptor placement, all of which impact the object-to-image receptor distance (OID) and source-to-image receptor distance (SID) (Stull *et al.,* 2013a; Nakashima & Duong, 2020). Minimising these distortion factors is crucial for producing interpretable x-ray images and therefore the Lodox® Systems was designed to primarily visualize radiopaque materials with minimal distortion, including minimal 2D superimposition of anatomical structures (Beningfield *et al.* 2003; Knobel *et al.,* 2006; Stull, 2013b). Lodox® Systems does this by using a collimated fan beam geometry that increases the SID and reduce the OID.

In contrast, traditional conventional x-ray modalities use a cone-beam geometry which produces distortion in both the slot direction (x-axis) and scan-axis (y-axis) (Stull *et al.,* 2013b). The Lodox®

Systems, however, significantly minimises distortion along the y-axis by utilising a collimated fan beam geometry (Beningfield *et al.,* 1999; Stull *et al.,* 2013b). This fan beam is directed vertically through the patient onto a detector array, while the scanning arm, with the x-ray tube and detector mounted on opposite ends of a C-arm, traverses the full length of the patient (Beningfield *et al.,* 1999). This unique design minimises distortion while simultaneously producing a full-body, direct digital image in 10 to 13 seconds (Beningfield *et al.*, 1999; Knobel *et al.*, 2006; Stull *et al.*, 2013b).

Due to its design, the Lodox® System's ability to minimize distortion along the scan axis allows for a more accurate representation of the scanned object's original dimensions, compared to conventional x-ray modalities. Several studies have evaluated the system's performance for trauma imaging. For instance, Beningfield *et al*. (1999, 2003) and Chen *et al.* (2010) found that Lodox® Systems modalities, such as the Lodox® Scannex and Lodox® Statscan™, are diagnostically equivalent to conventional radiographs. These studies highlighted several key benefits, including a significantly lower radiation dose (3% to 5% lower than conventional x-rays), faster image succession (10 to 13 seconds), and improved workflow, all at a reduced financial cost (Beningfield *et al*., 1999, 2003; Chen *et al.,* 2010). Because of these advantages, the Lodox® System was recommended as a viable alternative to traditional conventional x-ray for evaluating acute trauma patients.

Subsequently, Lodox® Systems, especially the Lodox® Statscan™, have been widely adopted in South African medico-legal facilities, particularly those with high caseloads and limited resources, including a shortage of staff and limited access to advanced postmortem radiographic equipment (Boffard *et al.,* 2006; Knobel *et al.,* 2006; Deyle *et al.,* 2010; Dempers *et al.,* 2018; du Plessis *et al.,* 2020; LODOX®, 2023a). The Lodox® Statscan™ is primarily used to assist in the postmortem examination of unnatural death cases including the identification of unknown human remains (Bernitz & Verster, 2017; du Plessis *et al.,* 2020; Reid *et al.,* 2020; Morele *et al.,* 2024). The advantages thereof, are that it can obtain image results similar to those of traditional radiographic modalities (e.g., mammography and sonography) but in a much safer environment for the staff/operator (Chen *et al.,* 2010; Boffard *et al.,* 2006), while providing minimally distorted full body 2D images in rapid succession (Amirlak *et al.,* 2009, Stull *et al.,* 2013a; Bernitz & Verster, 2017; Mamabolo *et al.,* 2020). Although the image quality of the Lodox® Statscan™ is relatively poor than that of CT scans and MRI images, the image quality is sufficient enough to visualize both skeletal and soft tissues in anteroposterior, lateral or oblique plane of views, without the need to re-adjust the body or stitch subsequent images (Beningfield *et al*., 2003; Boffard *et al.,* 2006; Amirlak *et al.,* 2009; Bernitz & Verster, 2017; Mamabolo *et al.,* 2020). Moreover, the produced radiographs can be visually enhanced and manipulated by zooming in and out, and by adjusting

the contrast to allow for better assessment of skeletal traits from a specific area of interest (Stull *et al.,* 2013b; Mamabolo *et al.,* 2020). Lodox scans can thus be used for the visualisation of skeletal tissue and the potential estimation of biological profile parameters of human remains, and unidentified decedents admitted to FPS facilities.

Forensic anthropologists in South Africa are mostly employed by tertiary institutions, primarily as academics rather than as law enforcement officers (Obertová *et al.*, 2016). Therefore, utilising Lodox scans for biological profile estimations can reduce the need to transfer skeletal remains to tertiary institutions forensic laboratories for anthropological assessment, potentially avoiding processes like human maceration, and instead allowing for a preliminary assessment of biological profile parameters (e.g., sex estimation) from x-ray radiographs. However, it is currently unknown if the traditional macroscopic, morphological skull and postcranial skeletal elements and traits outlined in the literature (Tables 2.1 and 2.2) can be visualised and/or observed, and accurately and repeatedly assessed for skeletal sex estimation from the produced Lodox® Statscan™ images. Additionally, the sex classification accuracies of South African-based morphological sex estimation methods are yet to be tested and validated for application on Lodox® Systems modalities, including Lodox® Statscan™. Therefore, this study focused on assessing the feasibility of skeletal sex estimation from adult Lodox® Statscan™ images based on the commonly assessed sexually dimorphic traits of the human skull, pelvis, and various postcranial bones.

2.5. Study Aim and Objectives

The aim of the current study was to investigate the observability, repeatability, and validity of macroscopic morphological skull and postcranial skeletal elements and skeletal traits for sex estimation from Lodox® Statscan™ radiographs of adult individuals of European descent.

The study objectives were to:

1. determine which skeletal elements (i.e., cranium, mandible, clavicle, scapula, rib costal cartilage, humerus, ulna, pelvic girdle, sacrum and femur) are observable on Lodox scans.
2. determine which skull and postcranial sexually dimorphic traits are observable and scorable from Lodox scans.
3. assess the intra- and inter-observer repeatability of the observable skeletal elements and associated sexually dimorphic skeletal traits from Lodox scans.
4. estimate the skeletal sex of the scorable sexually dimorphic traits of the skull and postcranial skeletal elements from Lodox scans.
5. assess the sex classification accuracies of the scorable sexually dimorphic traits for the estimation of morphological skeletal sex from Lodox scans.

CHAPTER 3: METHODS AND MATERIALS

The present study involved an exploratory, observational assessment of sexually dimorphic skull and postcranial traits from Lodox® Statscan™ images (hereon referred to as Lodox scans) of individuals of European ancestry. This chapter outlines the study sample used, the sources of data, and associated ethical considerations. The skeletal element and associated traits assessed, the methodology for their assessment from the Lodox scans, and the statistical analyses performed, including reliability, descriptive, and classification statistics are also included in this chapter.

3.1. Study Sample

3.1.1. Ethical clearance

This study was conducted under an ethical clearance waiver number W-CBP-220504-01 (Appendix 1) approved by the Cadaveric Collection Committee of the Department of Anatomical Sciences, School of Biomedical Sciences at the University of the Witwatersrand, Johannesburg, South Africa.

3.1.2. Inclusion and exclusion criteria

Lodox® Statscan™ offers an excellent resolution for visualising the human skeleton (Mamabolo *et al.,* 2020). As such, all available Lodox scans of cadavers from European ancestry with documented individual sex were assessed. However, skull and postcranial skeletal elements whereby the regions of interest were compromised by antemortem trauma/pathology, or any foreign object that might obscure visual assessment of a skeletal trait were excluded from the study per Lodox scan.

3.1.3. Study sample

A total of 152 full-body Lodox scans were assessed of which 150 met the inclusion criteria (listed below). The Lodox scans were all of adult individuals of European ancestry, comprising 72 males and 78 females. However, only 120 scans had known age-at-deaths and had an average age-at-death range of 39 to 101 years and an average age-at-death of 76 ± 12.94 years (Table 3.1). These 121 scans comprised 56 males and 65 females, with an average at-death of 75 ± 12.2 years for males and 78 ± 13.6 years for females (Table 3.1). These individuals succumbed to natural causes and donated their bodies to the Department of Anatomical Sciences, School of Biomedical Sciences, University of Witwatersrand, Johannesburg, to teach students and further scientific research (Brits *et al.,* 2020; Hutchinson *et al.*, 2020). The demographics of the current body donors in the Department of Anatomical Sciences is comprised mainly of individuals of European ancestry (Brits *et al.*, 2020), thus the study included all Lodox scans of individuals of European ancestry with varying nationalities including South African (n = 127), German (n = 3), British (n

= 2), Australian (n = 1), Dutch (n = 1), Lesothan (n = 1), Namibian (n = 1), Nigerian (n = 1), Swiss (n = 1), Tanzanian (n = 1), Zimbabwean (n = 1), and unknown nationalities (n = 12). All Lodox scans with documented/known sex were included for statistical analysis (n = 150 scans).

Table 3.1: Age distributions (in years) for Lodox scans of male and female individuals with documented ages-at-death.

	Known Age-at-deaths						Unknown Age-at-deaths	Total study
Sex	**Sample size**	**Minimum age**	**Maximum age**	**Mode**	**Mean**	**SD***	**Sample size**	**Sample size**
Male	56	39	94	79	75	12.20	16	72
Female	65	47	101	84	78	13.56	13	78
Total	121	39	101	84	76.5	12.94	29	150

*SD= Standard Deviation

The scans were anonymised before data collection commenced to protect the identity of the body donors; thus, the only utilised demographic information included in the study was their documented sex, age-at-death, and nationality. The documented sexes of the scans were unknown to observers and were only available to the principal investigator during the process of data analyses after all Lodox scans were assessed. The associated anatomical tissues visible on each scan included skeletal tissue and various soft tissues such as muscle tissue and external reproductive organs, as represented in various degrees of tissue density in shades of grey (Figure 3.1). The visibility of external reproductive organs potentially introduced biased into the study and assessment of skeletal traits of interest. However, it was minimised by assessing traits based on their respective established criteria for morphological assessment and visibility on assessed Lodox scans.

3.1.4. Lodox® Statscan™ scans

The Lodox® Statscan™ images used during this study were previously collected for research in the Department of Anatomical Sciences, School of Biomedical Sciences, University of the Witwatersrand, Johannesburg. All Lodox scans were taken in an anteroposterior plane of view with 110 kV, 160 mA, 2.08 Spatial Resolution (1-5p/mm), and 14 bits of contrast resolution at the Johannesburg FPS Medico-Legal Laboratory once the bodies had been embalmed. The scanning procedure involved placing individuals in a supine position on the Lodox® Statscan™ body table, in a standardised positioning of the head and all limbs into the anatomical position. However, the standard anatomical body position was not always achievable due to distinct challenges in positioning individuals due to stiffness resulting from formalin embalming.

3.2. Study Method

3.2.1. Lodox scan analysis

All the available Lodox scans were evaluated at the Department of Anatomical Sciences, University of the Witwatersrand, using DVS version 3.0, Digital X-Ray Diagnostic Viewer with Lucid™ image processing software (©Lodox™ 2005 Application Version 2.9.0.0) by the principal investigator.

3.2.2. Skeletal elements observations

The following skeletal elements: cranium, mandible, clavicle, scapula, costal cartilages, distal humerus, proximal ulna, pelvis, sacrum, and femur, were assessed to first ensure that they were observable for skeletal sex estimation on the 2-Dimensional (2D) Lodox x-ray scans (Figure 3.1). These skeletal elements were assessed per Lodox scan since each scan was associated with distinct potential limitations that could impede the visualisation of a specific element and morphological trait of interest. Therefore, each skeletal element was classified as either observable or unobservable per Lodox scan. An observable skeletal element (and trait) on an x-ray scan appears as a solid, dense, and radiopaque area, typically varying in shades of white against the darker greys of surrounding soft tissues (Figure 3.1) (Thrall, 2012). This appearance is due to the bone's higher density, which attenuates (absorbs and scatters) the x-rays more than other tissues (Berger, 2002; Thrall, 2012). Moreover, the description is based on principles of radiographic imaging, where denser materials block more x-rays, resulting in brighter areas on the x-ray scan, and subsequently resulting in brighter skeletal tissue compared to surrounding soft tissues (Berger, 2002; Thrall, 2012; Rowbotham & Blau, 2020). Observation also relied on knowledge of human osteology and the descriptions of human osteology by White *et al.* (2011) and Christensen *et al* (2014d), which provides details about the typical size, shape, and location of bones within the body, allowing for identification of specific skeletal elements (e.g., cranium, femur, rib, vertebra) based on their visual characteristics within the x-ray radiograph. In a standard anteroposterior x-ray scan, the anterior aspect of skeletal elements is most visible to the observer, however, in some scans, such as those with a tilted head, arm or hip, the lateral aspects of associated skeletal elements may also be observable (Figure 3.1). Subsequently, skeletal elements (or traits) that could not be visualised from Lodox scans, based on the above-mentioned descriptions were thus considered unobservable.

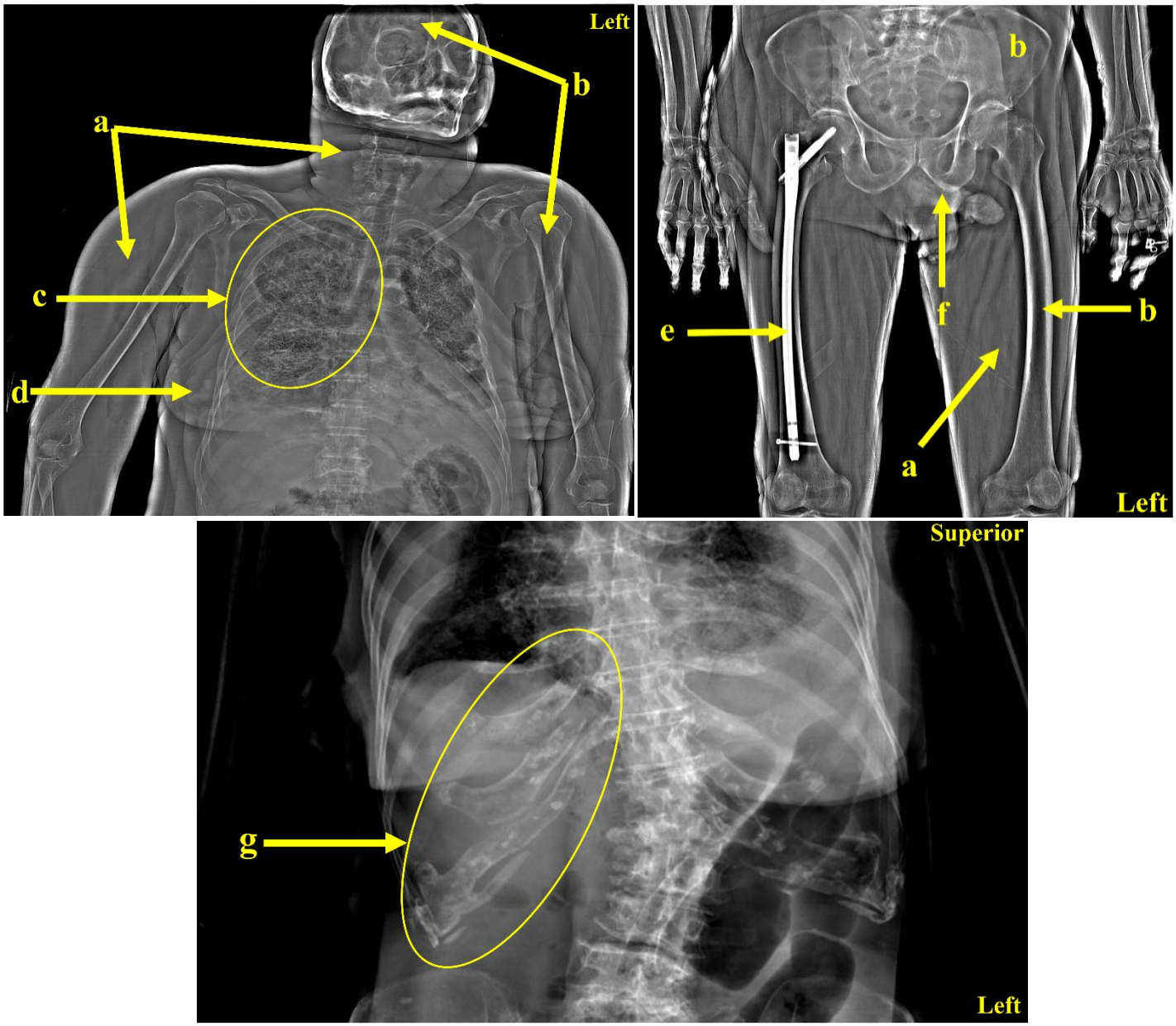


Figure 3.1: Examples of skeletal tissue and associated soft tissues visible from Lodox scans. Also evident is a tilted head on the top left scan. a = muscle tissue; b = bone; c = lung; d = breasts; e = internal prosthesis; f = male external reproductive organ; g = rib costal cartilages.

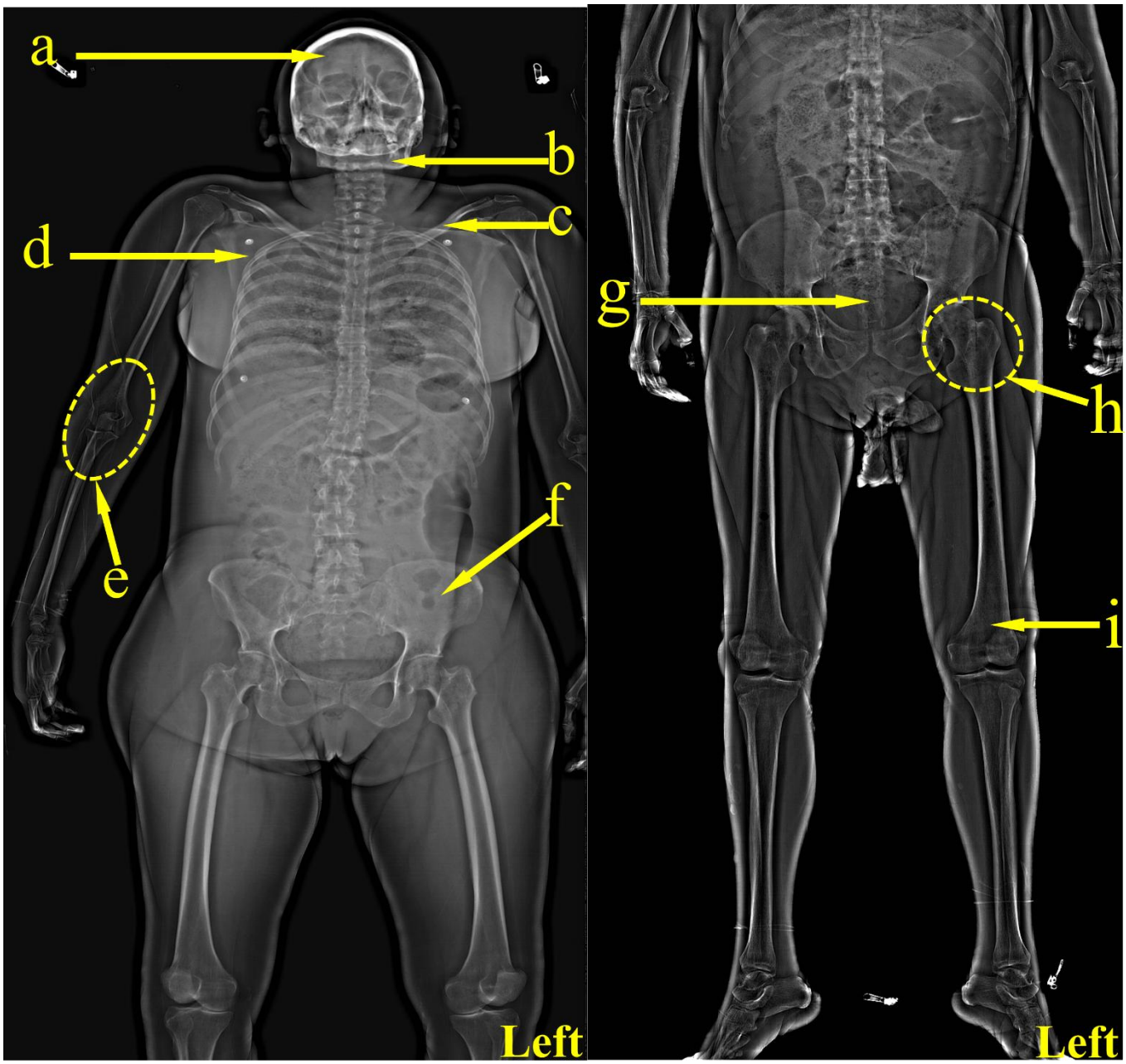


Figure 3.2: Skeletal elements assessed in the current study. a = cranium; b = mandible; c = clavicle; d = scapula; e = distal humerus and proximal ulna; f = pelvic girdle; g = sacrum; h = proximal femur; i = distal femur. See Figure 3.1 for the lower ribs' costal cartilages.

3.2.3. Skeletal traits assessed

Thirty-two macroscopic, morphological traits of the skull and postcranial elements, including the clavicle, scapula, costal cartilages, humerus, ulna, pelvis, and femur, that could potentially be assessed for adult skeletal sex estimation from Lodox scans were compiled from the available skeletal sex estimation literature (Tables 3.2, 3.3, and 3.4). These selected skeletal traits are associated with significant sex classification accuracies, with some being tested and validated for use on South African samples and therefore invaluable for the current study. As a standard procedure, these skeletal traits were observed from anterior-posterior views of the Lodox scans, and assessment was made on the left side only, using the respective dry bone morphological observation methods. In cases when the left skeletal element or trait was not observable, the trait was excluded (Langley *et al.,* 2016). Skeletal traits of observable skeletal elements were further assessed and scored for skeletal sex estimation (per Lodox scans), based on their respective sex estimation methods, trait description, and scoring procedures (Tables 3.3 and 3.4).

3.2.4. Skeletal trait scoring procedures

Sexually dimorphic traits of the observable skeletal elements (per Lodox scan) were evaluated to determine if they were scorable for morphological sex estimation. Skeletal traits deemed scorable were assessed qualitatively using their respective morphological scoring procedures detailed in Tables 3.3 and 3.4. Skeletal traits with ordinal sex characteristics were assessed and scored on a five-point ordinal scale (1 = female; 2 = probable female; 3 = ambiguous; 4 = probable male; 5 = male) based on their respective ordinal scoring trait descriptions for male and female characteristics (e.g., greater sciatic notch; 1 = wide, 2 =relatively wide, 3 = ambiguous, 4 = relatively narrow, and 5 = narrow) (Tables 3.3 and 3.4). Skeletal traits with nominal sex characteristics (e.g., pelvic brim shape; either round or heart-shaped) were scored on a two-point nominal scale (1 = female and 5 = male) based on their respective nominal scoring trait descriptions for male and female characteristics (Tables 3.3 and 3.4).

In this study, “female” and “male” represent the most certain scores for sex classification and are aligned with the terms suggested by the Standards for Sex Estimation in Forensic Anthropology (American Academy of Forensic Sciences Standards Board, 2019). In contrast, “ambiguous” represents a score for skeletal traits that possess morphological characteristics that are intermediate between male and female characteristics (American Academy of Forensic Sciences Standards Board, 2019). The “probable female” and “probable male” scores indicate a higher likelihood of one sex over the other, but without complete confidence, however, they were classified under female and male categories, respectively. Traits scored as 1 or 2 and 4 or 5 were classified into female and male categories, respectively. Skeletal traits scored as 3 were categorized as ambiguous

as they were open to multiple potential interpretations and therefore could not be classified into a specific sex category. Thereafter, the classified sex of a particular skeletal trait was compared to the respective individual's documented sex to determine the male and female correct sex classification accuracies of each skeletal trait. The overall combined male and female correct sex classification accuracy of a particular trait was also determined and reported as "combined sex classification accuracy". The accuracies of incorrectly classified sexes for each assessed skeletal traits were also determined, however, they were excluded from 'combined sex classification accuracies' as their inclusion would artificially overestimate the sex classification accuracy of a trait (Inskip *et al.,* 2019).

Table 3.2: Image illustrations of skeletal traits assessed for morphological sex estimation from Lodox scans.

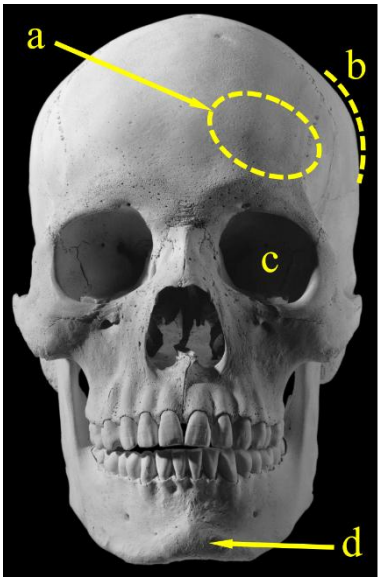
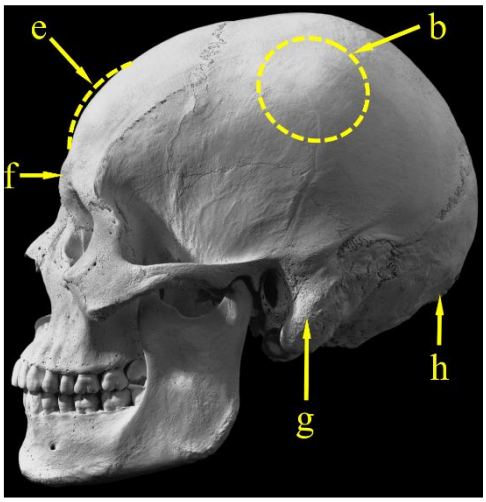
Skeletal elements	**Image illustrations of assessed skeletal traits**	**Key**
Skull	A  B 	a: Frontal eminence b: Parietal eminence c: Orbit d: Mental eminence e: Frontal slope f: Glabella g: Mastoid process h: Nuchal crest
Clavicle	C 	a: Costoclavicular tuberosity

Table 3.2: Continued…

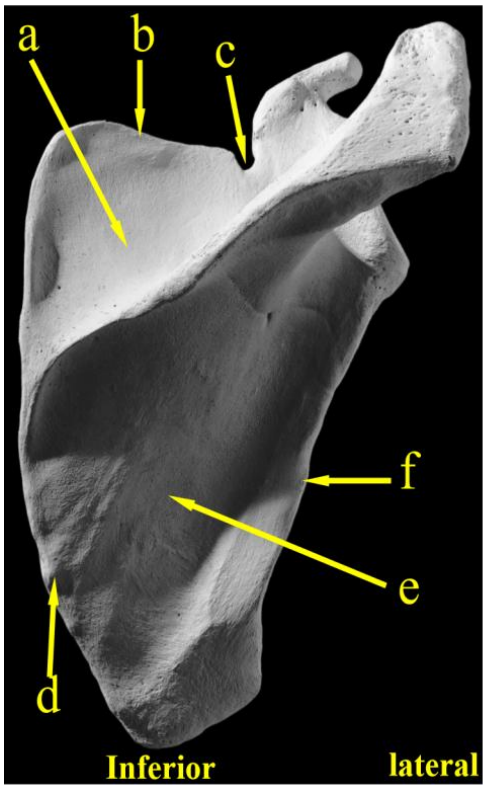
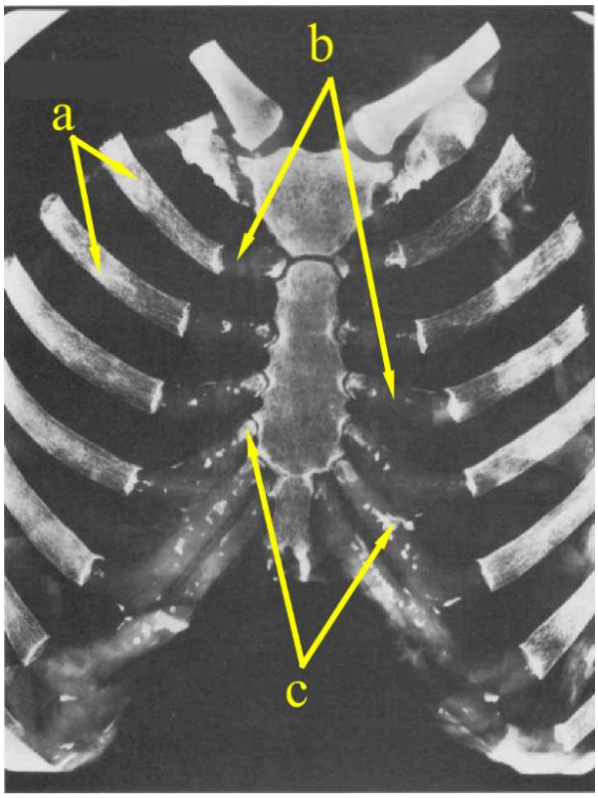
Skeletal elements	Image illustrations of assessed skeletal traits*	Key
Posterior scapula	D 	a: Supraspinous fossa b: Superior border c: Suprascapula notch d: Medial border e: Infraspinous fossa f: Lateral border
Rib costal cartilages	E* 	a: Rib b: Costal cartilage c: Ossification nodules

Table 3.2: Continued…

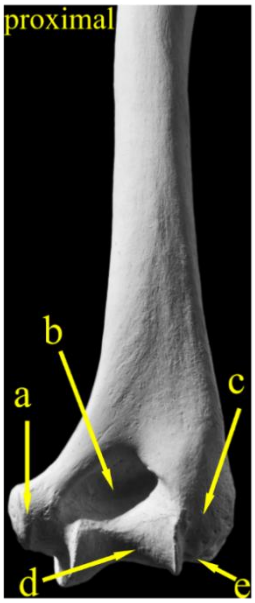
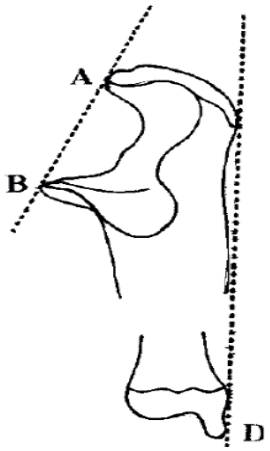
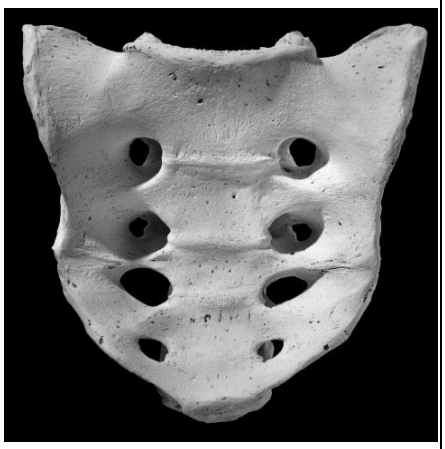
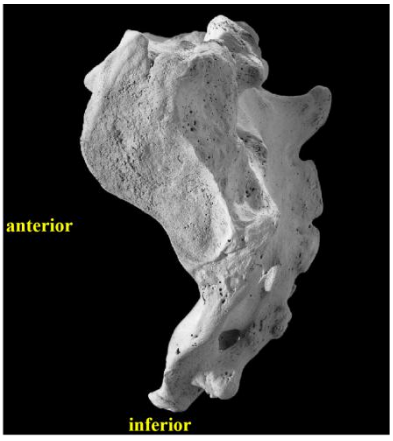
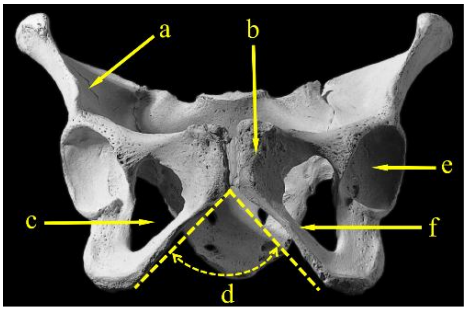
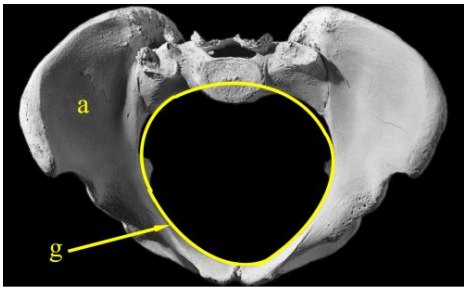
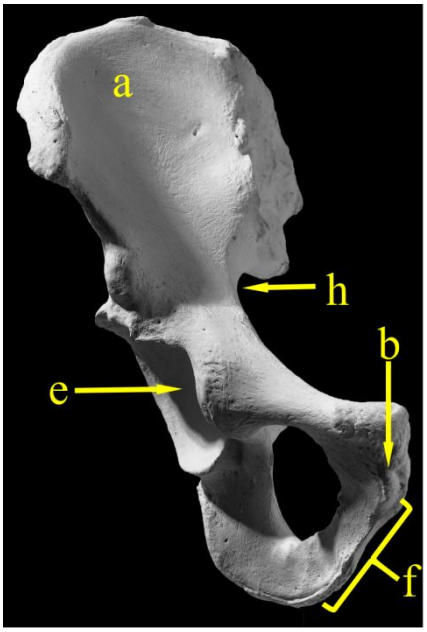
Skeletal elements	Image illustrations of assessed skeletal traits*		Key
Posterior distal humerus	F 		a: Medial epicondyle b: Olecranon fossa c: Lateral epicondyle d: Trochlea e: Posterior margin of capitulum
Proximal ulna	G 	H* 	a: Olecranon process b: Coronoid process d: Styloid process
Sacrum	I 	J 	

Table 3.2: Continued…

Skeletal elements	Image illustrations of assessed skeletal traits*		Key
Pelvis	K  L*  	M*  	a: Ilium b: Pubic bone body c: Obturator foramen d: Subpubic shape e: Acetabulum f: Ischiopubic ramus g: Pelvic brim h: Greater sciatic notch
Femur	N* 	O*  	ASIS: Anterior Superior Iliac Spine Q: Quadriceps Angle CP: Centre of Patella TT: Tibial Tuberosity

*: Images obtained from the Human Osteology Third Edition textbook by White *et al.* (2012) with the exceptions of images E, H, N, and O.
E*: An example of ossification of the costal cartilages in a woman. Image obtained from McCormick *et al.* (1985)
H*: Image illustration obtained from Purkait (2001).
L*: Pelvis viewed from a superior aspect.
M*: Right os coxae viewed from an anterior aspect.
N*: Image illustration for the measurement of the femoral neck shaft angle by Rogers (2021).
O*: Measurement of the quadriceps angle. Image illustration obtained from Raveendranath *et al.* (2009).

Table 3.3: Sexually dimorphic traits of the skull and associated assessment scores used in the present study.

Skeletal Traits	Description	Scoring	References of Estimation Method
Overall skull morphology	The relative, general size of the skull.	0 No assessment 1 Small 5 Large	Gupta *et al.*, 2022
Mastoid process	The morphology of the pyramidal-like bony projection at the base of the mastoid area, posterior to the external acoustic meatus (EAM) of each temporal bone.	0 No assessment 1 Very small with low volume. Short and narrow. Little projection of the mastoid process below the inferior EAM border. Digastric groove is usually visible. 2 Small. Short and/or narrow. Low volume. Slight projection of the mastoid process below the EAM border. Digastric groove is usually visible. 3 Medium volume. Projection of the mastoid process well below the inferior EAM border or longer than it is wide. Digastric groove may or may not be visible. 4 Large volume. Usually long and wide relative to the surrounding structures. Projection of the mastoid process below the inferior EAM border. Much wider or longer than the length/width of the EAM. 5 Very large. Very long and wide relative to the surrounding structures. Largest volume. Pronounced projection of the mastoid process below the inferior EAM border.	Walker, 2008; Krüger *et al.,* 2015; Klales & Cole, 2018

Table 3.3: Continued…

Skeletal Traits	Description	Scoring	References of Estimation Method
Nuchal crest (external occipital protuberance (EOP))	The morphology of a crest that lies on the ectocranial midline of the occipital area, where the occipital and nuchal planes meet for the attachment of the nuchal and trapezius muscles as well as the nuchal ligament.	0 No assessment. 1 Smooth. EOP is not evident. 2 Slight roughening or traces of the nuchal lines. EOP is not evident. 3 Nuchal lines and EOP are evident. EOP is rough and has a lip or edge with slight posterior projection. 4 Marked nuchal lines and EOP. EOP is pronounced with clear posterior projection but has not yet developed a pronounced hook or inferior projection. 5 Marked nuchal lines and EOP with a rough surface. EOP is very pronounced and can be hooked with marked posterior/inferior projection. A ledge or ridge to either side of the EOP may be present.	Krüger *et al.,* 2015; Klales & Cole, 2018
Frontal eminences	The relative size of the two prominent, round, anterolaterally located tubers on the external surface of the squamous part of the frontal bone.	0 No assessment. 1 Large. 5 Small.	İşcan & Steyn, 2013; Gupta *et al.,* 2022
Parietal eminences	The relative size of the rounded tubers centred on the ectocranial surface of each parietal bone	0 No assessment. 1 Large. 5 Small.	İşcan & Steyn, 2013

Table 3.3: Continued…

Skeletal Traits	Description	Scoring		References of Estimation Method
Orbit shape	The relative morphology of the bony structures of the cranium that form the eye socket.	0	No assessment.	İşcan & Steyn, 2013; Gupta *et al.,* 2022
		1	Round.	
		5	Squared.	
Forehead slope	The relative slope of the frontal bone.	0	No assessment.	İşcan & Steyn, 2013; Gupta *et al.,* 2022
		1	Round.	
		5	Steeper.	
Glabella morphology	The morphology of the most anteriorly projecting point in the mid-sagittal plane at the lower margin of the frontal bone, which lies above the nasal root and between the superciliary arches.	0	No assessment.	Walker, 2008; Krüger *et al.,* 2015; Klales & Cole, 2018
		1	Little to no anterior projection at midline or in the supraorbital region. Bone is smooth and nearly vertical.	
		2	Slight anterior projection at midline or along the supraorbital region. Bone may be slightly ridged or projecting beyond the landmark nasion.	
		3	Glabella and/or the brow ridges project anteriorly past the nasion landmark.	
		4	Glabella and the brow ridges project anteriorly past the nasion landmark and are rounded.	
		5	The region is massive and rounded (loaf-shaped) projection. Marked anterior projection past the nasion landmark.	

Table 3.3: Continued…

Skeletal Traits	Description	Scoring		References of Estimation Method
Mental eminence	The general morphology of the bony protuberance extending anterior to the mandibular alveolus, located along the midline of the mandible at the centre of the chin.	0	No assessment	Krüger *et al.,* 2015; Klales & Cole, 2018
		1	Pointed or rounded and smooth with no evidence of a projecting protuberance or tubercles.	
		2	Slightly delimited or roughened area at the protuberance with no tubercles.	
		3	Slightly or fully delimited projecting protuberance with anteriorly or inferiorly protruding tubercles that are close to the midline or mandibular symphyses.	
		4	Inverted T-shape with widely spaced anteriorly or inferiorly protruding tubercles. Mental trigon occupies a good portion of the anterior mandible.	
		5	Inverted T-shape with very widely spaced anteriorly or inferiorly protruding tubercles. Mental trigon takes up most of the anterior mandible.	

*Sex scores; 0 = No assessment: 1 = Female; 2 = Probable female; 3 = Ambiguous; 4 = Probable male; 5 = Male.

Table 3.4: Sexually dimorphic postcranial traits and associated assessment scores used in the current study.

Skeletal Traits	Description	Scoring	References of Estimation Method
Suprascapular notch	The morphology of the notch in the superior border of the scapula, medial to the base of the coracoid process.	0 No assessment. 1 Completely absent. 2 Shallow but present. 3 Well-marked, approximately a semicircle. 4 Very deep approaching a full circle. 5 A foramen.	Bainbridge & Tarazaga, 1956
Supraspinous fossa superior border	The slope of the superior border of the supraspinous fossa.	0 No assessment. 1 Convexly curved. 5 Downward slope toward the superior angle.	Scholtz *et al.,* 2010
Infraspinous fossa lateral border	The slope of the lateral border of the infraspinous fossa	0 No assessment. 1 Straight/steep lateral border. 5 Curved lateral border.	
Infraspinous fossa medial border	The slope of the medial border of the infraspinous fossa.	0 No assessment. 1 Straight/steep lateral border. 5 Curved medial border.	

Table 3.4: Continued…

Skeletal Traits	Description	Scoring	References of Estimation Method
Costoclavicular tuberosity	A tuberosity on the inferior surface of the sternal end of the clavicle. When present, it is broad with an irregular roughened surface	0 No assessment. 1 Absent. 5 Present.	Ishwarkumar, 2016
Costal cartilage ossification pattern	The typical morphology of ossification patterns of lower costal cartilages of 6^{th}-10^{th} ribs (in combination)	0 No assessment 1 Central foci of subperichondrial bands of ossification. 3 Ossification patterns are typically combinations of score 1 and 5. 5 Peripheral subperichondrial linear ossification.	McCornick *et al.*, 1985
Olecranon fossa	The shape of the largest fossa on the posterior surface of the distal humerus	0 No assessment 1 Superior half of the fossa presents as a gently curved arc. 2 Superior half of the fossa has curved walls and is mostly arc-like. 3 Superior half of the fossa is in between a triangle and an arc, with curved walls and a blunted apex. 4 The superior half of the fossa exhibits slightly curved walls and apex that resembles a rounded triangle. 5 The superior half of the fossa has roughly straight walls and a pointed apex that resembles a triangular appearance.	Vance *et al.,* 2011; Tallman & Blanton, 2020

Table 3.4: Continued…

Skeletal Traits	Description	Scoring		References of Estimation Method
Medial epicondyle angle	The angle of the posterior edge of the humerus medial epicondyle relative to the horizontal plane.	0	No assessment	Vance *et al.,* 2011; Tallman & Blanton, 2020
		1	The posterior edge of the medial epicondyle angles significantly posterior.	
		2	The posterior edge of the medial epicondyle angles slightly posterior.	
		3	The posterior edge of the medial epicondyle is parallel (i.e., in line) with other traits of the distal humerus (i.e., lateral epicondyle, posterior margin of capitulum)	
		4	The posterior edge of the medial epicondyle is slightly angulated anteriorly.	
		5	The posterior edge of the medial epicondyle is significantly angulated anteriorly.	
Trochlea constriction	The constriction of the midpoint portion of the trochlea	0	No assessment	
		1	The inferior border of trochlea is markedly constricted at midpoint (i.e., spool-shaped).	
		2	The inferior border of the trochlea is significantly constricted at midpoint.	
		3	The inferior border of the trochlea is constricted at midpoint.	
		4	The inferior border of the trochlea is slightly constricted at the midpoint.	
		5	The inferior border of the trochlea is smoothly arched and lacks midpoint constriction.	

Table 3.4: Continued…

Skeletal Traits	Description	Scoring	References of Estimation Method
Trochlea symmetry	The symmetry of the notch-shaped medial edge of the trochlea relative to the capitulum (lateral).	0 No assessment 1 The trochlea is mostly on, the same distal plane as the capitulum. 2 The trochlea extends slightly inferior to the capitulum. 3 The trochlea extends moderately inferior to the capitulum. 4 The trochlea extends significantly inferior to the capitulum. 5 The trochlea extends markedly inferior to the capitulum.	Vance *et al.,* 2011; Tallman & Blanton, 2020
Olecranon-coronoid angle	The angle formed by the olecranon and coronoid processes of the ulna relative to the posterior surface.	0 No assessment 1 Narrow, $14.73^{o} \pm 4.46^{o}$. 5 Wide, $22.26^{o} \pm 3.47^{o}$.	Purkait, 2001
Overall pelvis morphology	The relative size of the pelvis as a whole	0 No assessment 1 Large 5 Small	İşcan & Steyn, 2013
Pelvic brim morphology	The relative shape of the edge of the pelvic inlet, defined by linea terminalis that passes through the sacral promontory, the arcuate and pectineal line, and the upper margins of the pubic crest.	0 No assessment 1 Round/Elliptical 5 Heart-shaped	İşcan & Steyn, 2013; Berg, 2017

Table 3.4: Continued…

Skeletal Traits	Description	Scoring	References of Estimation Method
Subpubic shape	The shape of angle located inferior to the pubic symphysis of the pubic arch, formed by the convergence of the paired ischiopubic rami.	0 No assessment 1 U-shaped 5 V-shaped	Small *et al.*, 2012; İşcan & Steyn, 2013
Obturator foramen shape	The relative shape of the large foramen on the os coxae, encircled by the two pubic rami and the ischium	0 No assessment 1 Triangular 5 Ovoid	İşcan & Steyn, 2013
Greater sciatic notch	The morphology of the notch inferior to the posterior inferior iliac spine of the os coxae	0 No assessment 1 Wide 2 Relatively wide 3 Ambiguous/intermediate 4 Relatively narrow 5 Narrow and symmetrical	Gupta *et al.*, 2022
Subpubic contour	The lateral recurve which occurs in the ischio-pubic ramus just lateral to the lower margins of the pubic symphysis	0 No assessment 1 Well-developed concavity present inferior to symphyseal face and along most of the length of the inferior ramus. 2 Slight concavity is present inferior to symphyseal face that extends partially down inferior ramus. 3 Bone is nearly straight along the entire length of ischiopubic ramus with no obvious concavity or convexity observable.	Klales & Cole, 2018

Table 3.4: Continued…

Skeletal Traits	Description	Scoring		References of Estimation Method
Subpubic contour ***(continued)***		4	Slight convexity, especially pronounced along the middle portion of the inferior ramus. A very slight indentation may exist just below the symphyseal face and/or along the lower third; however, the middle portion of ramus is convex.	Klales & Cole, 2018
		5	Well-developed convexity, pronounced along the entirety of the inferior ramus.	
Ventral arc	An elevated ridge of bone running inferiorly and laterally across the ventral surface of the lateralmost extension of the pubic bone.	0	No assessment	Klales & Cole, 2018
		1	Arc present and oriented at an approximate angle of 40° or more relative to the symphyseal face. A large triangular portion of bone is located inferior to the arc, giving the pubis a squared-off appearance.	
		2	Arc present and oriented at an approximate angle of 25–40° relative to the symphyseal face. A small triangular portion of bone is located inferior to the arc, giving the pubis a somewhat squared-off appearance.	
		3	Arc (or bony ridge) present and oriented at a slight angle (less than 25°) relative to the symphyseal face. A slight, non-triangular portion of bone is located inferior to the arc.	
		4	Bony ridge present and oriented approximately parallel to the symphyseal face. Hardly any additional bone is present inferior to the arc. Bone has a sloping appearance on the inferior symphyseal face.	
		5	No arc present and therefore, no additional bone present inferior to the arc. Bone has a sloping appearance on the inferior symphyseal face.	

Table 3.4: Continued…

Skeletal Traits	Description	Scoring	References of Estimation Method
Acetabulum position	The relative direction of the hollow that forms the socket of the hip and articulates with the femoral head.	0 No assessment 1 Directed anterolaterally 5 Directed laterally	İşcan & Steyn, 2013
Ilium morphology	General morphology of the thin, blade-like bony structure superior to the acetabulum.	0 No assessment 1 Significant flare & broad 5 Minimal flare & narrow	Rowbotham, 2016; Berg, 2017
Sacrum morphology	The general morphology of the wedge-shaped bony structure located at the base of the lumbar vertebrae and connected to the pelvis to form the posterior pelvic wall.	0 No assessment 1 Short & wide 5 Long & narrow	İşcan & Steyn, 2013; Berg, 2017
Quadriceps angle	The angle formed by a line that connects the anterior superior iliac spine to the centre of the patella and a line that runs from the centre of the patella to tibial tuberosity.	0 No assessment 1 Wide; >14.5^{o} 5 Narrow; <10.9^{o}	Raveendranath *et al.*, 2009
Femoral neck shaft angle	The angle between the femoral neck axis and the femoral long axis of the shaft.	0 No assessment 1 Broad; 133.61^{o} ± 5.17^{o} 5 Narrow; 131.56^{o} ± 4.74^{o}	Rogers, 2021

*Sex scores; 0 = No assessment: 1 = Female; 2 = Probable female; 3 = Ambiguous; 4 = Probable male; 5 = Male.

3.3. Statistical Analysis

3.3.1. Repeatability assessment and analysis

To ensure repeatability of the assessment, 20 randomly selected Lodox scans, equally distributed by sex, were subjected to intra- and inter-repeatability assessment prior to the commencement of the study. For intra-repeatability, the 20 Lodox scans were re-assessed one week after their initial evaluation by the principal investigator. For inter-observer assessment, an independent observer assessed the same randomly selected set of 20 Lodox scans. This independent observer, a Master of Science in Medicine candidate with a Bachelor of Arts Honors qualification in Archaeology, had moderate knowledge of human anatomy and forensic anthropology but limited experience with visualising Lodox radiographs. The independent observer evaluated the observability of all skeletal elements and skeletal traits of interest based on White *et al.* (2011) and Christensen *et al.* (2014d) descriptions of human osteology and Thrall's (2012) descriptions of skeletal tissue appearance on radiographs, respectively. All skeletal traits of interest were assessed and scored based on their respective descriptions of visualisation and morphological assessment (Tables 3.3 and 3.4).

Quadratic weighted Cohen's Kappa scores were computed in the Statistical Package for the Social Sciences (SPSS) software (IBM Corporation, 2023) to assess inter- and intra-observer repeatability concerning the scores of ordinal skeletal traits (1 = female; 2 = probable female; 3 = ambiguous; 4 = probable male; 5 = male). Unweighted Cohen´s Kappa scores were computed in Microsoft Excel (Microsoft Corporation, 2024) to assess inter- and intra-observer repeatability concerning scores of nominal traits (1 = female; 5 = male), including the ability to observe skeletal elements and to score skeletal traits (1 = yes; 0 = no). The observer agreement was expressed as a value between zero and one, whereby zero represents no agreement and one represents a perfect agreement between observers in all their assessments (Sim & Wright, 2005). The following strengths of agreements in Table 3.5 were used as standards for Cohen´s Kappa coefficients (Viera & Garret, 2005).

Table 3.5: Cohen's Kappa strengths of agreements and associated coefficients, adapted from Viera & Garret (2005).

Cohen's Kappa coefficients	Interpretation
≤0.09	No agreement
0.10-0.20	Slight agreement
0.21-0.40	Fair agreement
0.41-0.60	Moderate agreement
0.61-0.80	Substantial agreement
0.81-0.99	Near perfect agreement
1.00	Perfect agreement

3.3.2. Data analysis

Prior to data analysis, the dataset of Lodox scans with known age-at-death underwent normality testing (using a Shapiro-Wilk test), descriptive summary statistics (including mean, standard deviation, mode, minimum and maximum age-at-death), skewness and kurtosis test functions. These analyses were conducted to determine whether the sample size of the Lodox scans with known age is representative of a normally distributed population, thus aiding in selecting an appropriate statistical test, including providing a concise and interpretable overview of the age-at-death dataset. Given that the sample sizes of male and female Lodox scans were not equally distributed, a two-sample unequal variance (Welch) t-test was used to test whether the means of the ages-at-death of males and females (n = 121) were statistically different and reflect a true difference in the population. Data analysis in this case was carried out using the Paleontological Statistics (PAST) computer software program (Hammer *et al.*, 2001).

The frequency distributions for the observability of skeletal elements were reported and presented as percentages (i.e., total observable skeletal element divided by study sample size (n = 150 scans) multiplied by 100%) (see equation (1)). Similarly, the frequency distributions for the observability of respective skeletal traits (Tables 3.3 and 3.4) were also reported and presented in two types of percentages, that is, 1) frequency of observable skeletal trait divided by total frequency of observable respective skeletal element (see equation (2)); and 2) frequency of observable skeletal trait divided by total study sample size (see equation (3)). The frequencies of scorable skeletal traits were also reported and determined in similar calculations.

The estimated sexes of scorable skeletal traits were then compared to their respective documented sexes, and the sex classification accuracies were determined, per respective skeletal trait. The sex classification accuracies of scorable traits were compared in two distinct ways to provide a comprehensive analysis. The first method involved dividing the number of correctly classified

male or female individuals for each trait by the total number of assessed scans in the study (see equations (4) and (5)). The second method focused on the subset of visible traits and calculated accuracy by dividing the number of correctly classified individuals (male/female) by the total number of scans where a specific trait was scorable. For both classification accuracy methods, the combined sex classification accuracy for a particular trait was then calculated as the average percentage of correctly classified male and female individuals (see equation (6)). The frequencies of skeletal traits classified as 'ambiguous' were also reported, compared to respective documented scans sexes. The associated proportions and classification frequencies were similarly calculated in two ways. However, the classification estimates of ambiguous classified traits were not included in the combined sex classification accuracy rate as ambiguity cannot be considered as correct nor incorrect estimation, and their inclusion might result in overestimated accuracies. All frequency counts and calculations were carried out in Microsoft Office Excel® computer software program (Microsoft Corporation, 2024).

A Pearsons Chi-squared test of independence was used to evaluate whether a specific score for a skeletal trait is more associated with either male or female morphology based on the sample. The same Pearsons Chi-squared test was also used to evaluate significant differences between the documented sex and the morphological skeletal sex estimation of a particular skeletal trait. Traits classified as 'ambiguous' were excluded from such test analysis as sex classification was not predicted due to the ambiguity of the trait. The proposed null hypothesis was that there should not be a relationship between the predicted sexes of assessed skeletal traits and the respective sexes of documented scans, i.e., significant statistical difference. Data analysis in this case was carried out using the PAST computer software program (Hammer *et al.*, 2001). A significant level (α) of 0.5 was applied for all statistical analyses.

$$accuracy\ for\ observable\ skeletal\ element = \frac{\text{total observable skeletal element}}{Total\ study\ sample\ (150)} X100\% \quad (1)$$

$$observable\ skeletal\ trait\ accuracy = \frac{\text{frequency of observable skeletal trait}}{\text{total frequency of observable skeletal element}} X100\% \quad (2)$$

$$observable\ trait\ accuracy\ per\ study\ sample = \frac{\text{frequency of observable skeletal trait}}{\text{total study sample (150)}} X100\% \quad (3)$$

$$correct\ male\ accuracy\ for\ a\ trait = \frac{The\ number\ of\ correctly\ classified\ males}{Total\ documented\ male\ scans\ (72)} X100\% \quad (4)$$

$$corect\ female\ accuracy\ for\ a\ trait = \frac{The\ number\ of\ correctly\ classified\ females}{Total\ documented\ female\ scans\ (78)} X100\% \quad (5)$$

$$correct\ combined\ accuracy\ for\ a\ trait = \frac{\%\ correct\ male + \%\ correct\ female}{2} X100\% \quad (6)$$

CHAPTER 4: RESULTS

4.1. Descriptive Statistics

The age of the dataset of Lodox scans with documented age-at-death (n = 121) was normally distributed (W = 0.97, *p-value* = 0.0043) with kurtosis and skewness results both less than one (-0.34 and -0.52, respectively. There were no statistically significant differences between the age-at-death of males (39-94 years, mean = 75 ± 12.2 years) and females (47-101 years, mean = 78 ± 13.7 years) (Welch t-test = 0.941, *p-value* = 0.349).

4.2. Observable Skeletal Elements

Observation of skeletal elements (and traits) on Lodox scans was based on the principle of radiographic images, that is, highly dense, radiopaque tissues typically appear in varying shades of white against the darker greys of surrounding soft tissues (Figure 3.1) (Berger, 2002; Thrall, 2012). Moreover, the identification of specific skeletal elements relied on White *et al.'s* (2011) and Christensen *et al.'s.* (2014d) description of human osteology, which provides details about the typical morphology and location of skeletal elements within the human body. As such, these allowed for visualisation of specific skeletal elements (and traits) on anteroposterior Lodox scans in relation to their anterior phenotypical characteristics (Figure 3.1). Therefore, eight out of ten skeletal elements assessed in the current study were observable in high frequencies from Lodox scans, ranging from 88% to 99% (Table 4.1). The most observable skeletal elements were the cranium and pelvic girdle, each observable in 99.3% of assessed Lodox scans, followed by the distal humerus and femur at 98% and 96.7%, respectively (Table 4.1).

The intra-observer repeatability agreements associated with observing skull and postcranial elements of interest from Lodox scans ranged from moderate to perfect repeatability agreements (Table 4.1). That is, the utilisation of Lodox scans showed near-perfect intra-observer agreement for the visual observability of lower rib costal cartilages, substantial agreement for the mandible and sacrum, and moderate agreement for the scapula. The remaining skeletal elements assessed had a perfect intra-observer repeatability agreement for observation on Lodox scans (Table 4.1). The inter-observer repeatability for observed skeletal elements ranged from slight to perfect agreements. The mandible and sacrum showed moderate agreement, while the scapula and rib costal cartilages exhibited fair and slight agreement, respectively (Table 4.1). All other skeletal elements demonstrated perfect inter-observer repeatability agreement.

Table 4.1: Counts and frequencies (in brackets) of observable skeletal elements from assessed Lodox scans (n = 150) with associated intra- and inter-observer Cohen's Kappa agreement scores (K).

Skeletal Element	Count Observable (Frequency)	Intra-observer agreement	Inter-observer agreement
Cranium	149 (**99.3%**)	1.00	1.00
Mandible	132 (88.0%)	0.64	0.46
Clavicle	138 (92.0%)	1.00	1.00
Scapula	137 (91.3%)	0.44	0.32
Lower ribs costal cartilages	65 (43.3%)	0.89	0.13
Distal humerus	147 (98.0%)	1.00	1.00
Proximal ulna	135 (90.0%)	1.00	1.00
Pelvic girdle	149 (**99.3%**)	1.00	1.00
Sacrum	43 (28.7%)	0.69	0.50
Femur	145 (96.7%)	1.00	1.00

*Bold percentages represent the highest frequency of observability

Colour codes: Slight agreement, fair agreement, moderate agreement, substantial agreement, near-perfect agreement, perfect agreement.

4.3. Observable and Scorable Skeletal Traits

Following the observation of the above-mentioned skeletal elements (per Lodox scan) (Table 4.1), the sexually dimorphic traits (of interest) associated with these skeletal elements were further assessed for observability and were ultimately scored for morphological sex estimation (Tables 3.3 and 3.4). The ability to score (i.e., scorability) a particular skeletal trait for morphological sex classification depended on its observability on a particular Lodox scans. Each observable skeletal trait (per Lodox scan) was morphologically scored using the criteria of the associated sex estimation method, with nominal skeletal traits scored as either 1 (female) or 5 (male), while ordinal traits were scored on a five-point scale: 1 = female, 2 = probable female, 3 = ambiguous, 4 = probable male, and 5 = male (Tables 3.3 and 3.4), as stated in the method chapter above. These scores were subsequently used to estimate the sex of the assessed trait from Lodox scans. For the purpose of further analysis, skeletal traits assigned scores of one (1) and two (2) were classified as 'female' whereas skeletal traits assigned scores of four (4) and five (5) were classified as 'male'. Skeletal traits assigned a score of three (3) were not given a sex classification but rather categorised as 'ambiguous'. Skeletal traits that were not observable and/or scorable from respective Lodox scans were categorised as 'unobserved'.

On average, the skeletal traits of the pelvic girdle were the most observable and scorable traits compared to the assessed traits of other skeletal elements, with the highest average observability (81%) and scorability (88%) frequencies (Figure 4.1). These were followed by the traits of the

mandible with 81% average observability and 76% average scorability. The average observability frequencies of the remaining skeletal traits, per skeletal elements, ranged from 0% (clavicle) to 51.3% (proximal ulna), while the average scorability frequencies ranged from 0% (clavicle) to 62.1% (cranium) (Figure 4.1).

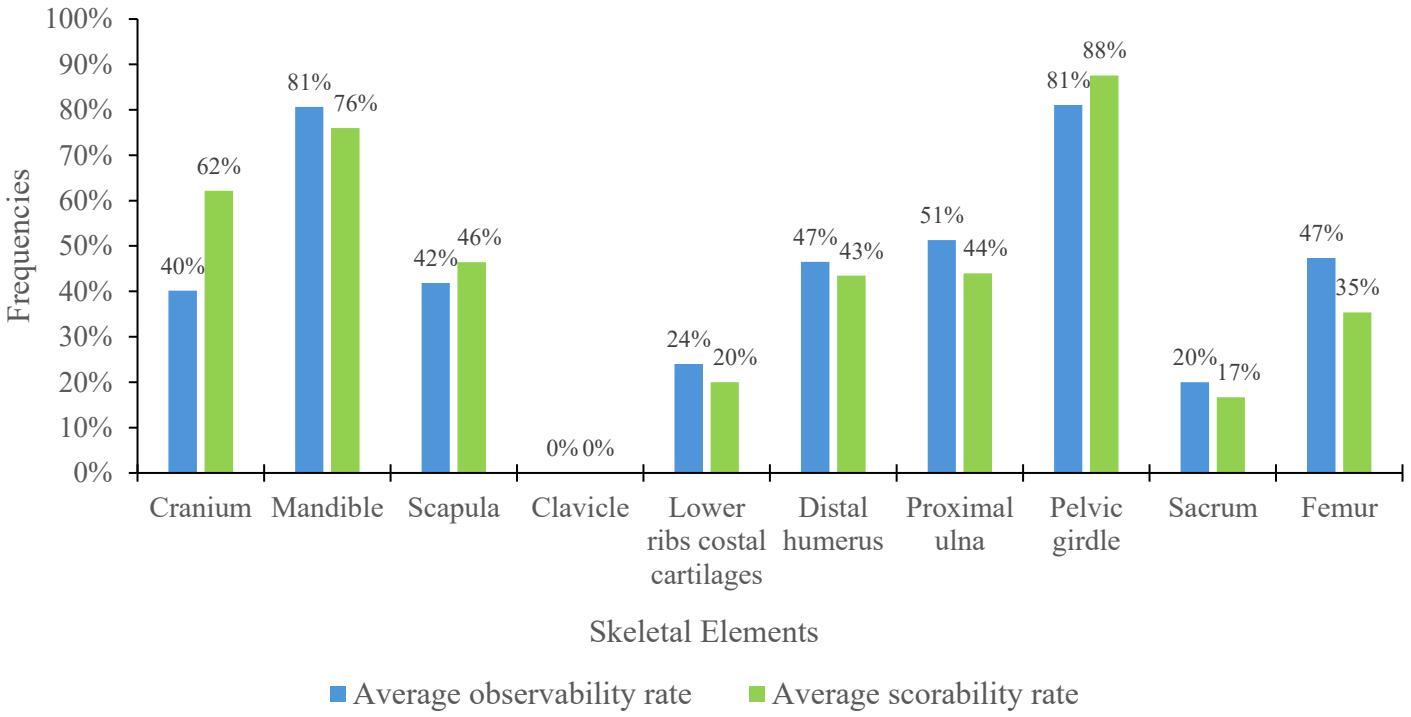


Figure 4.1: Visual representation to indicate skeletal element(s) with the most/least observable and/or scorable skeletal traits, on average frequencies. None-observable and/or -scorable skeletal traits were excluded from calculations of average frequencies.

4.3.1. Skull traits

4.3.1.1. Observability

Concerning skull traits assessed in the current study (Table 3.2), the orbit was the most observable trait, observable in 94.0% of the observable crania (140/149) of the Lodox scans (Figure 4.2). The second most observable trait was the overall skull morphology (90.6%, 135/149 scans), followed by the parietal eminence (87.9%, 131/149) (Table 4.2, Figure 4.2). The mastoid process and frontal eminence were the least observable cranial traits from assessed Lodox scans with observable crania and were only visible in 43.6% of mastoid processes (65/149 scans) and 7.4% of parietal eminences (11/149 scans), respectively (Table 4.2). The nuchal crest, forehead slope, and glabella were not observable from any of the assessed Lodox scans with observable crania. Subsequently, these traits were not assessed further for morphological sex estimation. The mental eminence was observable in 91.7% (n = 121 scans) of the Lodox scans with observable mandibles (n = 132 scans) (Figure 4.2). The differences in the observability frequencies of assessed cranial traits between the

total study sample (n = 150) and a subset of observable crania (n = 149) were consistently less than 1% while the mental eminence exhibited an 11.0% difference in observability frequencies (Table 4.2).

Visual observability of skull traits from Lodox scans exhibited intra- and inter-observer repeatability agreements ranging from slight to perfect agreements (Table 4.2). Perfect intra- and inter-observer agreements were achieved for the observation of the overall skull morphology from Lodox scans, whereas the mastoid process demonstrated the lowest levels of agreement, with fair intra-observer and slight inter-observer agreements. The majority of the remaining cranial traits demonstrated a variety of repeatability agreements, ranging from moderate to substantial repeatability agreements for observability on Lodox scans (Table 4.2). Nuchal crest, forehead slope, and glabella morphology, which were not observable in any assessed Lodox scans, demonstrated perfect intra- and inter-observer agreement, as both observers consistently recorded them as unobservable (Table 4.2). The mental eminence morphology had a moderate intra-observer agreement and a substantial inter-observer agreement for observation on Lodox scans (Table 4.2).

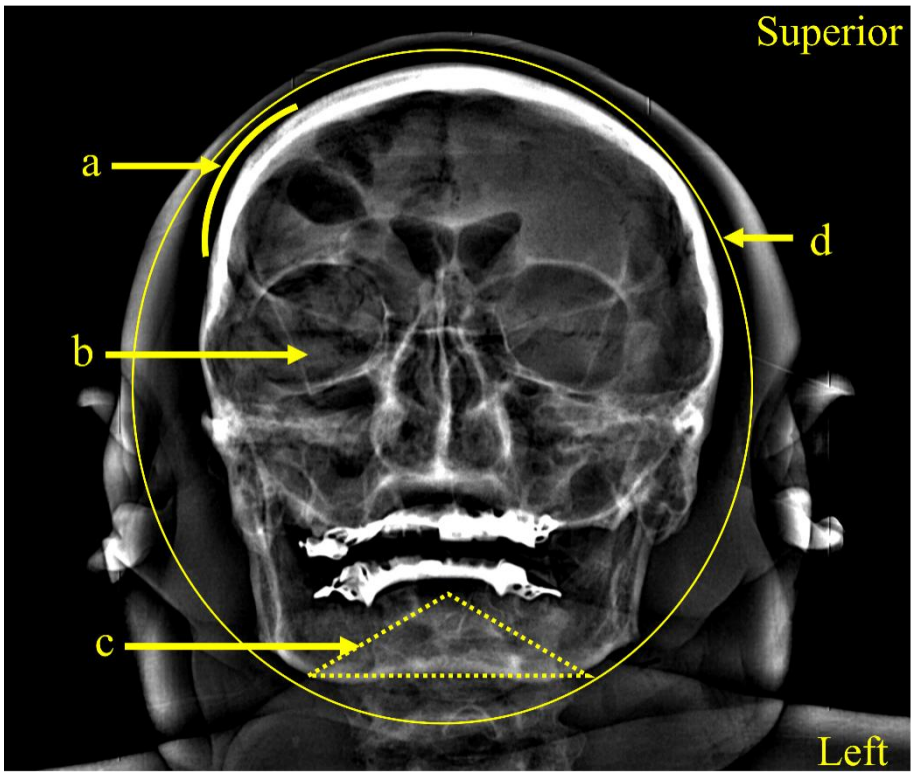


Figure 4.2: Example of skull traits with higher frequency (>89%) of observability from Lodox scans. a = parietal eminence; b = orbit morphology; c = mental eminence; d = overall skull morphology.

4.3.1.2. Scorability

Overall, the ability to score an observable skull trait from Lodox scans was greater than 87% (Table 4.2). Of the observable cranial traits, the orbit exhibited the highest frequency of scorability, scorable in 100% of the observable crania (140/140 scans), whereas mastoid process morphology exhibited the lowest frequency of scorability (87.7%, 57/65 observable). The parietal eminence, overall skull morphology, and frontal eminence were scorable in 97.7% (128/131 observable), 97.0% (131/135 observable), and 90.9% (10/11 observable) of observable crania, respectively. While most cranial traits showed only a 6-12% difference in scorability between a subset of respective observable cranial traits and the total sample (n = 150 scans), the scorability of the mastoid process and frontal eminence exhibited the greatest differences (49.7% and 84.2%, respectively) (Table 4.2). The mental eminence was scorable in 94.2% of observable mental eminences (114/121 observable), which represents 76.0% of the study sample size, an 18.2% difference.

The assessed scorable cranial traits exhibited levels of repeatability ranging from slight to perfect agreements (Table 4.2). For visual scoring on Lodox scans, the overall skull and parietal eminence morphologies both showed perfect intra-observer and moderate inter-observer agreements, while orbit shape showed substantial agreements for both intra- and inter-observer repeatability. The mastoid process and frontal eminence showed the lowest agreement levels for scorability (Table 4.2). The frontal eminence exhibited moderate intra- and inter-observer agreement, while the mastoid process showed moderate intra-observer and slight inter-observer agreements.

Table 4.2: Tabulated counts and frequencies (in brackets) of the observable and scorable morphological skull traits, and their respective intra- and inter-observer Cohen's Kappa coefficients (K).

Skeletal Traits	Observability				Scorability			
	Count observable (Frequency)	Percentage observable over total sample (n=150)	Intra-observer Agreement	Inter-observer Agreement	Count scorable (Frequency)	Percentage scorable over total sample (n=150)	Intra-observer Agreement	Inter-observer Agreement
Cranium (n = 149)								
Overall skull morphology	135 (90.6%)	90.0%	1.00	1.00	131 (97.0%)	87.3%	1.00	0.64
Mastoid process	65 (43.6%)	43.3%	0.29	0.19	57 (87.7%)	38.0%	0.50	0.13
Nuchal crest	0%	0%	1.00	1.00	0%	0%	-	-
Frontal eminence	11 (7.4%)	7.3%	0.64	1.00	10 (90.9%)	6.7%	0.50	0.58
Parietal eminence	131 (87.9%)	87.3%	0.69	0.48	128 (97.7%)	85.3%	1.00	0.48
Orbit shape	140 (**94.0%**)	**93.3%**	0.64	0.62	140 (**100%**)	**93.3%**	0.64	0.62
Forehead slope	0%	0%	1.00	1.00	0%	0%	-	-
Glabella	0%	0%	1.00	1.00	0%	0%	-	-
Mandible (n = 132)								
Mental eminence	121 (**91.7%**)	**80.7%**	0.50	0.77	114 (**94.2%**)	**76.0%**	0.40	0.34

*Bold percentages indicate the highest frequency of observability and/or scorability among all the traits for a particular skeletal element.

Dash (-) is indicative of traits where scorability was not conducted due to the not being observable from any assessed Lodox scans, thus not scorable.

Colour coding: Slight agreement, fair agreement, moderate agreement, substantial agreement, near-perfect agreement, perfect agreement.

Table 4.3: Skull traits observability and scorability differences between the total study sample (n = 150 scans) and a subset of observable and scorable trait.

Skeletal elements	Observability differences	Scorability differences
Cranium		
Overall skull morphology	0.6%	9.7%
Mastoid process	0.3%	49.7%
Frontal eminence	0.1%	84.2%
Parietal eminence	0.6%	12.4%
Orbit shape	0.6%	6.7%
Mandible		
Mental eminence	11.0%	18.2%

4.3.2. Postcranial traits

4.3.2.1. Observability

The observability of postcranial morphological traits from assessed Lodox scans varied, with a range of 14.6% to 98.0% from a subset of scans with observable skeletal elements (Table 4.4). Traits of the pelvic girdle were consistently highly observable compared to skeletal traits of other postcranial elements (Table 4.4). In particular, the pelvic brim was observable in 98.0% (146/149) of Lodox scans, followed by the overall pelvis morphology at 96.6% (144/149) (Table 4.4 and Figure 4.3). These were followed by the obturator foramen shape (91.9%, 137/149), subpubic bone shape (91.3%, 136/149), and acetabular position (91.3%, 136/149). The ventral arc was the least observable pelvic trait, observable on 87.9% (131/149) of assessed pelvic girdles, followed by the subpubic contour and ilium morphology both at 88.6% (132/149) observability rate.

The infraspinous fossa's lateral border was the most observable trait of the scapula, observable in 90.5% (124/137 scans) of assessed scapulae. It ranked as the sixth most observable postcranial trait overall (Table 4.4 and Figure 4.3). This was followed by suprascapula notch, with an observability of 56.2% (77/137), and the supraspinous fossa's superior border, with an observability of 21.9% (30/137). In contrast, the infraspinous fossa's medial border was the least observable scapula trait, and the least observable among all postcranial traits, at 14.6% (20/137) observability (Table 4.4). Among the distal humerus traits, the olecranon fossa's shape was the most observable, visible in 80.3% (118/147) of observable distal humeri (Table 4.4 and Figure 4.3). However, the observability of the trochlea constriction (54.4%, 80/147) and trochlea symmetry (55.1%, 81/147) were notably lower in comparison (Table 4.4)

The observability of the remaining postcranial traits ranged between 29.7% (quadriceps angle, 43/145 assessed femora) and 55.4% (costal cartilage ossification patterns, 36/65 assessed lower

ribs costal cartilages) (Table 4.4). The costoclavicular tuberosity, medial epicondyle angle, and greater sciatic notch were not observable from any of the assessed Lodox scans and thus were not assessed for morphological sex estimation. While most postcranial traits showed less than 5.7% difference in observability between a subset of the respective observable postcranial traits and the total sample, the observability of the costal cartilage ossification patterns and sacrum morphology exhibited the greatest differences (31.4% and 49.8%, respectively). All assessed observable pelvic traits exhibited the least differences in observability (0.6% and 0.7%) compared to the other postcranial traits (Table 4.5).

The intra- and inter-observer agreements associated with observing the postcranial traits of interest ranged from no agreements to a perfect agreement (Table 4.4). Seven of the assessed postcranial traits, including the most observable postcranial traits, had perfect intra- and inter-observer agreements. The observability of the costal cartilage ossification positions had a near-perfect intra-observer agreement and a fair inter-observer agreement. Moreover, visual observability of the morphologies of the suprascapular notch, supraspinous fossa's superior border, olecranon-coracoid angle, sacrum, femoral neck shaft angle, and quadriceps angle exhibited intra- and inter-observer agreements ranging from no agreement to fair agreement (Table 4.4). The observability of the remaining postcranial traits on Lodox scans exhibited substantial and moderate intra- and inter-observer agreements (Table 4.4). The non-observability of the costoclavicular tuberosity, medial epicondyle angle, and greater sciatic notch morphology, from any of the assessed Lodox scans, exhibited perfect intra- and inter-observer agreements.

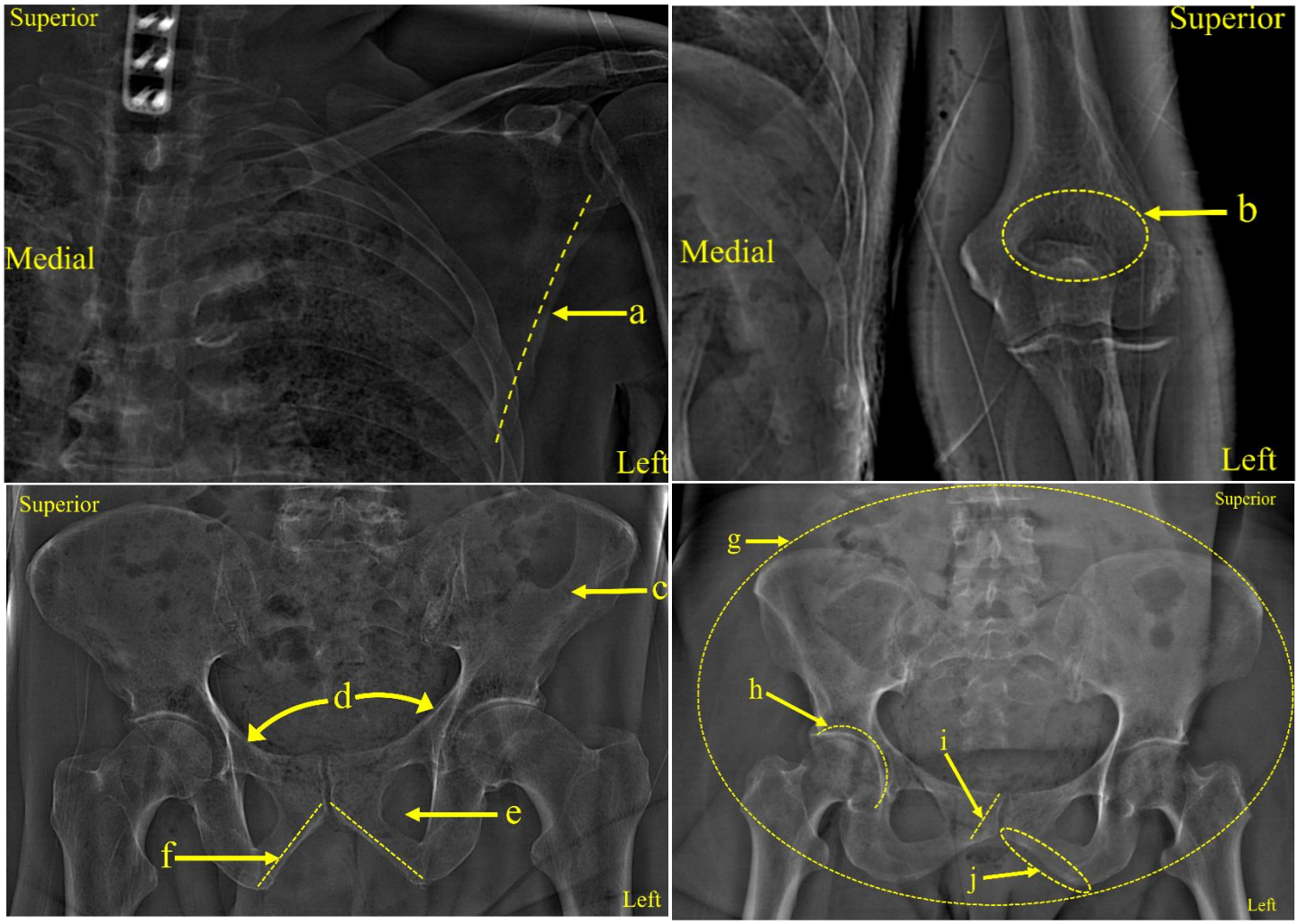


Figure 4.3: Image examples of postcranial traits with high frequency of observability (>80%) from Lodox scans. Images: Top left = scapula; top right = distal humerus; bottom images = pelvis. a = infraspinous fossa lateral border; b = olecranon fossa shape; c = ilium morphology; d = pelvic brim; e = obturator foramen shape; f = subpubic shape; g = overall pelvis morphology; h = acetabulum position; i = ventral arc; j = subpubic contour.

4.3.2.2. Scorability

With regard to the ability to score observable postcranial traits from Lodox scans, the frequencies of the most scorable postcranial traits ranged from 83.3% (costal cartilage ossification patterns (30/36 observable) and sacrum morphology (25/30 observable)) to 100% (infraspinous fossa's medial border (20/20 observable) and ilium morphology (132/132 observable)) (Table 4.4). The traits of the pelvic girdle were the most scorable postcranial traits, ranging from 93.2% (subpubic contour, 123/132 observable) to 100% (ilium morphology, 132/132 observable). Compared to other postcranial traits, pelvic traits were scorable in over 82.0% of the study sample size (n = 150 scans), ranging from 82.0% (subpubic contour, 123/150) to 93.3% (overall pelvis morphology and pelvic brim, 140/150) (Table 4.4). Although the infraspinous fossa medial border (100%, 20/20 observable), trochlea constriction (91.3%), trochlea symmetry (88.9%, 72/81 observable),

suprascapular notch (88.3%, 68/77 observable), olecranon-coronoid angle (85.7%, 66/77 observable), and the sacrum morphology (83.3%, 25/30 observable) were scorable in relatively higher frequencies from their respective observable skeletal elements, these traits were scorable in less than 50.0% of the total study sample size (n = 150) (Table 4.5). The least scorable postcranial trait was the femoral neck shaft angle (53.5%, 53/99 observable), while the supraspinous fossa superior border, costoclavicular tuberosity, medial epicondyle angle, greater sciatic notch, and the quadriceps angle were not scorable from any of the observable respective skeletal elements, thus morphological sex classification was not conducted.

The intra-observer agreements associated with the ability to score respective observable postcranial traits ranged from fair to perfect agreements, with the majority of the traits associated with either moderate or substantial intra-observer agreements (Table 4.4). The associated inter-observer agreements ranged from no agreement to perfect agreement (Table 4.4). Skeletal traits such as the infraspinous fossa lateral border and sacrum morphology exhibited the greatest difference in agreement levels between intra- and inter-observer repeatability, ranging between two and three agreement levels (Table 4.4). The scorability of the remaining postcranial traits exhibited no or a single level of differences between intra- and inter-observer repeatability.

Table 4.4: Tabulated counts of the observable and scorable morphological postcranial traits, associated frequencies in brackets, and their respective intra- and inter-observer Cohen's Kappa coefficients (K).

Skeletal Traits	Observability				Scorability			
	Count observable (Frequency)	Percentage observable over total sample (n = 150)	Intra-observer Agreement	Inter-observer Agreement	Count scorable (Frequency)	Percentage scorable over total sample (n = 150)	Intra-observer Agreement	Inter-observer Agreement
Scapula (n = 137)								
Suprascapular notch	77 (56.2%)	51.3%	0.24	0.18	68 (88.3%)	45.3%	0.20	0.09
Supraspinous fossa superior border	30 (21.9%)	20.0%	0.14	0.24	0%	0%	—	—
Infraspinous fossa lateral border	124 (**90.5%**)	**82.7%**	0.64	0.39	121 (**97.6%**)	**80.7%**	0.73	0.35
Infraspinous fossa medial border	20 (14.6%)	13.3%	0.69	0.50	20 (100%)	13.0%	0.79	0.63
Clavicle (n = 138)								
Costoclavicular tuberosity	0%	0%	1.00	1.00	0%	0%	—	—
Lower ribs costal cartilage (n = 65)								
Costal cartilage ossification pattern	36 (**55.4%**)	**24.0%**	0.90	0.24	30 (**83.3%**)	**20.0%**	0.72	0.47
Distal humerus (n = 147)								
Olecranon fossa	118 (**80.3%**)	**78.7%**	0.74	0.68	108 (**91.5%**)	**72.0%**	0.50	0.63
Medial epicondyle angle	0%	0%	0.79	0.41	0%	0%	—	—
Trochlea constriction	80 (54.4%)	53.3%	0.79	0.60	73 (91.3%)	48.7%	0.67	0.50
Trochlea symmetry	81 (55.1%)	54.0%	1.00	1.00	72 (88.9%)	48.0%	0.76	0.58

Table 4.4: Continued…

Skeletal Traits	Observability				Scorability			
	Count observable (Frequency)	Percentage observable over total sample (n=150)	Intra-observer Agreement	Inter-observer Agreement	Count scorable (Frequency)	Percentage scorable over total sample (n=150)	Intra-observer Agreement	Inter-observer Agreement
Proximal ulna (n = 135)								
Olecranon-coronoid angle	77 (**57.0%**)	**51.3%**	0.12	0.30	66 (**85.7%**)	**44.0%**	0.51	0.28
Pelvic girdle (n = 149)								
Overall pelvis morphology	144 (96.6%)	96.0%	1.00	1.00	140 (97.2%)	**93.3%**	1.00	1.00
Pelvic brim	146 (**98.0%**)	97.3%	1.00	1.00	140 (95.9%)	**93.3%**	1.00	1.00
Subpubic shape	136 (91.3%)	90.7%	1.00	1.00	130 (95.6%)	86.7%	0.64	0.46
Obturator foramen shape	137 (91.9%)	91.3%	0.64	0.64	128 (93.4%)	85.3%	1.00	1.00
Greater sciatic notch	0%	0%	1.00	1.00	0%	0%	—	—
Subpubic contour	132 (88.6%)	88.0%	1.00	1.00	123 (93.2%)	82.0%	0.64	0.62
Ventral arc	131 (87.9%)	87.3%	1.00	1.00	128 (97.7%)	85.3%	0.44	0.62
Acetabulum position	136 (91.3%)	90.7%	0.46	0.77	130 (95.6%)	86.7%	0.51	0.74
Ilium morphology	132 (88.6%)	88.0%	1.00	1.00	132 (**100%**)	88.0%	1.00	1.00
Sacrum (n = 43)								
Sacrum morphology	30 (**69.8%**)	**20.0%**	0.23	0.00	25 (**83.3%**)	**16.7%**	0.51	0.00

Table 4.4: Continued…

Skeletal Traits	Observability				Scorability			
	Count observable (Frequency)	Percentage observable over total sample (n=150)	Intra-observer Agreement	Inter-observer Agreement	Count scorable (Frequency)	Percentage scorable over total sample (n=150)	Intra-observer Agreement	Inter-observer Agreement
Femur (n = 145)								
Femoral neck shaft angle	99 (**68.3%**)	**66.0%**	0.13	0.00	53 (**53.5%**)	**35.3%**	0.42	0.05
Quadriceps angle	43 (29.7%)	28.7%	0.14	0.12	0%	0%	–	–

*Bold text indicates the highest frequency of observability and/or scorability among all the traits for a particular skeletal element.

Dash (–) is indicative of traits where scorability was not conducted due to the not being observable any assessed Lodox scans, thus not scorable.

Colour coding: No agreement, Slight agreement, fair agreement, moderate agreement, substantial agreement, near-perfect agreement, perfect agreement

Table 4.5: Postcranial traits observability and scorability differences between the total study sample (n = 150 scans) and a subset of observable and scorable trait. Non-observable skeletal traits are excluded.

Skeletal Traits	Observability differences	Scorability differences
Scapula		
Suprascapular notch	4.9%	43.0%
Supraspinous fossa superior border	1.9%	–
Infraspinous fossa lateral border	7.8%	16.9%
Infraspinous fossa medial border	1.3%	86.7%
Lower ribs costal cartilages		
Costal cartilage ossification position	31.4%	63.3%
Distal humerus		
Olecranon fossa	1.6%	19.5%
Trochlea constriction	1.1%	42.6%
Trochlea symmetry	0.7%	40.9%
Proximal ulna		
Olecranon-coronoid angle	5.7%	41.7%
Pelvic girdle		
Overall pelvis morphology	0.7%	3.9%
Pelvic brim	0.7%	2.6%
Subpubic angle shape	0.6%	8.9%
Obturator foramen shape	0.6%	8.1%
Subpubic contour	0.6%	11.2%
Ventral arc	0.6%	12.4%
Acetabulum position	0.6%	8.9%
Ilium morphology	0.6%	12.0%
Sacrum		
Sacrum morphology	49.8%	66.7%
Femur		
Femoral neck shaft angle	2.3%	18.2%
Quadriceps angle	1.0%	–

*Dash (–) indicates that scorability could not be assessed therefore differences could not be determined.

4.4. Skeletal Traits Sex Classification Accuracies

4.4.1. Sex classification accuracies per study sample

4.4.1.1. Skull traits

Regarding the morphological sex classification of scorable skull traits from assessed Lodox scans (males = 72 and females = 78), correct classification accuracy rates ranged from 6.9% to 80.6% for males, and from 5.0% to 74.4% for females (Table 4.6). The parietal eminence morphology achieved the highest accuracy in correctly classifying male sex (80.6%, 58/72), with only 11.1%

of males incorrectly classified as females. Females, however, had a lower correct classification accuracy of 47.4% (37/78) for parietal eminence morphology, with a 32.1% incorrect classification rate (Table 4.6). Orbit shape achieved the second-highest correct sex classification in males (72.2%, 52/72), with a 23.6% incorrect classification and a correct classification in 69.2% of females (54/78) with a 21.8% incorrect classification rate. Sex classification based on the overall skull morphology was the most accurate in females, correctly classifying females 74.4% (58/78) of the time, with a 14.1% incorrect classification rate, while males were correctly classified 63.9% (46/72) of the time, with a 22.2% incorrect classification rate (Table 4.6). Furthermore, sex classification based on the morphology of the mental eminence resulted in 56% (male:40/72 and females: 44/78) correct sex classification accuracies for both male and female individuals, with 16.7% and 14.1% male and female incorrect classification rates, respectively. Based on morphological sex estimation, the frontal eminence yielded the lowest classification accuracy for both males (6.9%, 5/72) and females (5.0%, 4/78) while the mastoid process had the second-lowest accuracy for both males (27.8%, 20/72) and females (36.0%, 28/78) (Table 4.6).

Overall, morphological sex estimation (over total study sample) based on the orbit shape resulted in the highest combined sex classification accuracy for skull traits (70.7%, 106/150), followed by the overall skull morphology (69.3%, 104/150), parietal eminence (63.3%, 95/150), mental eminence (56.0%, 84/150), mastoid process (32%, 48/150), and frontal eminence (6.0%, 9/150) from the skull traits (Table 4.6). The mental eminence is the only skull trait that demonstrated ambiguous sex characteristics; thus, sex classification was not conducted in 6.9% of males and 2.6% of females. Significant statistical differences existed between the predicted and documented sexes except for the frontal eminence (*p-value* = 0.06) (Table 4.6).

Table 4.6: Predicted sex classification counts and accuracy rates (in brackets) of skull traits morphological scored for sex estimation from 150 assessed Lodox scans.

Skeletal trait	Total classified scans	Male sex classifications (n = 72)				Female sex classifications (n = 78)				Chi-squared statistic [c]	Total incorrectly classified	Combined correct sex
		Correct	Incorrect	Ambiguous [a]	Unobserved [b]	Correct	Incorrect	Ambiguous [a]	Unobserved [b]			
Cranium												
Overall skull morphology	131 (87.3%)	46 (63.9%)	16 (22.2%)	0%	10 (13.9%)	58 (**74.4%**)	11 (14.1%)	0%	9 (11.5%)	45	27 (18.0%)	69.3%
Mastoid process	57 (38%)	20 (27.8%)	3 (4.2%)	0%	49 (68.1%)	28 (36%)	6 (7.7%)	0%	44 (56.4%)	27	9 (6.0%)	32.0%
Frontal eminence	11 (7.3%)	5 (6.9%)	0%	0%	67 (93.1%)	4 (5.0%)	2 (2.7%)	0%	72 (92.3%)	**5***	2 (1.3%)	6.0%
Parietal eminence	128 (85.3%)	58 (**80.6%**)	8 (11.1%)	0%	6 (8.3%)	37 (47.4%)	25 (32.1%)	0%	16 (20.5%)	32	33 (22.0%)	63.3%
Orbit shape	140 (93.3%)	52 (72.2%)	17 (23.6%)	0%	3 (4.2%)	54 (69.2%)	17 (21.8%)	0%	7 (9.0%)	37	34 (22.7%)	**70.7**%
Mandible												
Mental eminence	114 (76.0%)	40 (**56.6%**)	12 (16.7%)	5 (6.9%)	15 (20.8%)	44 (**56.4%**)	11 (14.1%)	2 (2.6%)	21 (26.9%)	35	23 (15.0%)	**56.0%**

a: Skeletal traits scored as 3 and therefore not classified as either ‘male’ or ‘female’.

b: Skeletal traits that were not observable and/or scorable from a particular Lodox scan, thus sex classification was not conducted.

c: Chi-squared statistics with degrees of freedom = 1, for predicted sex classifications vs documented sexes.

*: Fishers Exact statistics. Bold and underlined Chi-square/Fishers Exact statistic values indicate no statistical significance (p-value ≥ 0.05).

Note: Bold percentages indicate the highest accuracy amongst traits for a particular skeletal element.

4.4.1.2. Postcranial traits

Regarding the morphological sex classification of scorable postcranial traits from assessed Lodox scans (males = 72 and females = 78), pelvic traits provided the highest male and female correct sex classification accuracies compared to other postcranial traits, ranging from 63.9% to 77.8% for males and 52.6% to 80.8% for females (Table 4.7). The subpubic shape and obturator foramen shape both had the highest correct sex classification accuracies for males (78.8%, 56/72), with 13.9% and 8.3% incorrect classification rates, respectively. The ventral arc morphology had the second most correct sex classification accuracy for males (76.4%, 55/72), followed by the overall pelvis morphology (75.0%, 54/72), pelvic brim (70.8%, 51/72), and acetabular position (70.8%, 51/72) (Table 4.7). These traits had a male incorrect classification rate of 9.7%, 19.4%, 22.2%, and 18.1%, respectively. The remaining postcranial traits achieved correct male sex classification accuracies ranging from 0% (suprascapular notch) to 69.4% (i.e., subpubic contour), with incorrect male classification rates ranging from 1.4% (costal cartilage ossification patterns) to 33.3% (suprascapular notch) (Table 4.7).

Correct female sex classification using pelvic brim morphology achieved the highest accuracy at 80.8% (63/78), with an incorrect classification rate of 11.5%. This trait was followed by the morphologies of the overall pelvis (79.5%, 62/78), ilium (78.2%, 61/78), and the obturator foramen shape (70.5%, 55/78) (Table 4.7). These three pelvic traits had 12.8%, 9.0%, and 14.1% incorrect female classification rates, respectively. The remaining postcranial traits achieved correct female sex classification accuracies ranging from 9.0% (sacrum morphology) to 66.7% (subpubic shape and acetabulum position), with incorrect female classification rates ranging from 1.3% (sacrum morphology) to 26.9% (infraspinous fossa lateral border) (Table 4.7).

In general, the overall pelvis morphology had a combined sex classification accuracy of 77.3% (116/150), the highest for all assessed skeletal traits. The pelvic brim morphology had the second highest combined sex classification accuracy (76.0%, 114/150), followed by the obturator foramen shape (74.0%, 111/150), and subpubic bone shape (72.0%, 108/150). The combined correct sex classification accuracies of the remaining postcranial traits ranged from 11.3% (infraspinous fossa medial border) to 71.3% (ilium morphology) (Table 4.7). Moreover, the combined incorrect classification accuracies ranged from 2.0% (infraspinous fossa medial border and sacrum morphology) to 26.7% (infraspinous fossa lateral border) (Table 4.7). Significant statistical differences existed between the predicted and documented sexes for all assessed postcranial traits (*p-value* < 0.05), except for the suprascapular notch (*p-value* = 0.89) (Table 4.7).

Compared to assessed skull traits, seven postcranial traits included ambiguous classifications due to exhibiting ambiguous sex characteristics, intermediate between male and female sex characteristics, thus their sex was not predicted (Table 4.7). The subpubic contour had the highest rate of ambiguous classifications, with 11.1% for males classified as ambiguous and 7.7% for females were classified as ambiguous. This trait was followed by the ventral arc with 6.9% ambiguous classifications for males and 5.1% ambiguous classifications for female ventral arc morphologies. The costal cartilage ossification patterns and olecranon fossa shape each demonstrated 1.4% ambiguous classification for males, 5.1% and 2.6% ambiguous classification for females, respectively. The suprascapular notch only demonstrated ambiguous classification for males (2.8%) while the trochlea constriction and trochlea symmetry morphologies demonstrated ambiguous classifications for only females (3.8% and 2.6%, respectively).

Table 4.7: Predicted sex classification counts and accuracy rates (in brackets) of postcranial traits morphologically scored for sex estimation from 150 assessed Lodox scans.

Skeletal trait	Total Classified Scans	Male sex classifications (n = 72)				Female sex classifications (n = 78)				Chi-squared statistic [c]	Total incorrect	Combined correct sex
		Correct	Incorrect	Ambiguous [a]	Unobserved [b]	Correct	Incorrect	Ambiguous [a]	Unobserved [b]			
Scapula												
Suprascapular notch	68 (45.3%)	0%	24 (33.3%)	2 (2.8%)	46 (63.9%)	40 (51.3%)	2 (2.6%)	0%	36 (46.2%)	**0**	26 (17.3%)	26.7%
Infraspinous fossa lateral border	121 (80.7%)	38 (**52.8%**)	19 (26.4%)	0%	15 (21%)	43 (**55.1%**)	21 (26.9%)	0%	14 (17.9%)	14	40 (26.7%)	**54%**
Infraspinous fossa medial border	20 (13.3%)	3 (4.2%)	3 (4.2%)	0%	66 (91.7%)	14 (17.9%)	0%	0%	64 (82.1%)	8	3 (2%)	11.3%
Lower ribs costal cartilages												
Costal cartilage ossification pattern	27 (18%)	9 (**12.5%**)	1 (1.4%)	1 (1.4%)	62 (86.1%)	9 (**11.5%**)	6 (7.7%)	4 (5.1%)	58 (74.4%)	10	4 (4.7%)	**12%**
Distal humerus												
Olecranon fossa	108 (72%)	34 (**47.2%**)	11 (15.3%)	1 (1.4%)	26 (36.1%)	45 (**57.7%**)	15 (19.2%)	2 (2.6%)	16 (20.5%)	21	26 (17.3%)	**52.7%**
Trochlea constriction	73 (48.7%)	24 (33.3%)	7 (9.7%)	0%	41 (56.9%)	26 (33.3%)	13 (16.7%)	3 (3.8%)	36 (46.2%)	19	20 (13.3%)	33.3%
Trochlea symmetry	72 (48.0%)	24 (33.3%)	7 (9.7%)	0%	41 (56.9%)	27 (34.6%)	12 (15.4%)	2 (2.6%)	47 (47.4%)	22	19 (12.7%)	34%

Table 4.7: Continued…

Skeletal trait	Total classified Scans	Male sex classifications				Female sex classifications				Chi-squared statistic [c]	Total incorrect	Combined correct sex
		Correct	Incorrect	Ambiguous [a]	Unobserved [b]	Correct	Incorrect	Ambiguous [a]	Unobserved [b]			
Proximal ulna												
Olecranon-coronoid angle	66 (44.0%)	30 (**41.7%**)	2 (2.8%)	0%	40 (55.6%)	8 (**10.3%**)	26 (33.3%)	0%	44 (56.4%)	4*	28 (18.7%)	25.3%
Pelvic girdle												
Overall Pelvis morphology	140 (93.3%)	54 (75.0%)	14 (19.4%)	0%	4 (5.6%)	62 (79.5%)	10 (12.8%)	0%	6 (7.8%)	61	24 (16%)	**77.3%**
Pelvic brim	139 (92.7%)	51 (70.8%)	16 (22.2%)	0%	5 (6.9%)	63 (**80.8%**)	9 (11.5%)	0%	6 (8.0%)	57	25 (16.7%)	76.0%
Subpubic shape	130 (86.7%)	56 (**77.8%**)	10 (13.9%)	0%	6 (8.3%)	52 (66.7%)	12 (15.4%)	0%	14 (18.0%)	57	22 (15.7%)	72.0%
Obturator foramen shape	128 (85.3%)	56 (**77.8%**)	6 (8.3%)	0%	10 (13.9%)	55 (70.5%)	11 (14.1%)	0%	12 (15.4%)	70	17 (11.3%)	74.0%
Subpubic contour	123 (82.0%)	50 (69.4%)	8 (11.1%)	8 (11.1%)	6 (8.3%)	41 (52.6%)	10 (12.8%)	6 (7.7%)	21 (26.9%)	49	18 (12%)	60.7%
Ventral arc	128 (85.3%)	55 (76.4%)	7 (9.7%)	5 (6.9%)	5 (6.9%)	49 (62.8%)	8 (10.3%)	4 (5.1%)	17 (21.8%)	67	15 (10%)	69.3%
Acetabulum position	130 (86.7%)	51 (70.8%)	13 (18.1%)	0%	8 (11.1%)	52 (66.7%)	14 (17.9%)	0%	12 (15.4%)	44	27 (18%)	68.7%
Ilium morphology	133 (88.7%)	46 (63.9%)	18 (25%)	0%	8 (11.1%)	61 (78.2%)	7 (9.0%)	0%	10 (12.8%)	53	25 (16.7%)	71.3%

Table 4.7: Continued…

Skeletal trait	Total classified Scans	Male sex classifications				Female sex classifications				Chi-squared statistic [c]	Total incorrect	Combined correct sex
		Correct	Incorrect	Ambiguous [a]	Unobserved [b]	Correct	Incorrect	Ambiguous [a]	Unobserved [b]			
Sacrum												
Sacrum morphology	25 (16.7%)	15 (**20.8%**)	2 (2.8%)	0%	55 (76.4%)	7 (**9%**)	1 (1.3%)	0%	70 (89.7%)	14	3 (2%)	**14.7%**
Femur												
Femoral neck shaft angle	53 (35.3%)	19 (**26.4%**)	10 (13.9%)	0%	43 (59.7%)	18 (**23.1%**)	6 (7.7%)	0%	54 (69.2%)	9	16 (10.7%)	**24.7%**

a: Skeletal traits scored as 3 and therefore not classified as either ‘male’ or ‘female’.

b: Count and frequencies of not observed and/or scored traits from assessed Lodox scan, thus sex classification was not conducted.

c: Chi-squared statistics with degrees of freedom = 1, for predicted sex classifications vs documented sexes.

*: Fishers Exact statistics. Bold and underlined Chi-square/Fishers Exact statistic values indicate no statistical significance (p-value ≥ 0.05).

Bold percentages indicate the highest accuracy amongst traits for a particular skeletal element.

4.4.2. Sex classification accuracies per scorable skeletal traits

4.4.2.1. Skull traits

Based on the morphological sex classification of scorable skull traits from a subset of scorable skull traits per assessed Lodox scans, a narrow range of accuracy rates were observed compared to a range of accuracies observed in section 4.4.1.1 (Table 4.6). Overall, correct classification for males ranged from 69.9% to 87.0%, while it ranged from 76.1% to 100% for females (Table 4.8). The mastoid process proved to be the most accurate trait for classifying males, achieving an 87% correct classification rate (20/23). In contrast, it was slightly less accurate for females, with an 82.4% success rate (28/34). While orbit shape was the second most accurate trait for males at 75.4% (52/69), it had the lowest accuracy for females at 76.1% (54/71) and the highest incorrect classification rate at 23.9%. Contrarily, the frontal eminence was perfectly accurate for females (100%, 4/4) but was the second-lowest for males at 71.4% (5/7). When considering the overall skull morphology, females were more accurately classified at 84.4% (58/69) compared to males at 74.2% (46/72). The parietal eminence was the least reliable for males, with a 69.9% accuracy rate (58/83), and the second-lowest for females at 82.2% (37/45). The mental eminence also showed low accuracy, ranking as the second-lowest for both males (70.2%, 40/57) and females (77.2%, 44/57) (Table 4.8).

Overall, morphological sex estimation based on skull traits showed varying degrees of combined correct classification accuracy. The mastoid process had the highest accuracy at 84.2% (48/57) from a subset of scorable traits. The frontal eminence ranked second with an accuracy of 81.8% (9/11), followed by overall skull morphology (79.4%, 104/131). In contrast, orbit shape and the parietal eminence yielded the lowest combined accuracies for cranial traits, at 75.5% (106/140) and 74.2% (95/128) respectively, while the mental eminence yielded the lowest combined sex classification accuracy among all assessed traits skull traits, at 73.7% (84/114).

Table 4.8: Predicted sex classification counts and accuracy rates (in brackets) for sex estimation of morphologically observable and scorable skull traits from Lodox scans.

Skeletal trait	Total sex classified scans [a]	Male classifications*				Female classifications*				Combined correct sex
		Correct	Incorrect	Ambiguous [b]	Total male with classified scans [c]	Correct	Incorrect	Ambiguous [b]	Total female with classified scans [c]	
Cranium										
Overall skull morphology	131 (87.3%)	46 (74.2%)	16 (25.8%)	0%	62 (47.3%)	58 (84.1%)	11 (15.9%)	0%	69 (52.7%)	79.4%
Mastoid process	57 (38%)	**20 (87.0%)**	3 (13.0%)	0%	23 (40.4%)	28 (82.4%)	6 (17.6%)	0%	34 (59.6%)	**84.2%**
Frontal eminence	11 (7.3%)	5 (71.4%)	2 (28.6%)	0%	7 (63.6%)	**4 (100%)**	0%	0%	4 (36.4%)	81.8%
Parietal eminence	128 (85.3%)	58 (69.9%)	25 (30.1%)	0%	83 (64.8%)	37 (82.2%)	8 (17.8%)	0%	45 (35.2%)	74.2%
Orbital bone shape	140 (93.3%)	52 (75.4%)	17 (24.6%)	0%	69 (49.3%)	54 (76.1%)	17 (23.9%)	0%	71 (50.7%)	75.7%
Mandible										
Mental eminence	114 (76.0%)	**40 (70.2%)**	12 (21.1%)	5 (8.8%)	57 (50.0%)	**44 (77.2%)**	11 (19.3%)	2 (19.3%)	57 (50.0%)	**73.7%**

*: Non-scoreable skeletal traits were excluded from these calculations.

a: Chi-squared statistics are the same as those reported in Table 4.6.

b: Skeletal traits scored as 3 and therefore not classified as either ‘male’ or ‘female’.

c: Total and accuracy of classified males/females for a particular trait from a sub-set of Lodox scans with scorable respective trait (i.e., Total sex classified scans).

Bold percentages indicate the highest accuracy amongst traits for a particular skeletal element for each sex and combined classification accuracy.

4.4.2.2. Postcranial traits

An evaluation of morphological sex classification from scorable postcranial traits on a subset of sex classified Lodox scans yielded a slightly different range of accuracies compared to the total study sample data (Section 4.4.1.2, Table 4.7). For males, the range of correct classifications was 50.0% to 93.8%, although the suprascapula notch was an exception with a 0% correct male classification rate. Female correct classification accuracies had broader ranges, ranging from 23.5% to 100% (Table 4.9).

4.4.2.2.1. Scapula

In contrast to the findings in Section 4.4.1.2, sex classification based on scapula morphology yielded some of the highest accuracies, particularly for females, based on a subset of scorable respective scapula traits. The infraspinous fossa's medial border achieved a perfect 100% female classification accuracy (14/14 classified as females), and the suprascapula notch was highly accurate at 95.2% (40/42 classified as females). However, these same traits were notably poor for male classification (Table 4.9). The suprascapula notch had a 0% male classification accuracy (0/26 classified as males), while the infraspinous fossa's medial border showed only 50.0% accuracy (3/6 classified as males). These were the lowest and second-lowest male correct classification accuracies observed across all postcranial traits. Contrary to the above-mentioned scapula traits, the infraspinous fossa's lateral border had the lowest female classification accuracy among the scapula traits at 67.2% (43/64 classified as females), however, the highest male classification accuracy (66.7%, 38/57 classified as males).

4.4.2.2.2. Pelvic girdle

The traits of the pelvic girdle consistently provided the highest male and female sex classification accuracies compared to other postcranial traits, with ranges of 71.9% to 90.3% for males and 71.9% to 89.7% for females (Table 4.9). Similar to the findings in section 4.4.1.2, the obturator foramen shape and subpubic shape yielded the highest male classification accuracies among the pelvic traits. The obturator foramen shape was the most accurate pelvic trait for male classification (second highest amongst postcranial traits), achieving 90.3% accuracy (56/62 classified as males) with a low 9.7% incorrect classification rate. The subpubic shape was the second most accurate, with 84.8% (56/66 classified as males) male classification accuracy, but had a higher incorrect classification rate of 15.2%. In contrast to Section 4.4.1.2, the ventral arc provided a high classification accuracy for males, reaching 82.1% (55/67 classified as males) with a 10.4% incorrect rate. The remaining male classification accuracies for pelvic traits ranged from 71.9%

(ilium morphology) to 79.7% (acetabular position). Incorrect classification rates for these traits varied from 12.1% (subpubic contour) to 28.1% (ilium morphology). The subpubic contour and ventral arc were the only pelvic traits to have ambiguous classifications for males, at 12.1% and 7.5%, respectively.

For females, ilium morphology provided the highest classification accuracy at 89.7% (61/68 classified as females), followed by the pelvic brim at 87.5% (63/72 classified as females) and the overall pelvis morphology at 86.1% (62/72 classified as females). Ilium morphology also had the lowest incorrect classification rate at 10.3%, followed by pelvic brim morphology at 12.5%. In contrast, the subpubic contour achieved the lowest female classification accuracy among the pelvic traits at 71.9% (41/57), with an incorrect rate of 17.5%. The remaining female classification accuracies ranged from 78.8% (acetabulum position) to 83.3% (obturator foramen). Like the male classifications, the subpubic contour and ventral arc were the only traits with ambiguous female classifications, at 10.5% and 6.6%, respectively.

4.4.2.2.3. Distal humerus

In comparison to the findings in Section 4.4.1.2, sex classification based on scorable distal humerus traits demonstrated higher classification accuracies (Table 4.9). The trochlea constriction and trochlea symmetry both yielded the highest male classification accuracy at 77.4% (24/31 classified as males) with 22.6% incorrect classification rates. The olecranon fossa shape followed with a male classification accuracy of 73.9% (34/46 classified as males), accompanied by a 23.9% incorrect and a 2.2% ambiguous classification rate. For females, the olecranon fossa shape provided the highest accuracy at 72.6% (45/62 classified as females), with the lowest incorrect (24.2%) and ambiguous (3.2%) classification rates among the humerus traits. In contrast, trochlea symmetry and trochlea constriction had a lower accuracy of 65.9% for both (27/41 classified as females), with trochlea constriction having the highest incorrect (31.0%) and ambiguous (7.1%) classification rates. Trochlea symmetry achieved the second highest incorrect and ambiguous classifications at 29.3% and 4.9%, respectively.

4.4.2.2.4. Remaining postcranial traits

Morphological sex classification for the remaining postcranial traits, based on a subset of scorable traits, showed a wide range of accuracies, with ranges of 65.5% to 93.8% for males and 23.5% to 87.5% for females (Table 4.9). The olecranon-coronoid angle was the most effective single trait for male classification, achieving the highest accuracy at 93.8% (30/32 classified as males) (the highest amongst all postcranial traits). This was followed by the morphology of the sacrum at 88.2% (15/17 classified as males), the costal cartilage ossification pattern at 81.8% (9/11 classified

as males), and the femoral neck shaft angle at 65.5% (19/29 classified as males). Notably, these traits showed higher classification accuracies in this analysis compared to those in section 4.4.1.2. For females, the sacrum provided the highest classification accuracy at 87.5% (7/8 classified as females). The femoral neck shaft angle was the next most accurate at 75% (18/24 classified as females). However, the costal cartilage ossification pattern yielded a much lower accuracy of 47.4% (9/19 classified as females), while the olecranon-coronoid angle performed poorly for females, with a classification accuracy of 23.5% (8/34 classified as females).

4.4.2.2.5. Combined correct classification accuracies

Overall, the sacrum provided the highest combined sex classification accuracy among all postcranial traits, at 88.0% (22/25 classified scan). In contrast, the olecranon-coronoid angle had the lowest combined classification accuracy at 57.6% (38/66 classified scans). The pelvic traits consistently yielded high combined classification accuracies, ranging from 74.0% to 86.7% (Table 4.9). In contrast to the findings in section 4.4.1.2, the obturator foramen shape achieved the highest combined accuracy among pelvic traits and the second-highest among all postcranial traits, at 86.7% (111/128 classified scans). This was followed by the subpubic shape at 83.1% (108/130 classified scans). Similar to section 4.4.1.2, the subpubic contour yielded the lowest combined classification accuracy for a pelvic trait, though at a slightly improved 74.0% (91/123 classified scans). The infraspinous fossa's medial border delivered the third-highest combined classification accuracy at 85.0% (17/20 classified scans), representing a significant increase over the total study sample (Table 4.7). The remaining postcranial traits had moderate combined accuracies, ranging from 58.8% for the suprascapula notch (40/68 classified scans) to 73.1% for the olecranon fossa shape (79/108 classified scans) (Table 4.9).

Table 4.9: Predicted sex classification counts and accuracy rates (in brackets) for sex estimation of morphologically observable and scorable postcranial traits from certain Lodox scans.

Skeletal trait	Total sex classified scans [a]	Male classifications*				Female classifications*				Combined correct sex
		Correct	Incorrect	Ambiguous [b]	Total males with classified scans [c]	Correct	Incorrect	Ambiguous [b]	Total females with classified scans [c]	
Scapula										
Suprascapula notch	68 (45.3%)	0%	24 (92.3%)	2 (7.7%)	26 (38.2%)	40 (95.2%)	2 (4.8%)	0%`	42 (61.8%)	58.8%
Infraspinous fossa lateral border	121 (80.7%)	**38 (66.7%)**	19 (33.3%)	0%	57 (47.1%)	43 (67.2%)	21 (32.8%)	0%	64 (52.9%)	66.9%
Infraspinous fossa medial border	20 (13.3%)	3 (50.0%)	3 (50.0%)	0%	6 (30.0%)	**14 (100%)**	0%	0%	14 (70.0%)	**85.0%**
Rib costal cartilage										
Costal cartilage ossification pattern	27 (18%)	**9 (81.8%)**	1 (9.1%)	1 (9.1%)	11 (36.7%)	**9 (47.4%)**	6 (31.6%)	4 (21.1%)	19 (63.3%)	**60.0%**
Distal humerus										
Olecranon fossa shape	108 (72%)	34 (73.9%)	11 (23.9%)	1 (2.2%)	46 (42.6%)	**45 (72.6%)**	15 (24.2%)	2 (3.2%)	62 (57.4%)	**73.1%**
Trochlea constriction	73 (48.7%)	**24 (77.4%)**	7 (22.6%)	0%	31 (42.5%)	26 (61.9%)	13 (31.0%)	3 (7.1%)	42 (57.5%)	68.5%
Trochlea symmetry	72 (48.0%)	**24 (77.4%)**	7 (22.6%)	0%	31 (43.1%)	27 (65.9%)	12 (29.3%)	2 (4.9%)	41 (56.9%)	70.8%

Table 4.9: Continued…

Skeletal trait	Total sex classified scans [a]	Male classifications*				Female classifications*				Combined correct sex
		Correct	Incorrect	Ambiguous [b]	Total males with classified scans [c]	Correct	Incorrect	Ambiguous [b]	Total females with classified scans [c]	
Proximal ulna										
Olecranon-coronoid angle	66 (44/0%)	**30 (93.8)**	2 (6.3%)	0%	32 (48.5%)	**8 (23.5%)**	26 (76.5%)	0%	34 (51.5%)	**57.6%**
Pelvic girdle										
Overall Pelvis morphology	140 (93.3%)	54 (79.4%)	14 (20.6%)	0%	68 (48.6%)	62 (86.1%)	10 (13.9%)	0%	72 (51.4%)	82.9%
Pelvic brim	139 (92.7%)	51 (76.1%)	16 (23.9%)	0%	67 (48.2%)	63 (87.5%)	9 (12.5%)	0%	72 (51.8%)	82.0%
Subpubic shape	130 (86.7%)	56 (84.8%)	10 (15.2%)	0%	66 (50.8%)	52 (81.3%)	12 (18.8%)	0%	64 (49.2%)	83.1%
Obturator foramen shape	128 (85.3%)	**56 (90.3%)**	6 (9.7%)	0%	62 (48.4%)	55 (83.3%)	11 (16.7%)	0%	66 (51.6%)	**86.7%**
Subpubic contour	123 (82.0%)	50 (75.8%)	8 (12.1%)	8 (12.1%)	66 (53.7%)	41 (71.9%)	10 (17.5%)	6 (10.5%)	57 (46.3%)	74.0%
Ventral arc	128 (85.3%)	55 (82.1%)	7 (10.4%)	5 (7.5%)	67 (52.3%)	49 (80.3%)	8 (13.1%)	4 (6.6%)	61 (47.7%)	81.3%
Acetabulum position	130 (86.7%)	51 (79.7%)	13 (20.3%)	0%	64 (49.2%)	52 (78.8%)	14 (21.2%)	0%	66 (50.8%)	79.2%
Ilium morphology	133 (88.7%)	46 (71.9%)	18 (28.1%)	0%	64 (48.5%)	**61 (89.7%)**	7 (10.3%)	0%	68 (51.5%)	81.1%

Table 4.9: Continued…

Skeletal trait	Total sex classified scans [a]	Male classifications*				Female classifications*				Combined correct sex
		Correct	Incorrect	Ambiguous [b]	Total males with classified scans [c]	Correct	Incorrect	Ambiguous [b]	Total males with classified scans [c]	
Sacrum										
Sacrum morphology	**25 (16.7%)**	**15 (88.2%)**	2 (11.8%)	0%	17 (68.0%)	**7 (87.5%)**	1 (12.5%)	0%	8 (32.0%)	**88.0%**
Femur										
Femoral neck shaft angle	53 (35.3%)	**19 (65.5%)**	10 (34.5%)	0%	29 (54.7%)	**18 (75.0%)**	6 (25.0%)	0%	24 (45.3%)	**69.8%**

*: Non-scoreable skeletal traits were excluded from these calculations.

a: Chi-squared statistics are the same as those reported in Table 4.6.

b: Skeletal traits scored as 3 and therefore not classified as either ‘male’ or ‘female’.

c: Total and accuracy of classified males/females for a particular trait from a sub-set of Lodox scans with scorable respective trait (i.e., Total sex classified scans).

Bold percentages indicate the highest accuracy amongst traits for a particular skeletal element for each sex and combined classification accuracy.

4.4.3. Sex classification accuracies per skeletal element

The average sex classification accuracy of visually scorable skeletal traits, per observable skeletal element, was calculated to identify the most accurate skeletal element for morphological sex estimation from Lodox scans. To identify the most accurate skeletal element for sex estimation, this evaluation used two types of calculations to compare the average sex classification accuracy of skeletal elements, firstly compared against the total study sample (Figure 4.4) and secondly a subset of classified Lodox scans that excluded unobservable skeletal traits (Figure 4.5)..

Morphological sex classification accuracy from assessed Lodox scans varied across assessed skeletal elements. The pelvic girdle achieved the highest average correct sex estimation from the total study sample compared to the other assessed skeletal elements (71.2%, 107/150), with the mandible (56.0%, 84/150) performing slightly better than the cranium (48.3%, 72/150). Average classification accuracies for other skeletal elements ranged from 12.0% (low rib costal cartilages, 18/150) to 40.0% (distal humerus, 40/150) (Figure 4.4). Furthermore, the proximal ulna had the highest rate of incorrect sex classification (18.7%) from assessed Lodox scans, while other skeletal elements ranged from 2.0% (sacrum) to 15.3% (mandible and scapula) in incorrect classification rates (Figure 4.4). The mandible had the highest rate of ambiguous classifications at 4.7%, followed rib costal cartilages (3.3%), pelvic girdle (1.9%), distal humerus (1.8%) and scapula (0.4%). Average sex classification from the remaining skeletal elements; cranium, proximal ulna, sacrum, and femur, yielded no ambiguous classification (0%) of respective skeletal traits (Figure 4.4).

Similarly, morphological sex classification accuracy from a subset of Lodox scans with scorable skeletal traits varied among skeletal elements. However, average correct classification accuracies from the subsets were notably higher than those observed when evaluating the total study sample (Figurem4.5). For instance, the sacrum yielded the highest average correct classification accuracy at 88.0% (22/25), followed by the pelvic girdle (81.3%, 107/131), and the cranium (79.9%, 74/93). Sex classification using proximal ulna traits yielded the lowest average correct classification accuracy (57.6%, 38/66). The average correct classification accuracies of the remain skeletal elements ranged between 60.0% (low ribs costal cartilages) and 73.7% (mandible) (Figure 4.5). Proximal ulna had the highest average incorrect classification accuracy (42.4%), while other skeletal elements ranged from 12.0% (sacrum) to 30.2% (femur) (Figure 4.5). Low ribs costal cartilages yielded the highest average ambiguous classification of 16.7%, followed by the mandible (6.1%), distal humerus (3.2%), pelvic girdle (2.3%), and scapula (1.0%). Likewise, average sex classification from the cranium, proximal ulna, sacrum, and femur, yielded no ambiguous classification (0%) of respective skeletal traits (Figure 4.5).

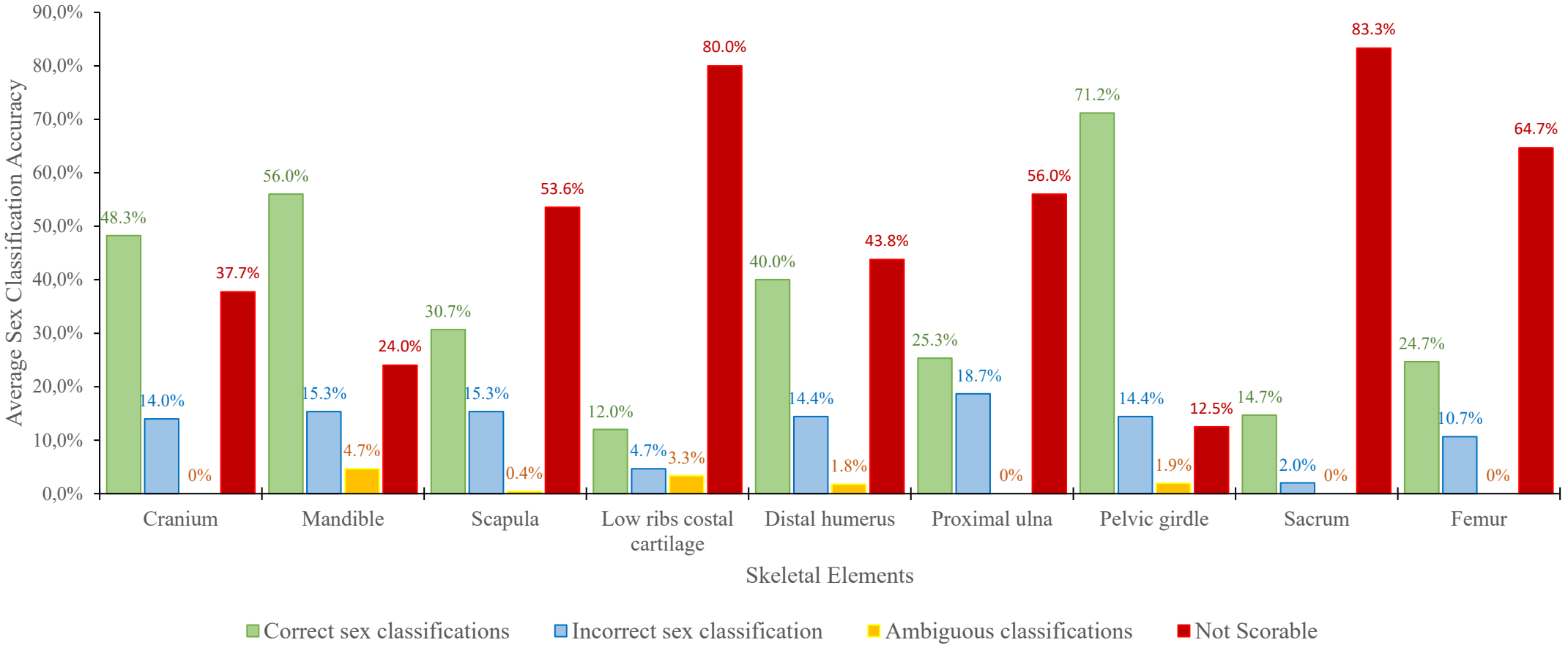


Figure 4.4: Visual representation of average sex classification accuracy of skeletal elements with scorable skeletal traits.

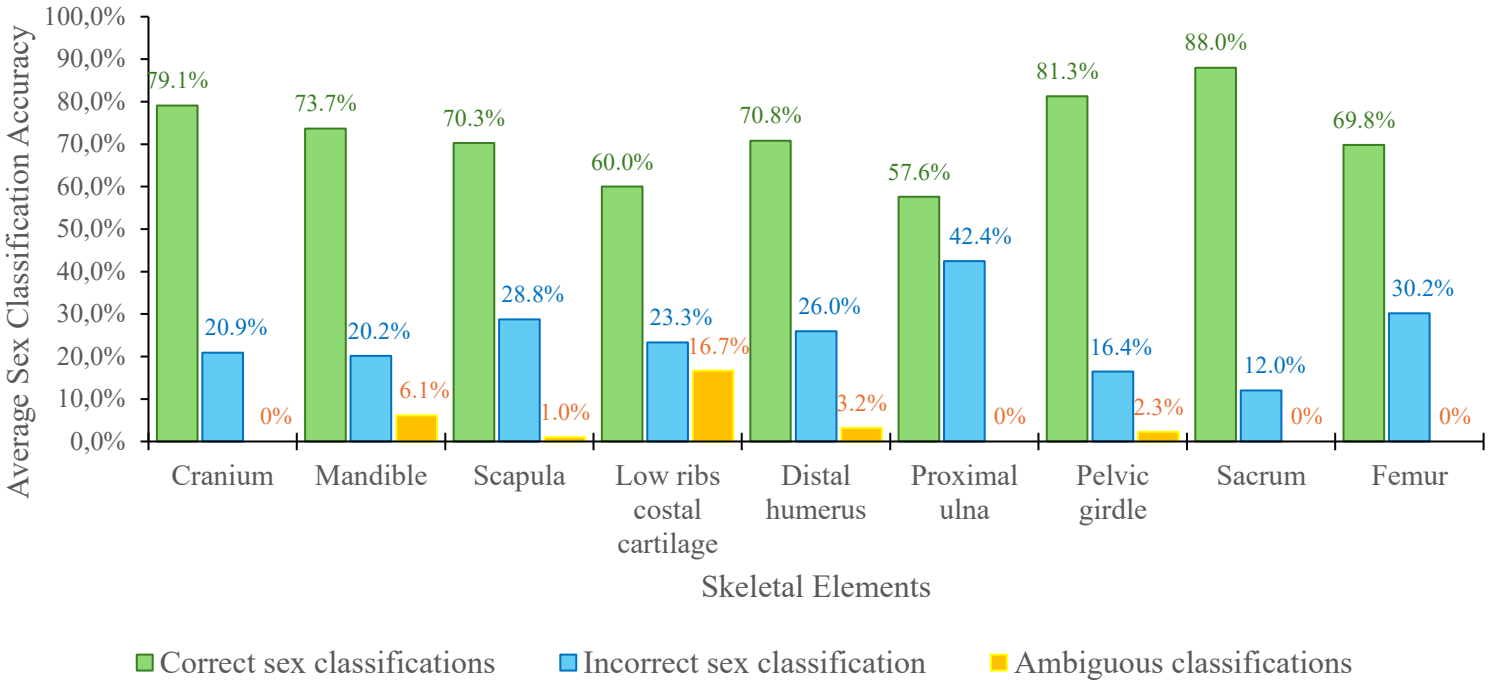


Figure 4.5: Visual representation of average sex classification accuracy of skeletal elements with scorable skeletal traits. Non-scorable elements and traits were excluded from these calculations.

4.4.4. Skeletal traits with over 75% sex classification accuracy

Although there is no universally fixed threshold for 'acceptable' sex classification accuracy due to variations in population, methodology, and statistical factors, studies frequently emphasize achieving accuracy rates above 80.0% (Mello-Gentil & Souza-Mello, 2022). Additionally, research indicates that applying posterior probability-informed thresholds (i.e., certainty levels between 0.75 and 0.95 before assigning sex) can yield accuracy rates significantly above chance (>50%), exceeding 75% for correct sex classification, therefore considered adequate for sex estimation (Jerković *et al.,* 2020; Avent *et al.,* 2022; Pilmann Kotěrová *et al.,* 2024). As such, a threshold of 75.0% correct classification was deemed as an acceptable accuracy for sex classification in the current study, as it aligns with posterior probabilities associated with accuracy rates significantly greater than 50.0% and not due to random chance (Avent *et al.,* 2022).

Out of the assessed skull and postcranial skeletal traits, only seven demonstrated the potential for accurate correct sex classification, achieving over 75.0% classification accuracy for males and/or females when evaluated from the total study sample (n = 150, i.e., parietal eminence, overall pelvis morphology, pelvic brim, subpubic shape, obturator foramen shape, ventral arc, and ilium morphology) (Figure 4.6). Of these skeletal traits, only the overall pelvis morphology exhibited correct sex classification accuracy exceeding 75.0% for both males and females, while the

remaining six traits demonstrated accuracy above this threshold in at least one sex (Figure 4.6). Of the skull traits, only parietal eminence morphology achieved a sex classification accuracy greater than 75.0%, specifically for males (80.6%).

When morphological sex classification was evaluated from a subset of Lodox scans with scorable skeletal traits, both skull and postcranial elements demonstrated a high potential for accurate sex estimation. All skull traits achieved over 75.0% classification accuracy for either males, females, or combined classifications (Table 4.8). Similarly, postcranial traits performed well, with only three traits (infraspinous fossa's lateral border, olecranon fossa shape, and femoral neck shaft angle) achieving below 75.0% classification accuracy for any sex or combined classifications (Table 4.9).

Male parietal eminences were observed to be less prominent (Table 4.10 A) compared to the more protruding female parietal eminences (Table 4.10 B). The morphologies of male pelves were larger overall (i.e., overall pelvis morphology), characterized by a narrow ilium and minimal flair (Table 4.11 A and C), while female pelves were smaller with broader ilia (Table 4.9 B and D). Moreover, male pelves (Table 4.11 C) had oval pelvic brims, V-shaped subpubic angles, and an ovoid obturator foramen shape, while female pelves (Table 4.11 B) were characterized by round/elliptical pelvic brims, U-shaped subpubic angles, and a triangular obturator foramen shape. Furthermore, the pubic bone in male pelves (Table 4.11 C) displayed a steep, straight subpubic contour and lacked a prominent ventral arc. Female pelves (Table 4.11 D), however, were characterized by a concave subpubic contour and a prominent ventral arc.

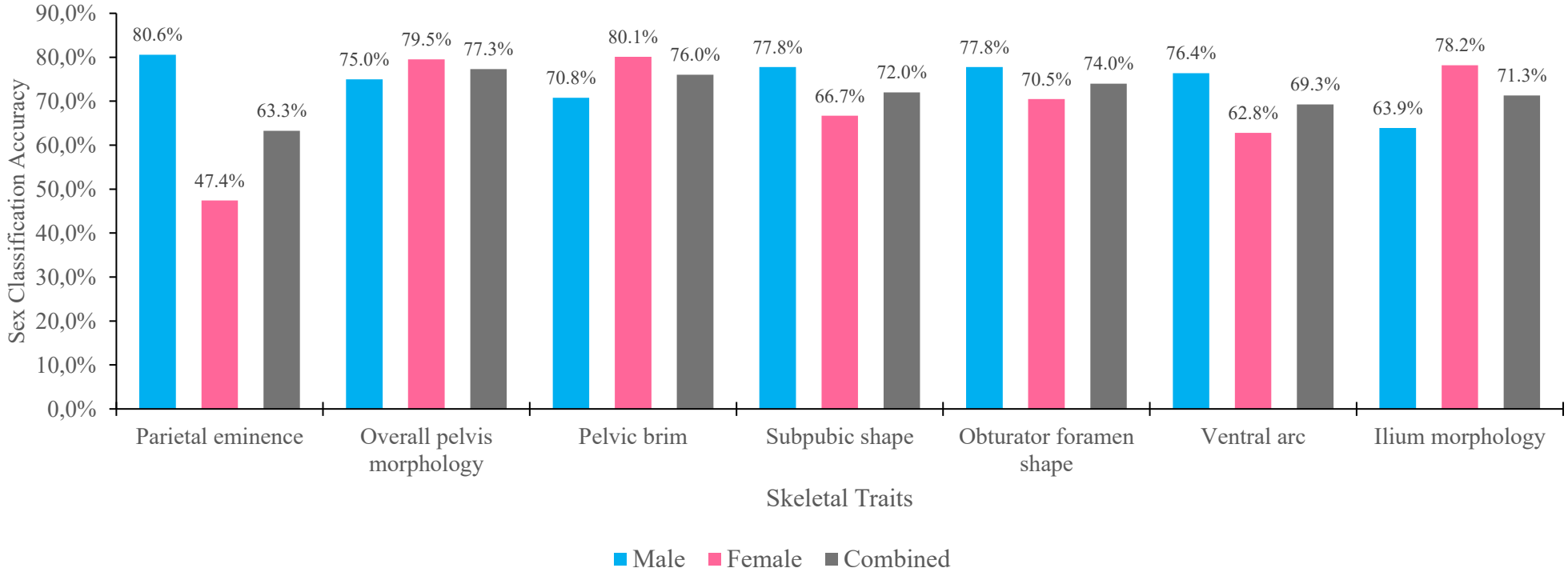


Figure 4.6: Visual representation of skeletal traits with at least over 75% correct sex classification accuracy either for males or females, or both sexes.

Table 4.10: Lodox® Statscan™ images illustrating male and female skulls and associated morphological skeletal traits.

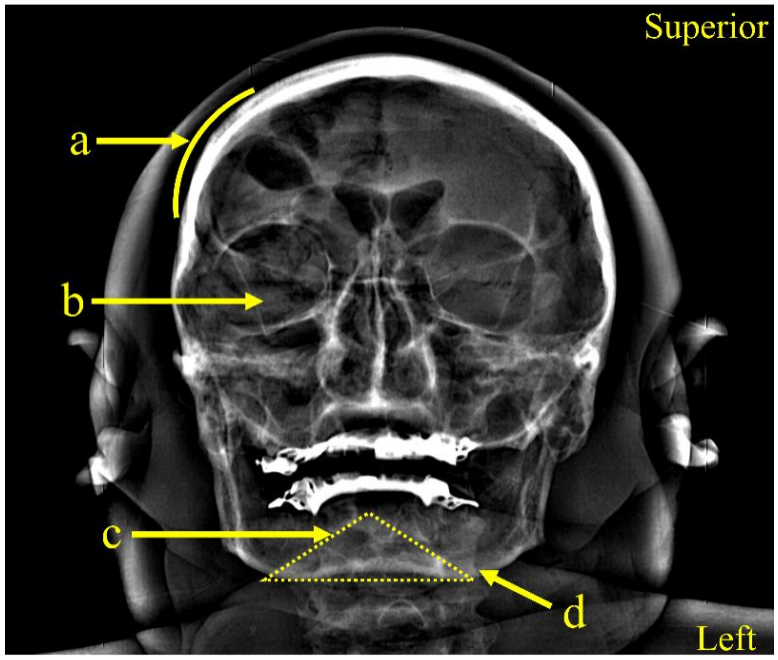
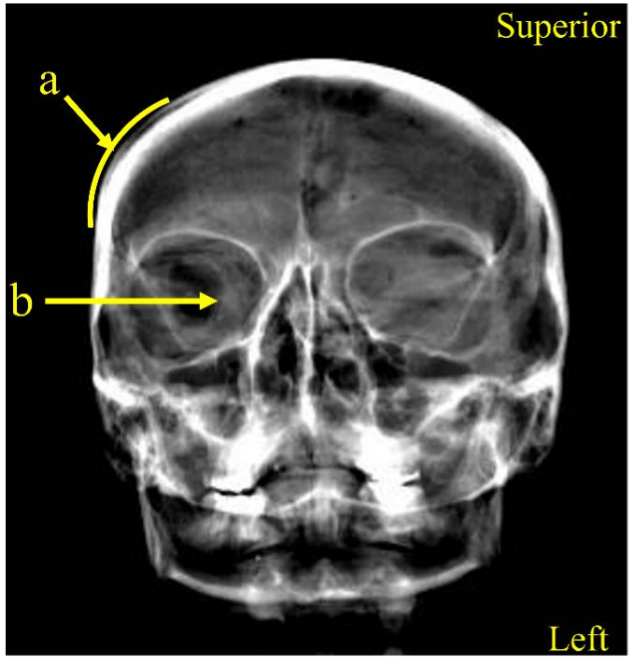
Skeletal Elements	Males	Females	Label descriptions
Skull	A 	B 	a = Parietal eminence b = Orbit shape c = Mental eminence d = Mental tubercle

Table 4.11: Lodox® Statscan™ images illustrating male and female pelves and associated morphological skeletal traits.

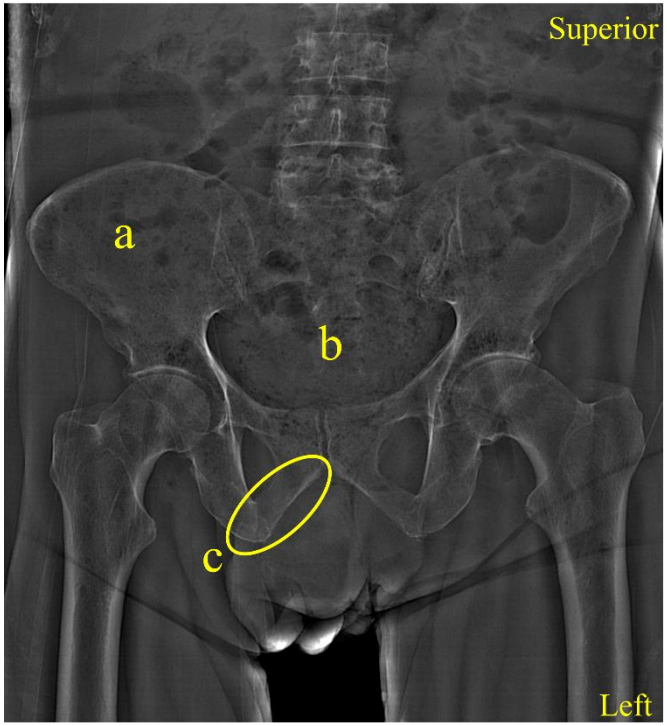
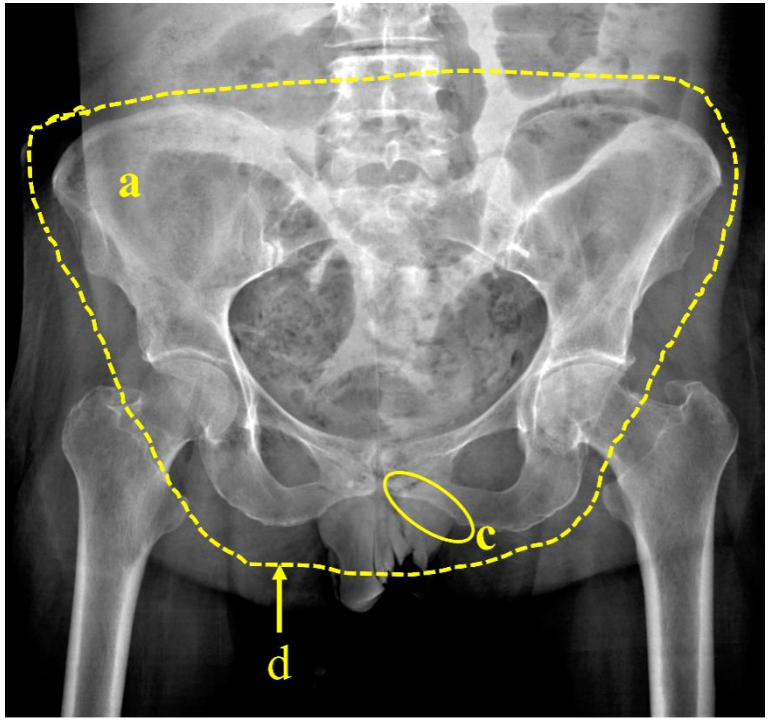
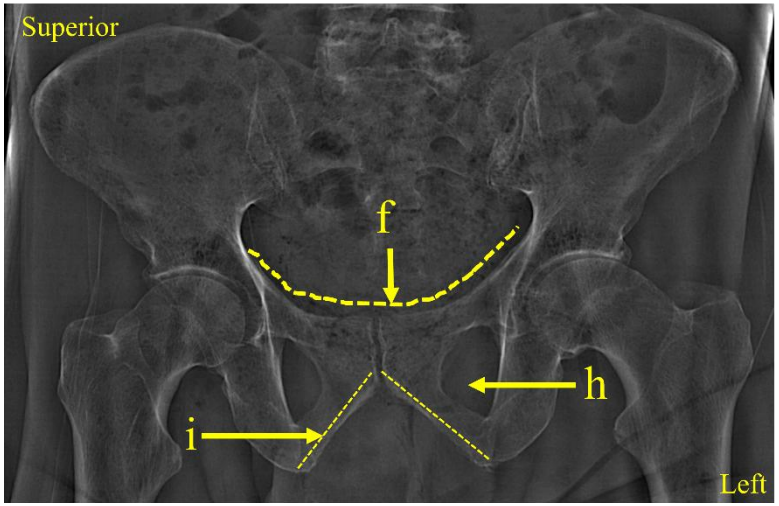
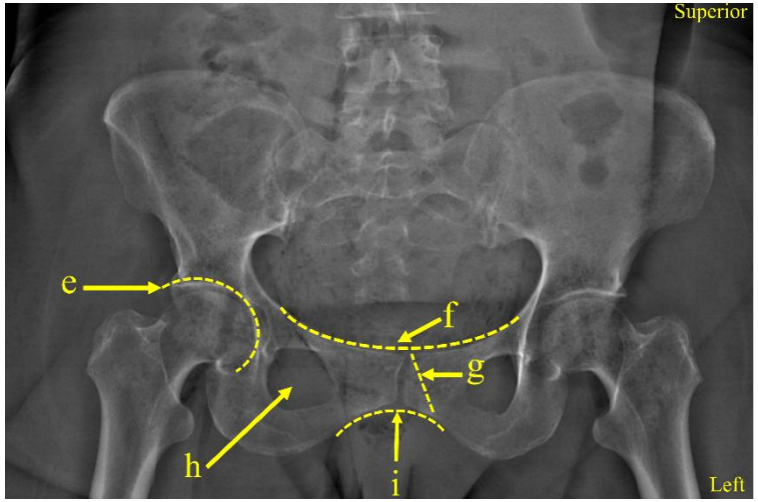
Skeletal Element	Males	Females	Label descriptions
Pelvis	A 	B 	a = Ilium morphology b = Sacrum morphology c = Subpubic contour d = Overall pelvis morphology

Table 4.12: Continued…

Skeletal Element	Males	Females	Label descriptions
Pelvis	C 	D 	e = Acetabulum position f = Pelvic brim g = Ventral arc h = Obturator foramen shape i = Subpubic shape

CHAPTER 5: DISCUSSION

Technological advances in digital photography have promoted the incorporation of radiographs in forensic anthropology to aid with the estimation of biological profile of human remains recovered in a medico-legal context (Garvin & Stock, 2016; Krishan *et al.,* 2016; Rowbotham & Blau, 2020; Zhang, 2022). Computed Tomography (CT) is a commonly utilised radiographic modality in forensic anthropology for anthropological analyses of human remains due to its detailed imaging and provision of 3D images of skeletal remains, allowing forensic anthropologists to examine bone structures and subtle fractures (in trauma analyses) for potential biological profile estimation (Teodoru-Raghina *et al.,* 2017; Rowbotham & Blau, 2020; Zhang, 2022). In addition, CT scans have demonstrated sex classification accuracy rates that are similar to those obtained through traditional metric and morphological dry bone analysis methods (Giurazza *et al.,* 2013; Mehta *et al.,* 2015; Garvin & Stock, 2016; Bertsatos *et al.,* 2020; Gillet *et al.,* 2020; Setiawati *et al.,* 2023; Maijanen *et al.,* 2024). However, CT scanners are expensive to obtain and maintain compared to x-ray modalities, and they involve higher radiation exposure that may pose health risks to staff operators (Safety, 2012; Garvin & Stock, 2016). Furthermore, CT scanners require specialized equipment, software, and operator expertise, including training in machine operation and CT scan interpretation (Schneider *et al.,* 2015; Garvin & Stock, 2016; Aldoihi & Hammami, 2018), as detailed above in the introduction/literature chapters. As such, Lodox® Systems modalities currently represent significant alternatives to how x-ray images could be utilised for forensic anthropological analyses of human remains, especially in South African medico-legal facilities (Boffard *et al,* 2006; Evangelopoulos *et al.,* 2009; Bernitz & Verster, 2017; du Plessis *et al.,* 2020). While the use of Lodox® Systems modalities (e.g., Lodox® Statscan™ and Lodox® Xmplar-dr™) has been well documented for skeletal imaging and skeletal trauma assessment (Boffard *et al.,* 2006; Pitcher *et al.,* 2008; du Plessis *et al.,* 2020; Morele *et al.,* 2024), their application for morphological skeletal sex estimation has not yet been explored. Therefore, the current study assessed the reliability and feasibility of the Lodox® Statscan™ to visualize skeletal elements and traditional skull and postcranial morphological traits from Lodox scans of adult individuals of European ancestry for morphological sex estimation.

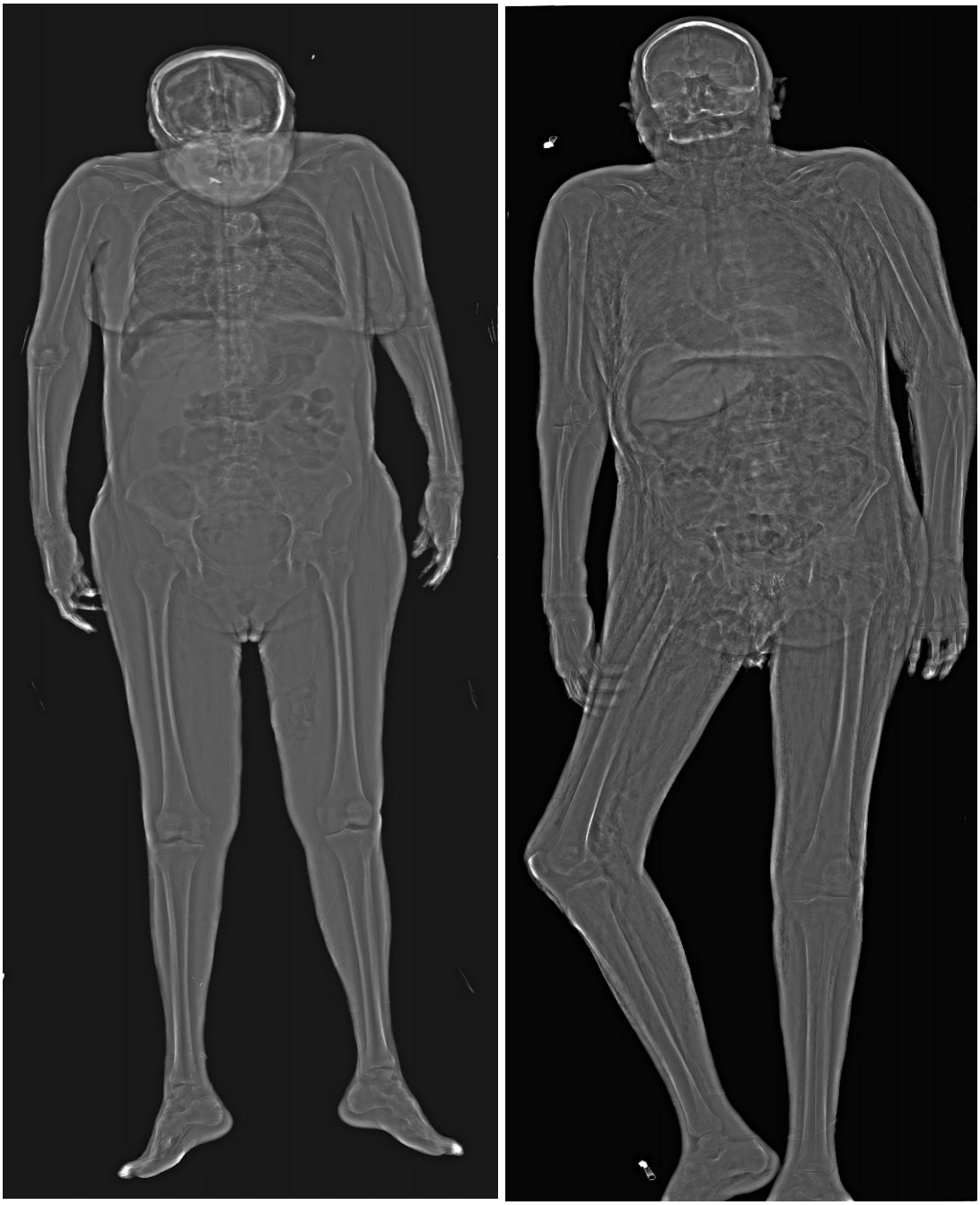
Therefore, this chapter discusses the study findings, by outlining and discussing the frequencies of skeletal elements and associated traits observable from Lodox scans, alongside the feasibility to morphological score such traits. Following this, observer repeatability is evaluated to determine the reliability and accuracy of Lodox scan-based skeletal trait observations, scoring and sex estimation. Finally, the limitations of Lodox scans for morphological sex estimation are addressed, specifically highlighting those encountered during this research.

5.1. Observability and Scorability of Skeletal Elements and Traits

5.1.1. Skeletal elements observability

The present study found that eight of the ten assessed skeletal elements were observable in over 88% (n =150 scans) of the assessed Lodox scans (i.e., cranium, mandible, clavicle, scapula, distal humerus, proximal ulna, pelvis, and femur). The observability frequencies of the rib costal cartilages (43.3%) and sacrum (28.7%) from Lodox scans were relatively poor, most likely due to the elements being less radiopaque and being obscured by the presence of soft tissues, interfering with their visibility on x-ray scans (Figure 5.1).

The cranium and pelvis showed the highest observability frequencies, each visible in 99.3% of the 150 scans. The 0.7% non-observability of the cranium resulted from a single scan where the cranium was dissected cross-sectionally in a transverse section, creating a view that shows the interior cranial base rather than the outer surface of the cranium (Figure 5.1 A). The 0.7% non-observability of the pelvis was due to excessive soft tissue (likely fat and muscle) obscuring the pelvic region in one scan (Figure 5.1 B). Soft tissue interference in addition to image distortion and 2D superimposed anatomical structures hindered the observability of other skeletal elements, including the distal humerus (98.0%), femur (96.7%), clavicle (92.0%), scapula (91.3%), proximal ulna (90.0%), and mandible (88.0%), consequently preventing 100% observability across these elements. Despite these limitations, the current study demonstrates that minimal soft tissue interference, image distortion and superimposed anatomical structures can yield high observation frequencies for skeletal elements observed from Lodox scans, especially those with high radiopacity.



A B

Figure 5.1: Lodox scans that represent 1% non-observability of the cranium (A) and pelvis (B). Evident in image A is a cross-sectionally dissected cranium, creating a view that shows the interior cranial base. Also, evident in image B is an example of low patient contrast, extensive soft tissue presence throughout the individual's body and a bent knee, indicating an individual not scanned in a standard anatomical position. Siding: Left is towards the right.

5.1.2. Skeletal traits observability

Morphological skeletal traits associated with the above-mentioned skeletal elements were assessed for their observability in Lodox scans for potential sex estimation. Fourteen of the 32 assessed

traits showed high frequencies of observation from assessed Lodox scans, ranging from 80% (olecranon fossa) to 98% (pelvic brim morphology).

5.1.2.1. Skull traits

Three of the eight cranial traits (overall skull morphology, orbit shape, and parietal eminence morphology) were consistently observable in higher frequencies (over 87.9%, n = 149) from assessed Lodox scans. This high observability is most likely attributed to the utilisation of anteroposterior plane of views to visualize the assessed cranial traits, which is crucial for optimal visualisation of these traits for accurate morphological assessment from the anterior aspect of the skull (White *et al.,* 2011; Christensen *et al.*, 2014d). Additionally, the mental eminence, a mandibular trait, also demonstrated high observability from Lodox scans (91.7%), a result likely attributed to its anterior positioning. Minimal soft tissue interference associated with the skull regions of these traits also likely contributed to the high accuracies achieved, particularly given that the degree of soft tissue thickness can vary across distinct skull regions (Park *et al.,* 2023). Contrary to the overall skull morphology, parietal eminence, and orbit shape, Lodox scans poorly visualised the mastoid process (43.3%) and frontal eminence (7.3%), while the nuchal crest, forehead slope, and glabella were unobservable. The achieved observability frequencies of the mastoid process and frontal eminence were primarily limited to Lodox scans associated with a head tilted towards the right, thus slightly exposing the lateral aspect of the cranium (or skull) and allowing observation of the two traits although with limited assessment of associated morphologies. This limited visibility stems from the anteroposterior imaging plane, as these traits, particularly for sex estimation, are optimally observed from a lateral view of the cranium (or skull) (Klales, 2020a). This indicates that the anteroposterior imaging plane of Lodox scans is insufficient for capturing and visualising these specific cranial traits (mastoid process, frontal eminence, nuchal crest, forehead slope, and glabella), particularly for potential morphological assessment. As such, a lateral imaging plane of view should be explored for the assessment and morphological sex estimation of these traits, particularly given that the Lodox® Statscan™ allows for the scanning of individuals from the lateral aspect, as well from an oblique plane of view (Vellema, 2014; Mamabolo *et al.,* 2020; Morele *et al.,* 2024).

The current study findings are comparable to 3D CT scans studies that have demonstrated observation and assessment of the skull and associated skull traits for various anthropological analyses, including the orbits, parietal eminences and the mental eminence (Saitou *et al.,* 2011; Stull *et al.,* 2014; Fahrni *et al.,* 2017; Dereli *et al.,* 2018; Abegg *et al.,* 2021). Contrary to the current study findings, 3D CT scans provide holistic, 3D visualisation of morphological features in anteroposterior, lateromedial, and oblique planes of view, providing a visualisation of a

multitude of morphological skull features, including traits that were unobservable (glabella, nuchal crest,) or observable in poor frequencies (mastoid process, forehead) from the assessed anteroposterior Lodox scans (Richtsmeier *et al.,* 1995; Saitou *et al.,* 2011; Stull *et al.,* 2014; Braun *et al.,* 2022). Nevertheless, the current study provides extensive information on the frequencies of observing various morphological skull traits from x-ray scans.

The interpretation of these findings requires consideration of the differences in observation frequencies between the study sample (n = 150) and a subset of Lodox scans with observable respective skull traits. This comparison is essential for ensuring that the interpretations of the findings are not skewed by uneven data distribution but rather indicate the utility in the observation a particular trait from a subset of Lodox scans with observable respective skeletal element. Notably, the assessed cranial traits demonstrated relatively low differences, ranging from 0.6% achieved by the overall skull morphology, parietal eminence, and orbit shape to 0.1% achieved by the frontal eminence. These findings signify a relatively higher precision and consistency in the observation of assessed cranial traits from Lodox scans, regardless of whether the traits are observed from a total study sample or a subset of observable crania.

Contrary to cranial traits, the mental eminence morphology exhibited a comparatively high difference in observation frequency (11.0%), demonstrating a relatively low consistency in the observation of the mental eminence from Lodox scans that yields lower observability frequency based on the study sample (80.7%), but higher frequency based on a subset of observable mandibles (91.7%). These findings highlight the need for caution when generalizing subset-based scorability of the mental eminence from Lodox scans to overall sample contexts and thus cranial traits, particularly anteriorly observable cranial traits, should be of primary preference for observation on Lodox scans for potential morphological sex estimation, given their low range of observability frequencies. The current study's findings further indicate that anteroposterior Lodox scans, including having minimal soft tissue interference and image distortions, are suitable for visualisation of anteriorly positioned and/or observable cranial (overall skull morphology, parietal eminence, and orbit shape) and mandibular (mental eminence) traits. However, the inclusion of lateromedial Lodox scans are justified, as it will most likely be suitable for visualisation of laterally positioned observable cranial traits such as the mastoid process, nuchal crest, frontal eminence, forehead slope, and the glabella, as these traits are optimally observed from a lateral view of the cranium (Klales, 2020a).

5.1.2.2. Postcranial traits

Postcranial trait observability in Lodox scans revealed that traits of the pelvic girdle, scapula, and distal humerus exhibited the highest frequencies (over 80%). Notably, most of the traits of the pelvic girdle were consistently observable in high frequencies, with eight of the nine assessed traits (overall pelvis, pelvic brim, subpubic shape, obturator foramen shape, subpubic contour, ventral arc, acetabulum, and ilium morphology) demonstrating high observation (n = 149), ranging from 87.9% (ventral arc) to 98.0% (pelvic brim). In contrast to the pelvic girdle's extensive traits observability, the scapula and distal humerus each presented only one highly observable trait: the infraspinous fossa's lateral border (90.5%, n = 124) and olecranon fossa (80.3%, n = 118), respectively. The remaining traits associated with these skeletal elements were either poorly (below 22%) or moderately (54-57%) observable from Lodox scans. Consistent with the highly observable skull traits, the high observation frequencies of traits of the pelvic girdle, scapula (infraspinous fossa's lateral border), and distal humerus (olecranon fossa) from Lodox scans are likely attributed to minimal soft tissue interference, minimal image distortion and 2D superimposed anatomical structures associated with the assessed Lodox scans, including optimal visualisation of these traits from an anterior plane of view.

In contrast to the abovementioned traits, soft tissue presence around the thoracic region most likely interfered with the effective visualisation and potential observability of the remaining postcranial traits (Figure 5.1 B). As such, this resulted in poor (i.e., <50%) and/or moderate (i.e., 50-79%) observability frequencies for the suprascapular notch (56.2%, n = 137), supraspinous fossa's superior border (21.2%, n =137), infraspinous fossa's medial border (14.6%, n = 137), and costal cartilage ossification patterns (55.4%, n = 65). Similarly, moderate observation frequencies were achieved for the observations of the sacral morphology (69.8%, n = 43) most likely due to extensive soft tissue interference in the sacral region (Figure 5.1 B). Additionally, poor and/or moderate observation frequencies were achieved for the trochlea symmetry (55.1%, n = 147), trochlea constriction (54.4%, n =147), femoral neck shaft angle (68.3%, n = 145) and quadriceps angle (29.7%, n = 145). These findings are most likely because of suboptimal positioning of the individual during the scanning processes (e.g., bent elbow or knee) (Figure 5.1 B), potentially resulting in image distortions and overlapping skeletal structures on these skeletal regions (Figure 5.2). These factors subsequently impacted effective visualisation and accurate observation of these traits from Lodox scans. Traits requiring observations from inferior view such as the costoclavicular tuberosity (White *et al.,* 2011; Ishwarkumar, 2016), distal humerus medial epicondylar angle (White *et al.,* 2011; Scholtz *et al.,* 2010; Tallman & Blanton, 2020) and those requiring observations from a posterior-oblique views such as the greater sciatic notch (White *et*

al., 2011; Gómez-Valdés *et al.,* 2012; Klales, 2020a), are subsequently less effectively visualised from an anterior plane of view, thus they were not observed from all assessed anteroposterior Lodox scans assessed in the current study.

As with the skull traits, accurate interpretation of the assessed postcranial trait observability from Lodox scans requires consideration of the percentage differences between the trait observability for the full study sample (n = 150) and the observable traits subsets. Notably, sacral morphology demonstrated a relatively high 49.8% difference in observability, that is, 69.8% observability within a subset of observable sacra but a 20.0% observability within the total study sample. This was followed by the costal cartilage ossification patterns, which exhibited the largest observed difference among postcranial traits, with a 31.4% difference in observability resulting from a 24.0% observability from a subset of observable rib costal cartilages, but 55.4% observability within the total study sample. This indicates the inconsistency in the observation of these skeletal traits from Lodox scans, highlighting that these traits may show higher observability frequencies when assessed on a subset of visible respective skeletal elements, but significantly lower observability when considering a larger sample size.

The remaining postcranial traits demonstrated relatively lower differences, below 5.7% (olecranon-coronoid angle), with the pelvic girdle traits exhibiting minimal differences (0.6% or 0.7%) compared to the other postcranial traits. Hence, the observations of pelvic traits from Lodox scans can be deemed the most consistent regardless of their observation from a subset of observable pelves or total study sample. These findings indicate that the observability of a particular skeletal trait on Lodox scans significantly depends on the visibility of its respective skeletal element as the observability differences (from study sample versus subset) are relatively lower for majority of the assessed postcranial traits. The findings further indicate that inherent 2D x-ray imaging limitations can also hinder the observability of a trait even though its respective skeletal element is observable in high frequencies from Lodox scans. For instance, the costoclavicular tubercle was not observable in any of the visible clavicle due to the limitations of 2D x-ray scans to visualise the inferior surface of the clavicle. Nevertheless, the current study findings indicate that similar to skull traits, the observability of postcranial traits from Lodox scans is significantly influenced by the skeletal traits anatomical position, soft tissue interference, the imaging plane used (anteroposterior in this case), and the interference of distortion and overlapping anatomical structures. As such, skeletal traits within regions with minimal soft tissues and optimally visualised from an anterior plane of view are most likely to yield higher observability frequencies from anteroposterior Lodox scans, including minimum percentage differences for the observability frequencies between the full study sample and observable subsets. Notably, the

pelvic girdle stands out as a skeletal element with traits demonstrating consistently high observability frequencies from Lodox scans compared to traits of other skeletal elements, thus suggesting Lodox scans are effective for visualising traits of the pelvic girdle.

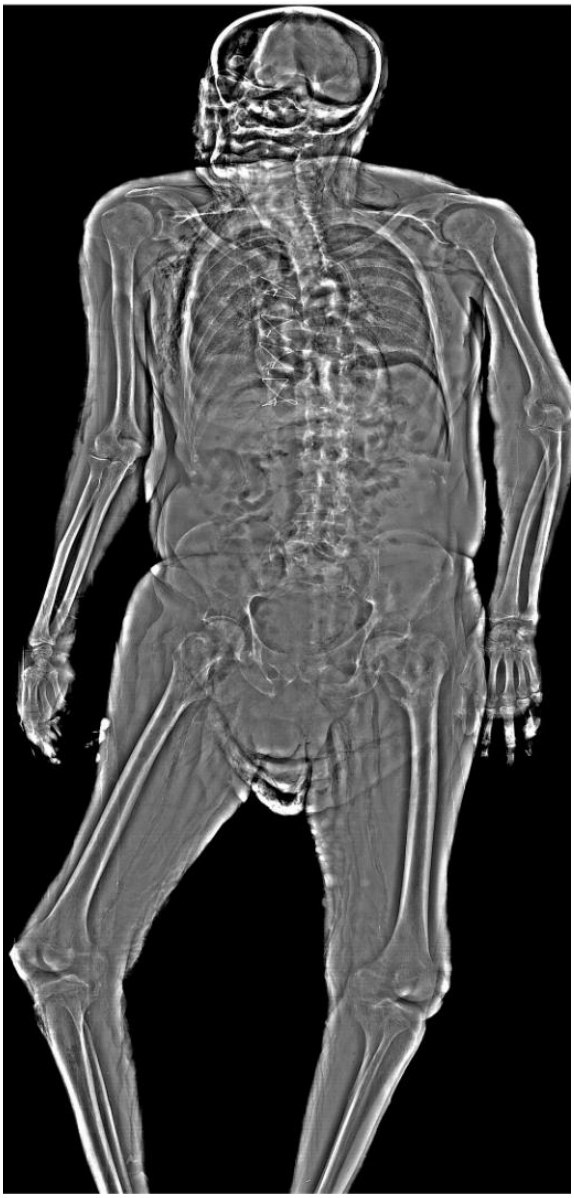


Figure 5.2: An example of a Lodox scan of an individual not scanned in a standard anatomical position, exhibiting image distortion and superimposed anatomical structures on the cranial, thoracic and pelvic regions. Left hand side is towards the right.

5.1.3. Skeletal traits scorability

When evaluating the feasibility of morphological assessment of the assessed skeletal traits for sex estimation, pelvic traits consistently exhibited high scoring frequencies, mirroring their high observability frequencies. Specifically, pelvic traits scored morphologically, based on their respective ordinal or nominal scoring scales, from Lodox scans (n = 150) ranged from 82.0% (subpubic contour) to 93.3% (overall pelvis and pelvic brim morphologies), thus surpassing the

scorability of traits of the skull and other postcranial skeletal elements. In addition to their high scorability frequencies, pelvic traits also demonstrated the lowest variability in scorability when comparing the total study sample to the subsets of scorable pelvic traits, mirroring the relatively low differences in observability frequencies. Specifically, these differences ranged from a minimum of 2.6% for pelvic brim morphology (study sample observability = 93.3%; subset observability = 95.9%) to 12.4% for ventral arc (study sample observability = 85.3%; subset observability = 97.7%; Table 4.5), further emphasizing the high chance of scoring pelvic traits both from the total study sample and a subset of Lodox scans with observable pelves.

In contrast to the consistent scorability of pelvic traits, only a selected few skull traits—orbit shape (93.3%), overall skull morphology (87.3%), parietal eminence morphology (85.3%), and mental eminence (76.0%)—achieved similar high scoring frequencies from assessed Lodox scans (n = 150 scans), consistent with their high observability frequencies. Moreover, skull traits showed considerably greater variability (compared to pelvic traits), with scorability differences between the study sample and the scorable subsets ranging from 6.7% for the orbit shape (study sample observability = 93.3%; subset observability = 100%) to 84.2% for the frontal eminence (study sample observability = 6.7.0%; subset observability = 90.9%; Table 4.3). Similarly, the infraspinous fossa lateral border (80.7%, n = 150) and olecranon fossa (72.0%, n = 150) showed scorability frequencies comparable to pelvic and the above-mentioned skull traits, also consistent with their high observability. However, like the aforementioned skull traits, these two postcranial traits also exhibited significant differences in scorability between the study sample and the scorable subsets, 16.9% for the infraspinous fossa's lateral border (study sample observability = 80.7%; subset observability = 97.6%) and 19.5% for the olecranon fossa (study sample observability = 72.0%; subset observability = 91.5%). These high differences, compared to pelvic traits, indicate that the ability to score the traits of the above-mentioned skull, scapular, and distal humerus from the total assessed Lodox scans (n = 150) was relatively low, but contrarily high when scored from a subset of scans with observable respective trait, further indicating their high chance of scorability from respective observable skeletal element.

The remaining assessed traits were either not morphologically scorable or exhibited relatively low scorability frequencies with relatively high differences in frequencies of scorability. For instance, the infraspinous fossa medial border exhibited the greatest difference in scorability frequencies between a subset of observable scapulae and a total study sample (86.7%), followed by the sacrum morphology (66.7%). Thus, such traits should not be of preference for morphological scoring from Lodox scans. These study findings highlight the need for caution when generalizing subset-based scorability of traits from Lodox scans to overall sample contexts and emphasize the superior

reliability of pelvic traits for morphological sex estimation in such analyses, given their low range of scorability frequencies.

5.1.4. Overall interpretation

The current study's findings indicate a potential relationship between the observability of a trait and how effectively it can be scored for morphological assessment from using Lodox scans. Thus, traits with relatively high observability frequencies subsequently exhibited relatively high scorability frequencies compared to those with relatively low or moderate observability frequencies. As such, both observability and scorability of a skeletal trait should be considered when using Lodox scans for morphological assessment, particularly for potential sex estimation from such x-ray scans. The current study findings also indicate that the same factors that influence observability; soft tissue presence, anatomical positioning of traits, anatomical plane of view, image distortion and superimposition of anatomical features, also influence scorability of morphological traits from Lodox scans. Skeletal traits associated with the minimum or lack of these factors are most likely to be more effectively observed and assessed morphologically for potential sex estimation. As a result, skull and postcranial traits with relatively high observability frequencies (>82%, e.g., orbit shape, parietal eminences, pelvic brim, ilium, acetabulum) subsequently exhibited relatively high scorability frequencies (>80%) from the assessed Lodox scans (n = 150). Moreover, the pelvic girdle consistently stands out as a skeletal element with traits that are consistently well-visualised and effectively assessed morphologically from anteroposterior Lodox scans, making it an important skeletal element for potential morphological sex estimation using Lodox scans. While certain non-pelvic postcranial traits exhibit moderate observability frequencies (50-79%), they also show greater variability in their scorability frequencies compared to skull and pelvic traits. This potentially indicate that even when these traits are observable from Lodox scans, their morphological assessment may be poor and/or less consistent, thus their preference for morphological assessment using Lodox scans should be tertiary to that of the pelvic (1st preference) and skull (2nd preference) traits.

The current study findings also align with the established capability of x-ray imaging to visualize skeletal tissue, including Lodox scans (Muehleman *et al.,* 2006; Pitcher *et al.,* 2008; Stull *et al.,* 2013b; Berger *et al.,* 2018; Rowbotham & Blau, 2020; Morele *et al.,* 2024). Additionally, the current study provides information on specific skeletal elements and traits that can be observed and assessed in high frequencies from Lodox scans. Moreover, visualisation of skeletal tissue is particularly evident on bony regions with higher bone density, which readily absorb more x-ray beams, producing more contrast on the x-ray detector (i.e., appears whiter than other tissues against a black background), thus the bone and/or skeletal traits are highly radiopaque and visible on x-

ray scans (Berger, 2002; Pitcher *et al.,* 2008; Franklin *et al.,* 2016; Rowbotham & Blau, 2020; Ou *et al.,* 2021). As a result, pelvic traits and selected skull traits were observed and morphologically assessed for sex estimation at higher frequencies, in addition to being positioned in a preferred anatomical position that is optimal for visibility (i.e., anterior), compared to most postcranial traits. In contrast, skeletal traits of the scapula, ulna, rib costal cartilages, and sacrum were observed and morphologically assessed at low frequencies from Lodox scans. Optimal visualisation of traits associated with the above-mentioned postcranial elements was most likely hindered by their suboptimal anatomical positioning for visualisation. For instance, the costoclavicular tuberosity can only be visualised from an inferior plane of view for optimum morphological assessment) (Scholtz *et al.,* 2010; White *et al.,* 2011; Ishwarkumar, 2016; Tallman & Blanton, 2020). Additionally, x-ray imaging factors, such as image distortion, 2D superimposed anatomical structures, and soft tissue interferences (Muehleman *et al.,* 2006; Pitcher *et al.,* 2008; Stull *et al.,* 2013b; Ahern & Brygel, 2014; Franklin *et al.,* 2016), also likely contributed to the reported low frequencies of observability and scorability of non-pelvic postcranial traits from Lodox scans.

Furthermore, six morphological traits (nuchal crest, forehead slope, glabella, costoclavicular tuberosity, medial epicondyle angle, and greater sciatic notch) were entirely unobserved in all the assessed Lodox scans. This is because these skeletal traits are typically visualised from anatomical planes other than the anteroposterior view of the assessed Lodox scans. For instance, the morphologies of the nuchal crest and glabella are best assessed in a lateral plane of view (Klales, 2020a). These traits, including those with moderate (50-79%) and/or poor (<50%) observability and scorability frequencies (i.e., mastoid process, frontal eminence, suprascapular notch, supraspinous fossa medial border, rib costal cartilage ossification patterns, trochlea constriction, trochlea symmetry, olecranon fossa, olecranon-coronoid angle, sacrum morphology, femoral NSA, and Q angle), should not be prioritized for morphological assessment using anteroposterior Lodox scans. In contrast, pelvic traits (pelvic brim morphology, overall pelvis morphology, obturator foramen shape, subpubic shape, acetabulum position, subpubic contour, ilium morphology, and ventral arc), followed by a select skull traits (overall skull morphology, parietal eminence, orbit shape, and mental eminence), and the supraspinous fossa's lateral border should be prioritization for observability and morphological assessment from Lodox scans (in the provided order), due to their relatively high frequencies of observability and scorability from the assessed Lodox scans (>80%, n = 150).

5.2. Repeatability of Observed Skeletal Elements and Traits

Reliable data collection is fundamental to generating accurate research findings in observational studies and for the development of methods. Assessing reliability is crucial in morphological sex

estimation studies, where subjective observer variations and interpretations are often involved. This involves ensuring repeatable and reproducible observations across different observers. Observer repeatability, also known as intra-observer agreement, measures how consistent a single observer is across repeated assessments. Therefore, high intra-observer agreements signify strong repeatability in the assessment of observations/measurements (Blanchard, 2010; McHugh, 2012; Popović *et al.,* 2017). Reproducibility (i.e., inter-observer agreement) assesses the consistency of observations between different observers; thus, high inter-observer agreements indicate good reproducibility in the assessment of observations (Blanchard, 2010; McHugh, 2012; Popović *et al.,* 2017). Therefore, reliability is established when a method or assessment criteria yield consistent results across repeated observations by the same observer and repeated observations by distinct observers. Establishing robust repeatable and reproducible observations ensures that study findings reflect true biological variation and not subjective, inconsistent observations amongst distinct observers (McHugh, 2012).

In the current study, reliability in observing skeletal elements and traits, and the ability to morphologically score such traits from Lodox scans was established in two ways. Observations were made twice by the principal investigator and once by an independent observer, using the same Lodox scans. Intra- and inter-observer agreements were then quantified using Cohen's Kappa statistics, interpreted based on qualitative agreement levels (i.e., no, slight, fair, moderate, substantial, near-perfect, and perfect agreements (Table 3.5), thus providing a measure of repeatability, reproducibility, and subsequently, reliability in the observation and feasibility of scoring morphological traits from anteroposterior Lodox scans.

5.2.1. Repeatability of observed skeletal elements

Most skeletal elements assessed in this study demonstrated substantial to perfect agreements (K>0.61) for intra-observer repeatability (cranium, mandible, clavicle, rib costal cartilages, distal humerus, proximal ulna, pelvic girdle, sacrum, and femur) and inter-observer repeatability (cranium, clavicle, distal humerus, proximal ulna, pelvic girdle, and femur) for observation. This strong repeatability likely correlates with the high frequency of observation (>88%) associated with these skeletal elements, facilitated by Lodox scans' ability to effectively visualize bone material (Stull *et al.,* 2013b; Stull *et al.,* 2017; Morele *et al.,* 2024). These findings support the reliability of Lodox scans to visualize skeletal elements for morphological assessments and potential sex estimation. However, certain elements, such as the mandible, scapula, rib costal cartilages, and sacrum, demonstrated lower inter-observer agreements compared to intra-observer agreements for visual observability (i.e., slight to moderate inter-observer agreement). The disagreements in repeatability agreements are likely due to the level of experience in assessing

Lodox scans by the different observers, particularly in cases where elements are obscured by other tissues. The principal investigator's prior experience and familiarity with Lodox scans, in addition to their double assessment of the same scans for repeatability, likely contributed to their higher intra-observer agreements. In contrast, the inter-observer, who only assessed the scans once and had less familiarity, showed lower agreement on specific elements like the mandible, scapula, rib costal cartilages, and sacrum. Furthermore, the inherent challenges of 2D imaging, including Lodox scans, likely played a role in the differences between inter- and intra-observer agreements. Factors such as image distortions, soft tissue interference, and overlapping anatomical structures can make it difficult to visualise skeletal elements effectively and introduce subjectivity into the assessments, leading to disagreements between observers (Stull *et al.,* 2013b; Nakashima & Duong, 2020). Nevertheless, the current study findings demonstrate the Lodox scan's reliability in effectively visualising the skull and various postcranial elements, especially when obscuring factors are minimal.

5.2.2. Repeatability of observed skeletal traits

Compared to the skull and other postcranial skeletal traits, the assessed pelvic traits demonstrated notable reliability (highly repeatable and reproducible) for observation from Lodox scans. This reliability was evident in the perfect intra- and inter-observer repeatability agreements for several pelvic traits, including overall pelvic morphology, pelvic brim, subpubic bone shape, subpubic contour, ventral arc, and ilium morphology. However, exceptions were noted for the acetabular position and obturator foramen shape which exhibited poor intra- and inter-observer repeatability agreements for observation (respectively). This was most likely due to the traits being situated in pelvic regions that are prone to image distortion, spatial resolution limitations, internal prosthesis, and overlapping anatomical structures, compared to the other pelvic traits (Figure 5.3). These factors potentially impacted their effective observations from Lodox scans, leading to increased subjective observations/interpretations between distinct observers. Nevertheless, given the relatively high observation frequencies associated with these pelvic traits, the achieved intra- and inter-observer repeatability agreements are most likely reflective of the feasibility of Lodox scans to effectively and reliably visualize these pelvic traits for observation and potential morphological sex estimation.

Visualisation of skull traits on Lodox scans also demonstrated notable reliability, with intra- and inter-observer repeatability agreements ranging from moderate to perfect. However, the mastoid process exhibited the lowest Cohens Kappa repeatability coefficients for both intra- and inter-observation (fair and slight agreements, respectively) most likely due to the trait requiring visualisation from the lateral aspect of the cranium for optimal observation (White *et al.,* 2011;

Christensen *et al.*, 2014d), especially for morphological sex estimation (Klales & Cole, 2018; Klales, 2020a). This is also reflective of its poor observation frequency from Lodox scans, thus further indicating that anteroposterior Lodox scans are not sufficient and reliable for optimal visualisation of the mastoid process. In contrast, the moderate to perfect intra- and inter-observer agreements associated with the overall skull morphology, parietal eminence, orbit shape, and mental eminence, are most likely reflective of the reliability and sufficient capability of Lodox scans to visualize these traits for effective observation and potential morphological assessment. In contrast, the achieved substantial intra- and perfect inter-observer repeatability agreements associated with the frontal eminence, as well as the perfect intra- and inter-repeatability agreements associated with non-observable cranium traits (nuchal crest, forehead slope, and glabella) are reflective of the reliability of anteroposterior Lodox scans to poorly and not effectively visualize these cranial traits. This is most likely due to the traits requiring visualisation from a lateral plane of view for optimal visualisation (White *et al.,* 2011; Christensen *et al.*, 2014d; Klales & Cole, 2018; Gupta *et al.,* 2022), thus they are less likely to be effectively visualised from anteroposterior Lodox scans.

Similar to skull traits, observation of selected distal humerus traits (olecranon fossa, trochlea constriction, and trochlea symmetry) from Lodox scans exhibited notable reliability, with intra- and inter-observer repeatability agreements ranging from moderate to perfect agreements. These intra- and inter-observer repeatability agreements are more likely reflective of the moderate observability of the trochlea constriction and symmetry, and high observability of the olecranon fossa on Lodox scans. Moreover, the perfect intra- and inter-observer agreements for the medial epicondyle are reflective of the reliability of anteroposterior Lodox scans to not visualize the trait, especially since the trait requires observation inferior to the distal humerus for optimal morphological assessment (White *et al.,* 2011; Tallman & Blanton, 2020). Therefore, the use of anteroposterior Lodox scans for observation of distal humerus traits is expected to consistently yield reliably high observability for the olecranon fossa, moderate observability for trochlea constriction and symmetry, and effectively no observation of the medial epicondyle, given the limitations of this scan orientation.

The remaining non-pelvic and non-distal humerus postcranial traits (i.e., traits of the scapula, rib costal cartilages, proximal ulna, sacrum and femur) demonstrated poor reliability for observation on Lodox scans. These traits exhibited intra- and inter-observer repeatability agreements ranging from no agreement to moderate agreement. Specifically, traits of the proximal ulna, sacrum, and femur exhibited the lowest Cohens Kappa coefficients for both intra- and inter-repeatability, ranging from no to fair observer agreements. These findings indicate the poor reliability of

anteroposterior Lodox scans to effectively visualize traits of these skeletal elements for optimal observation and potential morphological assessment. These findings are also reflective of the poor and moderate observability frequencies associated with observations of the respective traits from anteroposterior Lodox scans. This is most likely attributed to soft tissue interference, especially for the scapula, rib costal cartilages, and sacral traits (Figure 5.1B and 5.3), Suboptimal positioning (during scanning) that often leads to image distortion and overlapping anatomical structures (Dorion, 1983; Boffard *et al.,* 2006; Stull *et al.,* 2013a), especially for traits of the proximal ulna and femur (Figure 5.3). As such, these factors most likely limited effective and reliable observability of these postcranial skeletal traits from Lodox scans, resulting in significant subjective observation between observers.

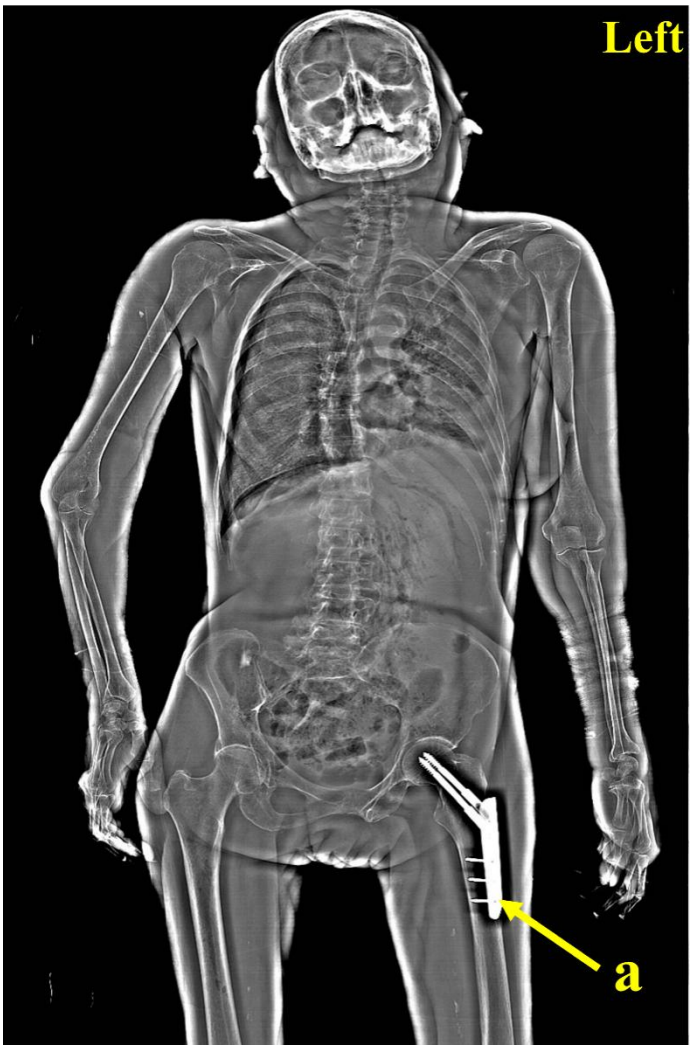


Figure 5.3: An example of a Lodox scan of an individual exhibiting image distortion, superimposed anatomical structures, and/or soft tissue interference in the thoracic, elbow, and pelvic regions, in addition to not being scanned in a standardised anatomical position. Both hands are partially pronated. a = internal prosthesis.

5.2.3. Repeatability of scored skeletal traits

5.2.3.1. Skull traits

The ability to morphologically score most of the observable cranial traits from the Lodox scans was primarily characterized by moderate and perfect intra-observer repeatability agreements and moderate inter-observer repeatability agreements (overall skull morphology, mastoid process, frontal eminence, and parietal eminence). The consistency in achieving moderate repeatability agreements are reflective of the feasibility to morphologically score the overall skull morphology and parietal eminence in relatively high frequencies (87.3% and 85.3%, respectively) from anteroposterior Lodox scans (n = 150). In contrast, the consistency in achieving moderate repeatability agreements for the morphologically scoring of the mastoid process and frontal eminence is reflective of the poor scorability frequencies associated with cranial traits (38.0% and 6.7%, respectively, n = 150). Furthermore, the ability to score the morphology of the orbit from Lodox scans demonstrated substantial intra- and inter-observer agreements, an indication of high reliability in the feasibility of scoring the trait from anteroposterior Lodox scans. Compared to traits of postcranial elements, particularly the pelvic traits, the achieved repeatability agreements are comparably lower. This is most likely due to the degree of image distortion associated with the cranium, resulting from challenges associated with aligning the cranium into anatomical position during the scanning process (Figure 5.3).

Except for the mastoid process and the frontal eminence, the achieved intra- and inter-observer repeatability agreements associated with overall skull morphology, parietal eminence, and orbit shape are consistent with their respective abilities to be morphologically scored from Lodox scans in high frequencies (> 85%, n = 150). Studies using dry bone analysis (Walker, 2008; Krüger *et al.,* 2015; Lewis & Garvin, 2016) and CT scans (Dereli *et al.,* 2018; Braun *et al.,* 2022; Kelley, 2022) have consistently shown moderate to near-perfect intra- and inter-observer agreement for the scoring of similar cranial traits in morphological sex estimation studies. For instance, Kelley (2022) utilising Cohen's Kappa statistics reported moderate intra-observer repeatability agreements in the morphological assessments of the mastoid process, glabella, and mental eminence (based on Buikstra & Ubelaker (1994) and Walker (2008) methods) from 3D volume rendered CT scans of adults from the New Mexico Decedent Imaging Database. Contrary to assessed cranial traits, scoring of the mental eminence from anteroposterior Lodox scans demonstrated fair intra- and inter-observer repeatability agreements. This lower agreement aligns with numerous findings from dry bone (Walker, 2008; Krüger *et al.,* 2015) and CT scan (Dereli *et al.,* 2018; Braun *et al.,* 2022) studies, which also reported fair or lower repeatability agreements for morphoscopic sex estimation of the mental eminence, thus recommending the exclusion of the

trait for the estimation of sex. For instance, based on the Walker (2008) traits, Klales (2020a) investigated the feasibility of using skull morphology for sex estimation from utilising the MorphoPASSE computer software program. Klales (2020a) recommended the exclusion of the mental eminence for morphological sex estimation due to low observer agreements and significant variations in the morphological expression of the trait ‘s shape, total area, and mental tubercles, which are often not all correlated (Klales & Cole, 2018). As such, the ability to score the mental eminence from anteroposterior Lodox scans, although scorable in relatively moderate frequencies (76.0%), can be deemed less reliable compared to cranial traits with relatively high observer repeatability agreements and scorability frequencies (i.e., overall skull morphology, parietal eminence, and orbit shape).

5.2.3.2. Pelvic traits

The repeatability agreements for the ability to score observable pelvic traits from Lodox scans were similar and/or within the same range of repeatability agreements as their respective trait observations agreements. That is, the ability to observe and morphologically score pelvic traits such as overall pelvis morphology, pelvic brim, and ilium was primarily characterised by perfect intra- and inter-observer repeatability agreements. In contrast, the observability and scorability of the acetabular position was characterized by moderate intra- and substantial inter-observer repeatability agreements. The consistency in the perfect scorability of these pelvic traits (with exception of the acetabulum position) between observers is most likely attributed to minimum soft tissue interference, minimal overlapping anatomical structures, and minimal distortion associated with the body/pelvic region. This subsequently favoured effective morphological assessment of these pelvic traits. Similar reasons are also most likely associated with the perfect intra- and inter-observer repeatability agreements for the scorability of the obturator foramen shape although the trait exhibited substantial intra- and inter-observer repeatability agreements for observation. Nevertheless, the consistency in these findings indicates the high reliability in morphologically scoring the overall pelvis morphology, pelvic brim, ilium, and the obturator foramen shape from anteroposterior Lodox scans.

In contrast, repeatability agreements to morphologically score the remaining pelvic traits (subpubic shape, subpubic contour, ventral arc, and acetabulum position) were poor and lower than those of the ability to observe these traits from Lodox scans (except for acetabulum position). These findings are likely attributed to the presence of overlapping skeletal structures (e.g., articulation of femoral head with acetabulum) and the potential suboptimal or angulated positioning of the pelvis during scanning, thus resulting in potential image distortion and 2D superimposition of the traits (Figure 5.3). This ultimately had an impact on the effective

morphological assessment and scoring of these pelvic traits, resulting in subjective morphological assessments of the traits by different observers, despite being observable in high frequencies. Nevertheless, the achieved moderate to perfect intra- and inter-observer repeatability agreements associated with these assessed pelvic traits are consistent with the relatively high frequencies of the ability to morphologically score the traits from Lodox scans. Moreover, the repeatability agreements between intra- and inter-observation are consistently within the same agreement levels or one agreement level below another, similarly indicating their reliability in their morphological assessment (scorability) from anteroposterior Lodox scans. Overall, the consistently high intra- and inter-observer repeatability agreements of assessed pelvic traits demonstrate the reliability in sufficiently and effectively morphologically assessing such traits from anteroposterior Lodox scans, in addition to their high scorability frequencies, compared to traits of the other postcranial elements.

These findings align with numerous studies evaluating the reliability of assessing morphology of pelvic traits for morphological sex estimation using dry bone analyses (Rogers & Saunder, 1994; Blanchard, 2010; Small *et al.,* 2012; Lesciotto & Doershuk, 2017), CT scan (Johnstone-Belford *et al.,* 2018; Setiawati *et al.*, 2022), or geometric morphometrics (Franklin *et al.,* 2014) approaches, all of which similarly reported moderate to perfect intra- and inter-observer repeatability agreements. Similar to analyses on dry bones, CT scans, and geometric morphometrics, the high intra- and inter-observer repeatability of the assessed pelvic traits from Lodox scans supports their reliable use in morphological assessments for sex estimation. This aligns with previous research, including studies by Rogers and Saunders (1994), Small *et al.* (2012), and Franklin *et al.* (2014), who found substantial to perfect agreement for key pelvic traits such as the ventral arc, subpubic contour, subpubic shape/angle. Lesciotto and Doershuk (2017) similarly reported moderate to substantial agreement. This overall consistency indicates that these traits are less challenging to score for morphological sex assessment.

5.2.3.3. Non-pelvic postcranial traits

The skeletal traits of the remaining postcranial elements demonstrated a wide variety of intra- and inter-observer repeatability agreements for scorability on Lodox scans, ranging from no to near-perfect intra- and inter-observer repeatability agreements. Morphological traits of the distal humerus consistently demonstrated moderate and substantial intra- and inter-observer repeatability agreements, consistent with their respective observability repeatability agreements. Similarly, the repeatability agreements to morphologically score traits of the scapula were consistent with those of the ability to observe the traits on Lodox scans. However, unlike the distal humerus traits, the scapula traits were primarily characterized by two to three differences in agreement levels between

intra- and inter-observation, particularly: fair and no repeatability (suprascapular notch), near-perfect and fair (infraspinous fossa's lateral border), and near-perfect and substantial (infraspinous fossa's medial border) intra- and inter-observer repeatability agreements, respectively. Moreover, postcranial traits of the rib costal cartilages, proximal ulna, sacrum, and femur also demonstrated intra- and inter-observer repeatability agreements that were different by at least two or three agreement levels. These were mainly characterized by moderate (olecranon-coronoid angle, sacrum morphology, and femoral NSA) and substantial (costal cartilage ossification patterns) intra-observer agreements, as well as no (sacrum morphology and femoral NSA), fair (olecranon-coronoid angle), and moderate (costal cartilage ossification patterns) inter-observer repeatability agreements. These findings are also reflective of the poor (< 50%) and/or moderate (50 – 79%) scorability frequencies associated with these respective traits (except for the infraspinous fossa lateral border) compared to the skull and pelvic traits. These findings may also be attributed to inherent limitations of x-ray imaging, mainly soft tissue interference, traits' suboptimal positioning during scanning, image distortion, 2D superimposition of anatomical structures, and the use of a suboptimal anatomical viewing plane for morphological assessment from Lodox scans. These factors most likely limited the effective morphological scoring of these postcranial traits, thus contributing to notable differences in repeatability agreements for scorability between observers, compared to the assessed traits of the skull and pelvis. As such, the achieved repeatability agreements are indicative of these postcranial traits being less reliable for morphological scoring from Lodox scans in comparison to skull and pelvic traits.

5.2.4. Overall interpretation

Notable differences that exist between the intra- and inter-observer repeatability agreements may also be attributed to variations in the observers' expertise with Lodox scan visualisation. That is, the principal investigator possesses greater familiarity with Lodox® Statscan™ scans and the associated software program to visualise Lodox scans including their application in the assessment of human remains compared to the inter-observer. Furthermore, the exclusive use of anteroposterior Lodox scans in the current study most likely influenced the overall reliability of observation and scorability of certain skull and postcranial traits, particularly those that would ideally be visualised from their preferred or optimal anatomical planes of view, consistent with their dry bone observation and morphological assessment. For instance, morphological traits such as the overall skull morphology, orbit shape, parietal eminence, infraspinous fossa lateral border, olecranon fossa, pelvic brim, and subpubic contour are best visualised from an anterior plane of view for optimum morphological assessment including morphological sex estimation (Scholtz *et*

al., 2010; İscan & Steyn, 2013; Klales, 2020a; Tallman & Blanton, 2020), thus these traits were effectively visualised and morphologically assessed on anteroposterior Lodox scans.

Challenges like the visual observation skeletal elements, image distortions, soft tissue presence, the skeletal trait's anatomical plane of view, and 2D superimposition of skeletal traits (see Figures 5.1 B, 5.2, and 5.3) most likely impacted the overall reliability of observing and morphologically scoring assessed postcranial traits from anteroposterior Lodox scans. These factors also likely contributed to the inconsistent and unreliable observer repeatability agreements associated with most postcranial traits, also reflecting the low accuracy associated with visualising and scoring such traits from Lodox scans compared to the skull and pelvic traits. Moreover, skeletal traits that were consistently unobservable from any of the assessed Lodox scans (e.g., nuchal crest, glabella, costoclavicular tuberosity, and greater sciatic notch) demonstrated perfect intra- and inter-observer repeatability agreements regarding their non-visibility. This consistent non-observability on anteroposterior Lodox scans with perfect repeatability indicates the reliability of such traits not observable from an anteroposterior plane of view of Lodox scans.

Despite these Lodox scans' limiting factors and non-observable traits, the current study's findings demonstrate that observation and scoring of skull and pelvic traits are consistent within the same observer and reproducible by a different observer, including not being overly influenced by individual observer variations. Moreover, the study findings align with those of previous studies that have evaluated and reported moderate to near-perfect repeatability agreement levels for morphological sex assessment of traditional skull and pelvic traits based on traditional dry bone assessments (Listi & Bassett, 2006; Williams & Rogers, 2006; Blanchard, 2010; Krüger *et al.*, 2015; Gupta *et al.,* 2022) and CT scans (Ramsthaler *et al.,* 2010; Decker *et al.*, 2011; Dereli *et al.,* 2018) analyses for morphological sex estimations, including those assessed in the current study. A study by Ramsthaler and colleagues (2010) utilised 50 volume-rendered cranial 3D CT scans of German individuals to morphologically evaluate a multitude of traditional cranial traits, including those assessed in the current study (i.e., glabella, orbit shape, frontal eminence, mental eminence, mastoid process, and forehead slope), morphologically assessed by two teams of two examiners each. Although repeatability agreements were only assessed between the two teams, instead of individual traits, a near-perfect inter-observer repeatability agreement in scoring assessed traits was reported between the two teams. Compared to the current study findings, the inter-observer repeatability agreement level reported by Ramsthaler and colleagues (2010) is at least different by one, two and three agreement levels to those reported for the orbit shape (i.e., substantial agreement), frontal eminence (i.e., moderate agreement), and mental eminence (fair agreement) in the current study, respectively. The significant difference in observer agreement levels between the

two studies likely stems from the focus of measurement. The Ramsthaler and colleagues (2010) study assessed the repeatability of the overall sex classification ability of their observers from 3D CT scans, whereas the current study measured the feasibility of classifying individual skeletal traits from Lodox scans. This distinction is crucial as a high agreement on the final sex classification does not necessarily indicate high agreement on each contributing trait. Moreover, the Ramsthaler and colleagues (2010) study reported near-perfect agreement was for the teams' collective ability to classify sex, not for the individual traits themselves. In contrast, the current study's lower observer agreement for specific traits (orbit shape, frontal eminence, and mental eminence) highlights the difficulty and inherent subjectivity of assessing these features in isolation, especially from 2D anteroposterior Lodox scans.

A study by Williams and Rogers (2006) based on percentage chance repeatability agreements, evaluated the reliability of the frontal eminence, mastoid process, orbit shape, forehead slope and parietal eminence for morphological sex estimation (among a total of 21 morphological skull traits), from a sample of 50 adult skulls of white European individuals. In contrast to the current study findings, only the frontal eminence and mastoid process traits were identified as highly reliable traits for morphological sex estimation due to exhibiting 8% intra-observer errors each, which is comparable to substantial to near-perfect Cohens Kappa agreement levels (McHugh, 2012), whereas in the current study these traits were associated with moderate and fair intra-observer repeatability agreements. Moreover, the orbit shape, forehead slope, and parietal eminence were reported to exhibit 12% (comparable to moderate to substantial agreements), 16% (comparable to fair to moderate agreements), and 20% (comparable to slight to moderate agreements) intra-observer error rates, respectively, thus deemed less reliable. Similarly, based on percentage chance repeatability agreements, Jilala and colleagues (2021) reported substantial intra- and inter-observer repeatability agreements on a study sexing contemporary Tanzanian skulls using Walker (2008) traits and dry bone assessment method, from all assessed Walker (2008) traits. From the current study findings, it is only the orbit shape that demonstrated intra-observer repeatability agreement (i.e., substantial intra-observer agreement) that is potentially similar to that reported by Williams and Rogers (2006) and the Jilala *et al.* (2021) study's findings.

The difference in intra-observer repeatability agreements between the current study and those by Williams and Rogers (2006) likely reflects the use of different statistical methods for measuring reliability in the observation of similar morphological skull traits between these studies (i.e., percentage agreements vs Cohens Kappa coefficients). However, it is important to note that percentage agreement can be misleadingly high as it does not account for agreement by chance, especially when a category is very common or rare. In contrast, the kappa statistics correct for

chance, however, it can also yield low values despite strong observer agreement, especially in cases where the prevalence of categories is highly skewed (Dettori & Norvell, 2020). Additionally, the assessment of real-bone skull traits specimen by Williams and Rogers (2006) compared to observation of similar skull traits from x-ray radiographs also likely attributed to the difference in intra-observer repeatability agreements between the two studies. That is, real-bone specimen provide a more comprehensive 3D of specimens as well as direct examination of morphological traits compared to 2D x-ray radiographs, which often suffer from superimposition of anatomical structures, obscuring subtle details and resulting in less accurate assessment of such traits (Safir *et al.*, 2012; DeMaio *et al.,* 2019; Allen, 2022). Nevertheless, the intra-observer repeatability agreements of the traits in comparison (except for the forehead slope) between the two studies are in close proximity in terms of Cohens Kappa agreement levels. Staying consistent with the sample of the current study findings, studies by Krüger *et al.* (2015) and Gupta *et al.* (2022) utilising skeletal samples of 161 Black South Africans (from the Raymond A. Dart Collection of Modern Human Skeletons, University of the Witwatersrand) and 245 black and white South Africans (from the Pretoria Bone Collection, University of Pretoria), respectively also reported moderate to near-perfect intra- and inter-observer repeatability agreements in the traditional dry bone assessments of Walker's (2008) traits, overall skull and frontal eminence morphologies, orbit shape, and subpubic angle for morphological sex estimation in adult South African study samples.

Additionally, Decker and colleagues (2011) utilised 100 abdominopelvic 3D CT scans of patients (from the University of South Florida College of Medicine) and evaluated the repeatability of various nonmetric pelvis sex estimation methods including the Phenice (1969) pelvic traits and the subpubic angle from CT-derived models. Contrary to the current study, inter-observer repeatability assessment for the subpubic angle/shape was based on a landmark placement and measurement error technique. Consistent with the current study findings, perfect repeatability agreements between observers were reported for Phenice's (1969) pelvic traits, with a 3.53% inter-observer error for the subpubic angle/shape, which is comparable with a relatively high Cohens Kappa agreement level (McHugh, 2012). The similarities and close proximity in the intra- and inter-observer agreement levels reported in the current study's and to those reported in CT scan (Decker *et al.*, 2011; Dereli *et al.,* 2018) and traditional dry bone (Listi & Bassett, 2006; Blanchard, 2010; Krüger *et al.*, 2015) studies are indicative of the potential capabilities of Lodox scans to yield comparably reliable morphological assessments of skull and pelvic traits for sex estimation. As such, the observer repeatability agreements reported in the current study for the observation and morphological scoring of the mastoid process, mental eminence, traits of the clavicle, scapula, rib costal cartilages, ulna, sacrum, and femur, from anteroposterior Lodox scans can be deemed

unreliable and limited, particularly for morphological sex assessment. In contrast, the current study's findings strongly support the use of anteroposterior Lodox scans for observation and morphological scoring of anteriorly positioned/observable skull (i.e., overall skull morphology, parietal eminence, and orbit shape) and pelvic traits for morphological sex estimation. This further renders primary preference for such skull and pelvic traits that are reliably observable and scorable in high frequencies (82-97%) for visualisation and morphological assessment on Lodox scans of adult individuals. Among these, pelvic traits should be prioritized for morphological assessment from Lodox scans for potential sex estimation, due to their highly reliable observer repeatability and reproducibility.

5.3. Sex Classification Accuracies

Similar to reliability, the assessment of accuracy is important in sex estimation studies. Without indicating how accurate (and reliable) a sex estimation method is, the method would lack validity (Blanchard, 2010). As such, a method's utility for sex estimation often relies on both its accuracy and reliability in estimation. A method that is reliable but inaccurate, or accurate but unreliable, can be deemed unuseful for estimating biological sex, as it will most likely produce either inconsistent results across researchers or yield low sex classification accuracies (Daniels, 2018).

5.3.1. Skull traits

Morphological sex estimation of traditional skull traits conducted from radiographic images (mainly 3D CT scans) has been reported to provide similar sex classification accuracies as traditional morphological sex estimation methods, with accuracies ranging between 81% and 95% from various studies (Ramsthaler *et al.,* 2010; Teodoru-Raghina *et al.,* 2017; Dereli *et al.,* 2018; Bertsatos *et al.,* 2020; Kelley, 2022; Bareša *et al.,* 2024). The current study also demonstrates the feasibility of morphological skull sex estimation from 2D anteroposterior Lodox scans. However, accurate sex estimation was limited to moderate classification accuracies of a selected skull traits, particularly when evaluated against the total study sample (overall skull morphology, mastoid process, frontal eminence, parietal eminence, orbit shape, and mental eminence). The classification accuracies ranged between 56.6% (overall skull morphology) and 80.6% (parietal eminence) for males, and between 47% (parietal eminence) and 74.4% (overall skull morphology) for females.

The observed differences in classification accuracies between the sexes likely stems from the nature of sexual dimorphism associated with the assessed morphological skull traits, with some traits exhibiting more pronounced and consistent morphological differences in one sex than the other (Christensen *et al.,* 2014c; Berg, 2017). The differences in sex estimation accuracy between males and females in the current study can be attributed to the variable expression of the assessed

sexually dimorphic skull traits. For instance, the parietal eminence, with an 80.6% accuracy for males, appears to be a more reliable indicator of male sex, suggesting that this trait is more consistently and distinctly expressed in males, particularly when assessed from Lodox scans. In contrast, the overall skull morphology demonstrated a higher accuracy for females, indicating that the morphological features of the female skull are more reliably classified as a whole. This difference highlights that not all morphological traits are equally accurate for sexing both sexes from Lodox scans. This is additionally supported by the perfect intra-observer agreement in the scorability of these traits, which confirms that the observed differences in classification accuracy are likely not due to observation errors but rather reflect genuine biological variation in how these traits appear on Lodox scans for males and females.

The moderate sex classification accuracies reported in the current study are primarily limited to skull traits observable and morphologically assessed in high frequencies (>80%, n = 150) from anteroposterior Lodox scans (i.e., overall skull morphology, parietal eminence, orbit shape, and mental eminence) compared to cranial traits that require visualisation from a lateral plane of view (i.e., mastoid process and frontal eminence). The low sex classification accuracies obtained for the mastoid process (males = 27.8% and females = 36%) and frontal eminence (males = 6.9% and females = 5%) were likely due to the use of an anteroposterior view which hindered effective morphological assessment as the traits require visualisation from a lateral cranial view for optimal morphological sex assessment (Klales & Cole, 2008). Additionally, the assessment of these traits was largely restricted to scans with a right-sided head tilt, only partially revealing the lateral skull. This limitation affected the scoring process, especially for the mastoid process, which was primarily assessed based on size (very small to very large) rather than the full range of recommended features (İşcan & Steyn, 2013; Klales & Cole, 2018). Specifically, the anteroposterior view hindered the observation and assessment of crucial sex characteristics of the mastoid process, such as its projection relative to the external acoustic meatus (of the temporal bone) and the presence (or absence) of a digastric groove, both essential for accurate sex classification (Klales & Cole, 2018). Similarly, the use of the anteroposterior Lodox scans hindered the effective assessment of the relative size of the frontal eminence (i.e., small or large) and subsequently resulted in low sex classification accuracies. While anterior plane of views are preferred for assessing overall skull morphology, parietal eminences, orbit shape, and mental eminences for optimal sex classification (İşcan & Steyn, 2013; Klales & Cole, 2018; Gupta *et al.,* 2022), the use of 2D anteroposterior Lodox scans did not provide sufficient detail for highly accurate morphological sex estimations comparable to those achieved with traditional dry bone analyses

(Krüger *et al.,* 2015; Gupta *et al.,* 2022) or CT scans (Teodoru-Raghina *et al.,* 2017; Kelley, 2022) when assessing similar cranial traits.

The sex classification accuracies achieved for males and females as well as the combined classification for the assessed traits fall below the commonly reported sex classification accuracies (80-95%) from studies employing similar assessments but utilising morphological dry bone analysis (Krüger *et al.*, 2015; Gupta *et al.,* 2022), geometric morphometric analysis (Toneva *et al.,* 2023), or CT scan (Teodoru-Raghina *et al.,* 2017; Dereli *et al.,* 2018; González-Colmenares *et al.,* 2019; Kelley, 2022) approaches. For instance, Gupta *et al.* (2022) also assessed various traditional skull traits for morphological sex estimation based on dry bone analyses of 161 skeletal samples of Black South Africans. Compared to the current study findings, Gupta and colleagues (2022) reported relatively higher classification accuracies for the glabella (males = 86.6% and females = 74.2%), frontal eminence (males = 78.1% and females = 80.6%), mastoid process (males = 73.2% and females = 67.7%), and mental eminence (males = 69.5% and females = 60%). Contrary to Gupta and colleagues (2022) sex classification accuracies for the overall skull morphology (males = 88.8% and females = 69.4%) and orbit shape (males = 88.5% and females = 62.9%), the current study achieved comparably higher female classification accuracies for these traits, 74.4% and 69.2%, respectively.

Similarly, Dereli and colleagues (2018) investigated morphological sex estimation from adult 3D CT scans (49 males and 36 females) by three observers, using the Walker (2008) traits. The authors reported classification accuracies ranging between 98% and 100% for males, and between 83% and 86% for females, with the glabella being the most effective trait for morphological sex estimation (accuracies range from 84.2-91.3% amongst observers). Similarly, Kelley (2022) evaluated the accuracy of morphological skull sex estimation using 3D volume rendered CT scans of adult individuals from New Mexico (242 males and 189 females), comprised of individuals of African American, Asian American, European American, Latin American, and Native American ancestry. The author assessed morphological skull traits based on Buikstra and Ubelaker (1994) and the Walker (2008) sex estimation methods. Although the study findings by Kelley (2022) do not specify classification accuracies per assessed skull traits but rather per population group, the reported classification accuracies are relatively higher than those achieved in the current study, particularly for individuals of European ancestry. Population-specific classification accuracies ranged between 81% and 87%, with the classification model for European American individuals achieving 81% combined classification accuracy (males = 80.5% and females = 81.6%). Contrary to Dereli *et al.* (2018), Gupta *et al.* (2022), and Kelley (2022), sex classifications of the glabella and nuchal crest traits were not possible to estimate in the current study due to the limitations of

anteroposterior Lodox scans to visualize the traits that were not being observable from all anteroposterior Lodox scans.

None of the other assessed Walker (2008) traits (i.e., mastoid process and mental eminence), including the overall skull morphology, frontal eminence, parietal eminence, and orbit shape, achieved sufficiently higher accuracy rates to be used in combination to improve the obtained accuracy rates. These findings are most likely due to inherent limitations associated with x-ray imaging (including Lodox scans) to distort images, superimpose anatomical structures, obscure observation with soft tissue presence (Muehleman *et al.,* 2006; Stull, 2013b; Ahern & Brygel, 2014; Franklin *et al.,* 2018) as well as offer a limited anatomical plane of view compared to traditional dry bone analyses and 3D CT scans techniques, thus inhibiting accurate morphological assessment of skull traits from Lodox scans. Therefore, it is likely that anteroposterior Lodox® Statscan™ scans do not provide sufficient image quality for accurate skeletal sex estimation from skull traits, particularly given that 3D CT scans can achieve accuracy rates comparable to those obtained through traditional dry bone analyses approaches.

While sex classification of skull traits generally yielded moderate accuracy compared to other sex estimation approaches like dry bone or CT scan analyses, the study found that focusing on a subset of observable and scorable traits notably improved accuracy. The assessed traits demonstrated the potential for skull sex estimation using Lodox scans, achieving accuracies over 75.0% for male, female, or combined classification. The mastoid process, in particular, demonstrated exceptionally high accuracies (>82.0%) across all classifications. In contrast, the frontal eminence, parietal eminence, orbit shape, and mental eminence were found to be reliable and accurate indicators specifically for female classification (Table 4.9). For these traits, accuracies of over 75.0% were achieved for either male or female or combined classification, further demonstrating the potential for using Lodox scans for skull sex estimation, albeit with limited applicability. For instance, Th mastoid process demonstrated particularly high accuracies (>82.0%) for male, female, and combined classification, while the and frontal eminence, parietal eminence, orbit shape, and mental eminence were a reliable and accurate indicators for female classification from Lodox scans (Table 4.9). These findings suggest that while Lodox scans have limitations, specific traits can still be used for highly accurate sex estimation, especially when the traits are clearly scorable on 2D anteroposterior scans.

5.3.2. Postcranial traits

Numerous postcranial skeletal traits have been investigated and assessed for morphological sex estimation, with up to 96% accuracy rates, even on studies utilising radiographic modalities

(Krogman and İşcan, 1962; Phenice, 1969; McCormick & Stewart, 1983; Rogers, 1999; Prado *et al.,* 2009; Scholtz *et al.,* 2010; Ali *et al.,* 2020; Rogers *et al.,* 2021). Similar to the skull, morphological assessment of various postcranial traits for sex estimation is feasible from Lodox scans but mainly limited to selected postcranial traits (e.g., pelvic traits), especially when evaluated against the total study sample. Similar to skull traits, the achieved pelvic traits classification accuracies were relatively moderate compared to those achieved in dry bone analyses (Rogers & Saunders, 1994; Kenyhercz, 2012; Inskip *et al.,* 2019; Gupta *et al.,* 2022), geometric morphometric analyses (Djorojevic *et al.,*2014; Cox, 2021), and CT scan (Decker *et al.,* 2011; Colman *et al.,* 2019; Ali *et al.,* 2020) approaches (80-96% classification accuracies). The moderate classification accuracies reported in the study ranged between 63.9% (ilium morphology) and 77.8% (subpubic angle shape and obturator foramen shape) for males, and between 52.6% (subpubic contour) and 80.8% (pelvic brim) for females.

The use of anteroposterior Lodox scans offered high observability and scorability frequencies (>82%, n = 150) for assessed pelvic traits, they were insufficient for providing detailed morphological assessments required for accurate sex classification when compared to dry bone analyses (Kenyhercz *et al.,* 2017; Inskip *et al.*,2019; Gupta *et al.*, 2022) or CT scan (Ali *et al.*, 2020) approaches assessing similar assessed pelvic traits. The use of anteroposterior Lodox scans hindered the effective evaluation of key sex-discriminating features of certain pelvic traits, such as the detailed morphologies of the subpubic bone contour and ventral arc, and the orientation of the acetabulum, which are typically assessed with direct and highly detailed observation in dry bone sex estimation approaches (İşcan & Steyn, 2013; Klales & Cole, 2018). This subsequently resulted in low and relatively biased sex classifications for these pelvic traits compared to other assessed pelvic traits (i.e., subpubic contour: combined accuracy = 60.7%, males = 69.4%, and females = 52.5%; acetabulum position: combined accuracy = 68%, males = 70.8%, and females = 66%; ventral arc: combined accuracy = 69.3%, males = 76.4%, and females = 62.8%). Moreover, only the overall pelvis morphology yielded consistently high and acceptable classification accuracies (>75%) for both males (75.0%) and females (79.5%), and combined sex accuracy (77.3%). Although the pelvis is associated with high sexual dimorphism due to adaptations in female parturition (Berg, 2017), the morphologies of the other pelvic traits proved challenging to visualize with 2D Lodox scans to effectively yield highly accurate sex classifications. Therefore, achieving acceptable accuracies for either males or females classification was limited to a selected pelvic traits, further indicating that these traits, when assessed from 2D anteroposterior Lodox scans, are more consistently and distinctly expressed in one sex or the other (i.e., pelvic brim (females = 81%), subpubic shape (males = 78%), obturator foramen shape (males = 78%), ventral

arc (males = 76%), and ilium morphology (females = 78%)). Furthermore, the study's finding that the overall pelvis morphology had consistently high classification accuracy for both sexes indicates that while individual traits might be difficult to assess in 2D, the assessment of the pelvis as whole provides a more reliable and accurate sex classification from Lodox scans. That is, the collective appearance of a wider, broader female pelvis and a narrower, more robust male pelvis is easier to distinguish even with the limitations associated with a 2D anteroposterior Lodox scan.

Nevertheless, the current study findings align with those of Varzandeh *et al.* (2019) and Abdallah *et al.* (2021), who also reported moderate sex classification accuracies (67-77% and 60-68%, respectively) in morphometric assessment of pelvic traits assessed from anteroposterior pelvis x-ray scans of adult individuals. Moreover, the current study's findings are comparable with previous studies that have reported high classification accuracy rates for morphological skeletal sex estimation based on pelvic traits compared to traits of the skull (Inskip *et al.,* 2019; Gupta *et al.,* 2022). The high sex classification accuracy of the pelvic girdle (compared to the skull and other assessed postcranial elements) is primarily attributed to the pelvis being the most sexually dimorphic skeletal element due to adaptations for parturition, to accommodate the passage of a foetus in females, subsequently resulting in significant sex differences in pelvic shape and size (Christensen *et al.,* 2014c; Klales, 2020b). Additionally, the high sex classification accuracy associated with the pelvis is also most likely attributed to the pelvis' high reliability for visual assessment and scoring for morphological sex estimation as reported in numerous study findings that have investigated its reliability in morphological sex estimation (e.g., Blanchard, 2010; Klales *et al.,* 2015; Colman *et al.,* 2019; Inskip *et al.,* 2019; Gupta *et al.,* 2022). Thus, the assessed pelvic traits yielded consistently higher sex classification accuracies compared to the skull and other postcranial traits, in addition to being reliable for observation and morphological scoring on Lodox scans.

Although the assessed pelvic traits exhibited the highest sex classification accuracies among the postcranial skeletal elements (61-77% combined sex classification accuracies), these accuracy rates fall notably below the commonly reported range achieved in pelvic morphological sex estimation studies utilising dry bone analyses (generally 85-96% combined accuracies) or CT scans (generally 85-95% combined accuracies) (e.g., Patriquin *et al.,* 2003; Listi & Bassett, 2006; Bierry *et al.,* 2010; Stull *et al.,* 2013a; Klales *et al.,* 2015; Kenyhercz *et al.,* 2017; Joon & Rohatgi, 2021; Zhang, 2022, 2024). For instance, Inskip and colleagues (2019) evaluated macroscopic sex estimation using various pelvic traits, including iliac morphology, ventral arc, subpubic angle, and subpubic contour, from a genetically sexed medieval skeletal collection (66 individuals). Contrary to the current study findings, Inskip and colleagues (2019) reported significantly higher

classification accuracies for the aforementioned pelvic traits, specifically 87.5% and 77.8% for male and female iliac morphologies (respectively), 93% and 100% accuracies for male and female the ventral arcs (respectively), and 100% accuracies for both male and female subpubic angles and subpubic contours. Similarly, Rogers and Saunders (1994) on a sample of 49 skeletons of Canadian ancestry evaluated morphological sex estimation using 17 morphological pelvic traits, including those assessed in the current study (i.e., obturator foramen shape, acetabulum position, ventral arc, subpubic contour, pelvic brim, and ilium morphology). Rogers and Saunders (1994) reported combined sex classification accuracies significantly higher than those reported in the current study, specifically 93% for the obturator foramen shape, 91% for the acetabulum position, 86% for the ventral arc, 83.8% for the subpubic contour, 83.7% for the ilium, and 80% for the pelvic brim. In contrast, the current study achieved relatively lower classification accuracy rates for these traits (61-77% combined accuracies).

Similarly, a multitude of dry bone pelvis morphological sex estimation studies, such as those by Patriquin *et al.* (2003), Bierry *et al.* (2010), Small *et al.* (2012), Kenyhercz (2012) Kenyhercz *et al.* (2017), Gupta *et al.* (2022), as well as Jager and Eliopoulos (2024), have reported relatively high sex classification accuracies (over 80% combined sex accuracies), across distinct population groups (including South Africans) in morphological sex estimations of the subpubic contour, subpubic angle/shape, obturator foramen shape, and ventral arc morphology in adult individuals. Similar to dry bone analyses approaches, Ali and colleagues (2020) reported a 94% combined accuracy of subpubic angle/shape (males = 94% and females = 94%) for sex estimation from multidetector CT scans of 100 contemporary Malaysian adult individuals. In contrast, the current study achieved lower classification accuracies for similar assessed morphological pelvic traits (61-77% combined accuracies). This was most likely due to limitations associated with assessing morphological skeletal traits from anteroposterior 2D x-ray images, such as overlapping anatomical structures and soft tissues, further masking the precise morphology of the traits and yielding less accurate assessment for se sex estimation.

The remaining assessed postcranial traits yielded classification accuracies below 60%, thus rendering the use of Lodox scans unsuitable and impractical for morphological sex estimation from these postcranial traits. The relatively moderate sex estimation accuracies achieved from Lodox scans, compared to dry bone and CT scans analyses, may be attributed to limitations in x-ray image quality to provide reliable and accurate assessment of adult postcranial skeletal sex (Ahern & Brygel, 2014; Huda & Abrahams, 2015; Ou *et al.,* 2021). This further indicates the superiority of traditional dry bone analyses (and CT scans) for accurate pelvic (and other postcranial traits) morphological sex estimation compared to the current study's utilisation of Lodox scans (Klales,

2013; Zhang, 2022, 2024). While the utilisation of Lodox® Statscan™ radiographs should not be of primary preference for morphological sex estimation of postcranial traits, particularly for the scapula, distal humerus, sacrum, and femur, in forensic anthropological analyses, the current study findings indicate that moderately accurate sex estimation can be achieved from anteriorly observable pelvic traits. As such, Lodox scans may serve as a valuable preliminary tool for sex estimation in emergencies where dry bone analyses are not immediately feasible or readily available.

Sex classification of postcranial traits from Lodox scans yielded poor and moderate accuracies compared to studies utilising dry bone, geometric morphometric, and CT scan analyses. However, the study found that focusing on a subset of observable and scorable traits provides notably high classification accuracy for majority of postcranial traits. For these traits, accuracies of over 75.0% were achieved for either male, female or combined classification, demonstrating the potential for using Lodox scans for sex estimation, albeit with limited applicability. For instance, postcranial traits such as costal cartilage ossification patterns, and the olecranon-coronoid angle demonstrated particularly high accuracies for male classification, while infraspinous fossa's lateral border and sacrum morphology were a reliable and accurate indicator for both sexes (Table 4.9). These findings suggest that despise the limitations of Lodox scans, focusing on specific traits that are clearly observable and scorable in 2D anteroposterior views significantly improves morphological sex classifications, yielding highly accurate sex estimations.

5.4. Lodox Scans Limitations for Morphological Skeletal Sex Estimation

The capabilities of the Lodox® Statscan™ to effectively visualize skeletal elements and locating foreign metal objects in medico-legal cases while also providing rapid full-body imaging have been well documented (Knobel *et al.,*2006; Evangelopoulos *et al.,* 2009; Mamabolo *et al.,* 2020; Morele *et al.,* 2024). The current study's findings support the established capabilities of the Lodox® Statscan™ to reliably visualize human skeletal elements. However, the utilisation of Lodox scans to visualize morphological skeletal traits for sex estimation proved to be challenging, resulting in comparatively low to moderate sex classification accuracies. This is notable considering that the assessed traits have been previously validated based on dry bone analysis for application in South African individuals of European ancestry (Scholtz *et al.,* 2010; Klales *et al.,* 2012; Small *et al.*, 2012; Stull *et al.,* 2013a; Krüger *et al.*, 2015; Ishwarkumar *et al.*, 2016; Kenyhercz *et al.,* 2017; Gupta *et al.,* 2022).

These findings are most likely attributed to inherent limitations in x-ray radiography, which may not always provide sufficient detail for visualisation of intricate anatomical structures such as

morphological skeletal traits (Williams *et al.,* 2007; Franklin *et al.,* 2016; DeMaio *et al.,* 2019; Allen, 2022). Moreover, certain assessed Lodox scans exhibited distortions (non-proportional scaling of the radiographed object) at certain skeletal regions of interest, effectively contributing to less accurate assessment of such skeletal regions (e.g. elbow and knee regions). However, the linear-slot scanning design and the use of collimated fan beam geometry by the Lodox® Statscan™ in addition to placing the body table to the lowest position (approximately 6 cm) from the detector significantly minimises image distortion by employing a greater SID and low OID (Pitcher *et al.,* 2008; Stull *et al.,* 2013b; Chimhundu *et al.,* 2014). In contrast, traditional conventional x-ray modalities typically utilise cone beam geometry which produces distortion in both x- and y-axis (Stull *et al.,* 2013b; Pauwels *et al.,*2015). As such, these Lodox® Statscan™ features collectively contribute to reducing image distortion, especially along the scan-axis (y-axis) and on individuals placed in a supine anatomical position (Boffard *et al.,* 2006; Stull *et al.,* 2013b). As such, image distortion was extensive on body regions (and skeletal elements and traits) that were not positioned in an optimal anatomical position during the scanning process, such as a tilted head, bent elbow or knee (Figures 5.2 and 5.3).

Similarly, certain Lodox scans exhibited 2D superimposition of skeletal elements and traits because of the overlapping nature of internal body structures to be compressed onto a single 2D plane by x-ray modalities (Dorion, 1983), in addition to the scanned individual not being placed in an optimal anatomical position (Figure 5.2). Moreover, the contrast resolution of the radiographs, defined as the degree of greyscale differentiation between anatomical structures (Clark, 2018), also likely influenced the accurate assessment of morphological traits for sex estimation. This is because regions with low contrast (many shades of grey) or high contrast (few shades of grey) may have hindered the observer's ability to accurately assess the morphology of certain traits, potentially impacting the sex classification accuracy of associated traits. Although the Lodox® Statscan™ imaging software (©Lodox™ 2005 Application Version 2.9.0.0) offers digital image contrast adjustment postprocessing, the patient contrast cannot be manipulated digitally postprocessing as it is determined by how effectively the patients' anatomical structures absorb x-ray beams and how the corresponding energy is transferred to the image receptor (DeMaio *et al.,* 2019). Consequently, Lodox scans with very low or high subject contrast in skeletal elements or traits (Figure 5.1 A) likely resulted in a less accurate visual assessment of such skeletal traits even though the digital contrast could be manipulated.

Consequently, these limiting factors (image distortion, 2D superimposed anatomical structures, patient contrast) hindered accurate visualisation and morphological assessment of affected skeletal elements and traits of interest, evident in the difficulty in assessing distorted and overlapping

observable skeletal traits. This likely led to inaccurate visual morphological assessment and potential misclassification of skeletal sex, particularly for traits like mental eminence, suprascapular notch, costal cartilage ossification patterns, olecranon-coronoid angle, femoral neck shaft angle, and quadriceps angle. Consequently, observation and morphological scoring frequencies for these skeletal traits were notably moderate and lower than their respective traditional dry bone methods. Additionally, these factors ultimately impacted the overall sex classification accuracy of such skeletal traits (if not all), resulting in higher misclassification and low accuracy rates, even though the traits were observable and scorable in high frequencies. As such, this study's findings highlight that while Lodox® Statscan™ scans are reliable for documenting and identifying skeletal elements and traits, their utility for morphological sex estimation is limited compared to alternative approaches of morphological sex estimation, particularly those that offer minimum to no obscuration of assessed morphological skeletal traits (e.g., traditional dry bone morphological assessment).

5.5. Study Limitations and Recommendations for Future Research

5.5.1. Limitations

The visibility of soft tissues, including external reproductive organs in Lodox scans, presented challenges that could potentially have biased the assessment of morphological traits for sex estimation (Figure 5.4). To maintain professionalism and research integrity, biased assessment was minimised by assessing skeletal traits scientifically based on their visibility on Lodox scans and according to their respective established criteria of morphological assessment, independent of the visibility of external reproductive organs. This approach was reflected in the relatively similar and comparable reliability agreements for both observation and scorability and significant statistical differences between the predicted sexes and documented sexes. These findings suggest an independent observation and assessment of skeletal traits, demonstrating the genuine applicability of Lodox scans for morphological sex estimation of skull and postcranial skeletal traits.

The presence of extensive soft tissue interference (Figure 5.1) and internal prostheses (Figure 5.3) on certain Lodox scans obscured and limited the potential visualisation and assessment of respective traits of interest (e.g., rib costal cartilages, scapula traits, sacrum, and femur). Additionally, the Lodox® Statscan™ is an outdated x-ray modality, no longer manufactured by the Lodox® Systems (Pty) Ltd company. As such, it is most likely to yield inferior image quality (compared latest Lodox® Systems modalities) that can compromise accurate visualisation and assessment of morphological skeletal traits of interest, especially when obscured by soft tissue interference and internal prostheses. These factors further reduced the number of skeletal elements

and traits that could be assessed on the Lodox scans, thereby limiting the accuracy of morphological sex estimation.

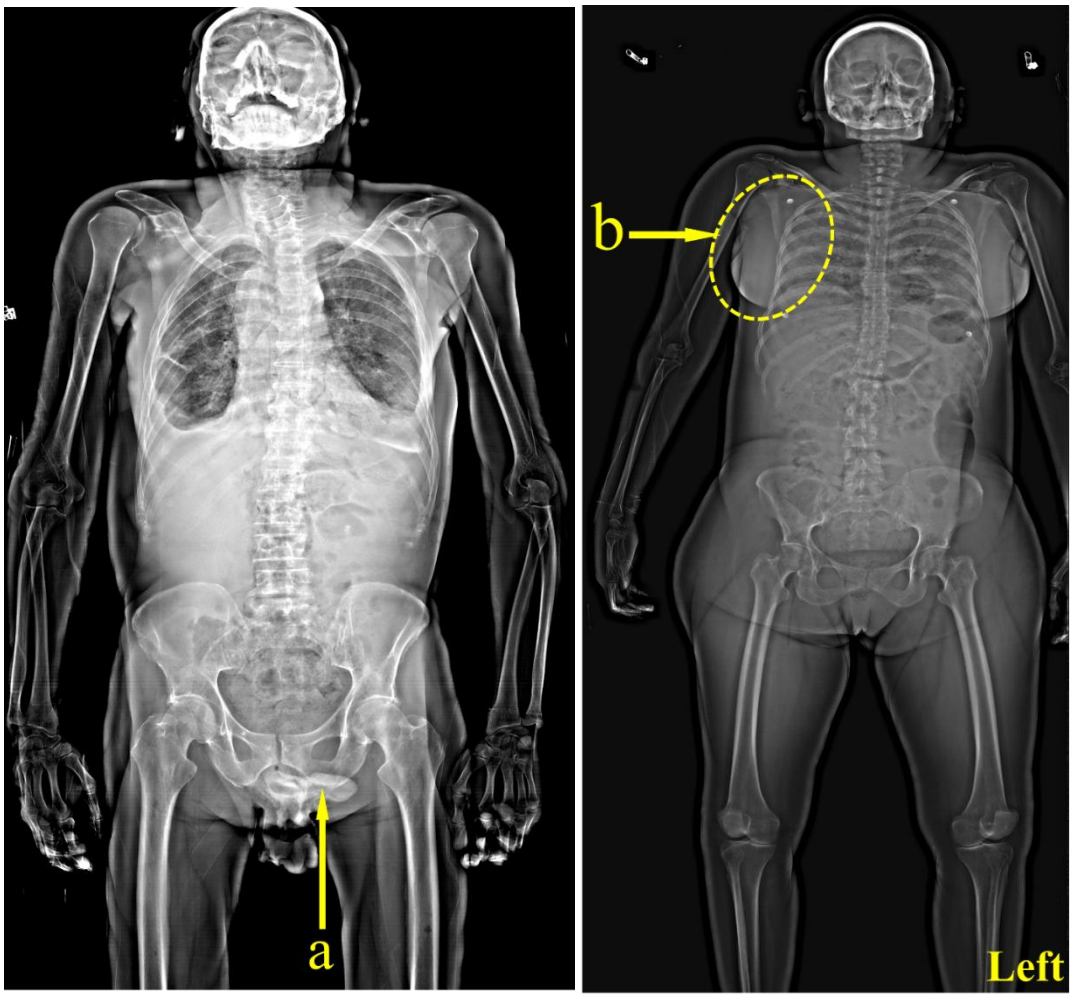
Another factor which posed as a study limitation is that the utilised Lodox scans were of individuals scanned only in an anteroposterior plane of view. The reliance on a single anatomical plane of view (i.e., anterior) restricted a comprehensive visualisation of the skull and postcranial skeletal elements and their associated traits. This limitation more often hinders the accurate assessment of traits of interest, as a holistic perspective consisting of multiple anatomical planes (i.e., anterior, lateral, oblique) is often crucial for a thorough assessment of morphological skeletal traits. Hence, skeletal traits mainly visible from lateral and/or oblique plane of views (e.g., nuchal crest, forehead slope, glabella, medial epicondyle angle, and greater sciatic notch) were not observable from any of the assessed Lodox scans, inhibiting their assessment for morphological sex estimation. As such, a standard procedure for Lodox scanning that includes multiple anatomical viewing planes that comes with the Lodox® Statscan™ functionality is warranted to accommodate visualisation of such traits (i.e., i.e., anterior, lateral, and oblique scans).

Additionally, the assessed Lodox scans are of individuals who were not all taken in a typical standardised anatomical position during the scanning process due to individual body variations including challenges of positioning individuals due to rigor mortis that occurs in the body after death, in addition to formalin embalming for tissue preservation. That is, certain scans were characterized by individuals who were not lying supine, facing directly anteriorly, upper limbs positioned naturally at the sides of the body, palms of the hands facing anteriorly, and the feet lying parallel to each other facing anteriorly (Christensen *et al.,* 2014d) on the Lodox® Statscan™ machine body table during the scanning process (Figures 5.1, 5.2, and 5.3). Nevertheless, the results of the current study do demonstrate the utility of Lodox® Statscan™ radiographs to visualise skeletal elements and traits as well as morphological sex estimation of certain sexually dimorphic traits, particularly those of the pelvis.

A limited sample size of Lodox scans (150 scans) and restricted demographic information of the sample (individuals of European ancestry with average age-at-death of 76.5 ± 12.94 years) also posed as a limitation to the current study, as compared to other morphological sex estimation studies that utilised relatively larger sample sizes (i.e., over 300 scans/skeletal remains) and diverse population groups (e.g., black and white South Africans) (Rogers *et al.,* 2000; Bruzek, 2002; Vance *et al.,* 2011; Klales *et al.,* 2012; Krüger *et al.*, 2015).

5.5.2. Recommendations for future research

Given that the utilised x-ray scans are from an outdated x-ray modality (i.e., Lodox® Statscan™), the current study's methodology should be re-assessed using the Lodox Systems' latest x-ray modality for forensic imaging, the Lodox® eXero-dr™ (LODOX®, 2023a). Moreover, all anatomical viewing planes (anteroposterior, lateral, oblique) should be explored and utilised to enhance visualisation and assessment of skeletal elements and traits to potentially improve classification accuracy rates. Given that calibrated measurements of skeletal elements can be obtained from Lodox scans (using ©Lodox™ 2005 Application Version 2.9.0.0), the investigation of metric sex estimation of the observable skeletal elements from the current study should be explored for skeletal sex estimation. This would allow for the comparison of the best application of Lodox® Statscan™ for skeletal sex estimation of adult human remains, and subsequent biological profile estimation.



A B

Figure 5.4: Examples of Lodox scans showing soft tissues of external reproductive organs. Image A is a Lodox scan of a male individual and image B is a Lodox scan of a female individual. a = male penis; b = breast. Left hand side is towards the right.

CHAPTER 6: CONCLUSION

The following conclusions can be drawn from the data presented in this study:

Objective 1: Determine which skeletal elements (i.e., cranium, mandible, clavicle, scapula, rib costal cartilage, humerus, ulna, pelvic girdle, sacrum and femur) are observable on Lodox scans.

1. For observation of skeletal elements from Lodox scans:
    a) Eight out of ten of the assessed skeletal elements (cranium, mandible, clavicle, scapula, distal humerus, proximal ulna, pelvic girdle, and femur) were observable in over 88% of the assessed Lodox scans.
    b) The cranium and pelvic bones were the most observable skeletal elements, each observable in 99.3% of the assessed Lodox scans.
    c) The rib costal cartilages and sacrum were observed in lower frequencies (≤43%), thus not preferable for visualisation from Lodox scans for morphological sex estimation.
    d) Soft tissue interference, image distortion and 2D superimposition of anatomical structures hindered the 100% observability of all assessed skeletal elements from Lodox scans

Objectives 2: Determine which skull and postcranial sexually dimorphic traits are observable and scorable from Lodox scans.

1. For observation and morphological scoring of skull traits (n = 150):
    a) Four skull traits (overall skull morphology, parietal eminence, orbit shape and mental eminence) were observed and scored in over 89% and 76% of the assessed Lodox scans, respectively.
    b) The mastoid process and frontal eminence were observed and scored in less than 44% and 38% of the assessed Lodox scans.
    c) The nuchal crest, forehead slope, and glabella were not observable from all assessed Lodox scans.
    d) The utilisation of anteroposterior Lodox scans significantly impact the effective visualisation of the mastoid process, frontal eminence, nuchal crest, forehead slope, and glabella from Lodox scans as these traits are optimally visualised from the lateral aspect of the cranium.
2. For observation and morphological scoring of postcranial traits (n = 150):
    a) Pelvic traits were the most frequently observed and scored postcranial traits, observable and scorable in over 87% and 82% of assessed Lodox scans, respectively.

b) Selected traits of the scapula (infraspinous fossa's lateral border) and the distal humerus (olecranon fossa) were the second and third most observed and scored postcranial traits, observable in 82.7% and 78.7% respectively, and scorable in 80.7% and 72% respectively.
c) The observations of the remaining postcranial traits were poor, ranging from 20% (sacrum) to 66% (femoral neck shaft angle), with scorability frequencies ranging from 17% (sacrum) to 48% (trochlea symmetry) of the assessed Lodox scans.
d) The costoclavicular tuberosity, medial epicondyle angle, and greater sciatic notch were not observable nor scorable in the assessed Lodox scans, due to the traits being optimally visible from lateral and/or oblique planes of view.
e) Interference of soft tissues, image distortion, and superimposed anatomical structures significantly impacted the effective visualisations of non-pelvic postcranial traits from assessed Lodox scans.

Objective 3: Assess the intra- and inter-observer repeatability of the observable skeletal elements and associated sexually dimorphic skeletal traits from Lodox scans.

1. For the reliability of observable skull and postcranial elements:
   a) Observation of seven skeletal elements (cranium, clavicle, distal humerus, proximal ulna, pelvis, & femur) from Lodox scans demonstrated perfect intra- and inter-observer repeatability, and were most reliable for visualisation on Lodox scans.
   b) The remaining skeletal elements (mandible, scapula, rib costal cartilage, and sacrum) had lower and dissimilar intra- and inter-observer repeatability agreements.
2. For the reliability of observation and scoring of skull traits:
   a) Only overall skull morphology exhibited perfect intra- and inter-observer repeatability for observations and achieved perfect intra-observer and moderate inter-observer agreement for scorability.
   b) The mastoid process exhibited the lowest repeatability agreements; fair intra- and slight inter-observer agreements for observation, and moderate intra- and slight inter-observer agreements for scorability.
   c) The nuchal crest, forehead slope, and glabella morphologies exhibited perfect repeatability agreements for non-visualisation from any of the assessed Lodox scans.
   d) The remaining skull traits had lower and dissimilar intra- and inter-observer repeatability agreements for observation and scorability.
3. For reliability of observation and scoring of postcranial traits:
   a) Observations of all assessed pelvic traits, except the obturator foramen shape (substantial repeatability) and acetabulum position (moderate intra- and substantial inter-observer

repeatability), exhibited perfect intra- and inter-observer repeatability. Scorability for assessed pelvic traits demonstrated intra- and inter-observer repeatability ranging from moderate to perfect agreement.

b) The remaining assessed postcranial skeletal traits demonstrated a range of intra- and inter-observer repeatability for both visual observability and scorability, consisting of slight, fair, moderate, and substantial levels of repeatability agreements.
c) The costoclavicular tuberosity, medial epicondyle angle, and greater sciatic notch had perfect repeatability agreements for non-visualisation from all assessed Lodox scans.

Objective 5: Assess the sex classification accuracies of the scorable sexually dimorphic traits for the estimation of morphological skeletal sex from Lodox scans.

1. For sex classification accuracy of scorable skull and postcranial traits:
   a) Moderate accuracy for skeletal sex classification was primarily achieved using pelvic traits (61-77% combined accuracy) and a selected few skull trait (63-71% combined accuracy).
   b) The remaining postcranial traits primarily achieved lower sex classification accuracies (≤54% combined sex accuracies) compared to the skull and pelvic traits.
   c) The reported accuracy rates (61-78% for pelvic traits and 63-71% for selected skull traits) are relatively lower than the reported range of accuracies (80% to 95%) achieved by alternative traditional and CT scan morphological sex estimation approaches, thus indicating the limitations for high accuracy of morphological sex estimation of skull and pelvic traits from Lodox scans.

This study indicated that Lodox scans are moderately accurate and reliable in visualising skeletal elements, including pelvic traits, and selected skull and postcranial traits. However, using Lodox scans for morphological sex estimation yielded low to moderate sex classification accuracies compared to alternative approaches (i.e., dry bone analysis, CT scans). This finding indicates that the use of Lodox® Statscan™ scans may not be a highly accurate and reliable approach for estimating the morphological skeletal sex of adult individuals from x-ray radiographs, but rather a reliable tool for observing skeletal elements and some of their associated traits. Given the limitations of morphological assessment for sex estimation from Lodox scans, alternative approaches, such as metric methods, should be explored for sex estimation using the highly observable skeletal traits identified in the current study. In addition, the current applicability of Lodox® Statscan™ for sex estimation requires refinement to optimize its accuracy for morphological sex estimation of human remains, especially where the identity of the remains is unknown and required for estimation of other biological profile parameters. It is assumed the

current utilisation of Lodox® Statscan™ for morphological sex estimation can yield moderate sex classification accuracies for morphological skull and pelvis traits and poor accuracies for other morphological postcranial traits.

REFERENCES

Abdallah, R.S., El Sayed, H.R. and Abdel Moawed, D.M.N. (2021). Forensic assessment of sex using pelvic X-rays in Libyan population in Tripoli. *Zagazig Journal of Forensic Medicine* **19(1)**: 91-101.

Abegg, C., Balbo, I., Dominguez, A., Grabherr, S., Campana, L. and Moghaddam, N. (2021). Virtual anthropology: a preliminary test of macroscopic observation versus 3D surface scans and computed tomography (CT) scans. *Forensic Sciences Research* **6(1)**: 34-41.

Adams, D.C., Rohlf, F.J., and Slice, D.E. (2004). Geometric morphometrics: ten years of progress following the 'revolution'. *Italian Journal of Zoology* **71(1)**: 5-16.

Ahern, G. and Brygel, M. (2014). *Exploring Essential Radiology* (eds), New York: McGraw-Hill Education LLC.

Airan, N. and Dwivedi, A.K. (2018). A comparative study of carrying angle among males and females in Garhwal region of Uttarakhand. *Medpulse International Journal of Anatomy* **6(2)**: 13-17.

Aldoihi, S. and Hammami, O. (2018). User experience of CT scan: a reflection of usability and exertions in *2018 IEEE/ACS 15th International Conference on Computer Systems and Applications (AICCSA).* IEEE:1-6.

Ali, S.H.M., Omar, N., Shafie, M.S., Ismail, N.A.N., Hadi, H. and Nor, F.M. (2020). Sex estimation using subpubic angle from reconstructed three-dimensional computed tomography pelvic model in a contemporary Malaysian population. *Anatomy & Cell Biology* **53(1)**: 27-35.

Allen, C.M. (2022). *Digital Radiographic Exposure: Principles & Practice,* Missouri: University of Missouri.

Aly, S.M., Shrestha, B., Hong, D.J., Omran, A. and Wang, W. (2016). Identification of age and sex based on knee radiography. *Forensic Science International* **267**: 231.e1-231.e7.

American Academy of Forensic Sciences Standards Board (2019). Standard for Sex Estimation in Forensic Anthropology (1st ed.). *AAFS Standards Board, LLC.* Available at: https://www.aafs.org/asb-standard/standard-sex-estimation-forensic-anthropology (Accessed: 14 January 2025).

Amirlak, B., Zakhary, B., Weichman, K., Ahluwalia, H., Forse, A.R. and Gaines, R.D. (2009). Novel use of Lodox Statscan in a level one trauma centre. *Ulusal Travma ve Acil Cerrahi Dergisi* **15(6)**: 521-528.

Austin, D. and King, R.E. (2016). The biological profile of unidentified human remains in a forensic context. *Academic Forensic Pathology* **6(3)**: 370-390.

Avent, P.R., Hughes, C.E. and Garvin, H.M. (2022). Applying posterior probability informed thresholds to traditional cranial trait sex estimation methods. *Journal of Forensic Sciences* **67(2)**: 440-449.

Bainbridge, D. and Tarazaga, S.G. (1956). A study of sex differences in the scapula. *The Journal of the Royal Anthropological Institute of Great Britain and Ireland* **86(2)**: 109-134.

Bareša, T., Jerković, I., Bašić, Ž., Jerković, N., Dolić, K., Dujić, G., Borić, M.Ć., Mršić, D.B., Krešić, E., Čavka, M. and Kružić, I. (2024). Walker's traits for sex estimation in modern Croatian population using MSCT virtual cranial database: validation and development of population-specific standards. *Forensic Imaging* **36**: 200578 https://doi.org/10.1016/j.fri.2024.200578.

Bass, W.M, 2003. *Human Osteology: a laboratory and field manual* (4th edition, 9th printing), Columbia: Missouri Archaeological Society.

Beningfield, S.J., Potgieter, J.H., Bautz, P., Shackleton, M., Hering, E., De Jager, G., Bowie, G., Marshall, M., Cox, G., Pagliari, G. and Coetzee, N., 1999. Evaluation of a new type of direct digital radiography machine. *South African Medical Journal* **89(11)**: 1182-1188.

Beningfield, S., Potgieter, H., Nicol, A., Van As, S., Bowie, G., Hering, E. and Lätti, E., 2003. Report on a new type of trauma full-body digital X-ray machine. *Emergency Radiology* **10(1)**: 23-29.

Berg, G.E. (2013). ‘‘Determining the sex of unknown human skeletal remains”, in Tersigni-Tarrant, M.A. and Langley, N.R. (eds), *Forensic Anthropology: an introduction*, New York: CRC Press, 139-160.

Berg, G.E. (2017). “Sex estimation of unknown human skeletal remains”, in Langley, N.R., Tersigni-Tarrant, M.A. (eds), *Forensic Anthropology: a comprehensive introduction*, Second Edition, New York: CRC Press, 143-161.

Berger, A. (2002). How does it work?: bone mineral density scans. *BMJ: British Medical Journal* **325(7362)**: 484-484.

Berger, M., Yang, Q. and Maier, A. (2018). “Chapter 7 X-ray Imaging” in Maier A., Steidl S. and Christlein V. (editors) *Medical Imaging Systems: an introductory guide*, Cham (CH): Springer, 119-145.

Bernitz, H. And Verster, J. (2017). Lodox® digital imaging–a tool for dental identification in single and mass fatality situations. *South African Dental Journal* **72(3)**: 118-121.

Bertsatos, A., Chovalopoulou, M.E., Brůžek, J. and Bejdová, Š. (2020). Advanced procedures for skull sex estimation using sexually dimorphic morphometric features. *International Journal of Legal Medicine* **134(5)**: 1927-1937.

Bharati, S., Demarchi, D.A., Mukherji, D., Vasulu, T.S. and Bharati, P. (2005). Spatial patterns of anthropometric variation in India with reference to geographic, climatic, ethnic and linguistic backgrounds. *Annals of Human Biology* **32(4)**: 407-444.

Bharati, S., Som, S., Bharati, P. and Vasulu, T.S. (2001). Climate and head form in India. *American Journal of Human Biology: The Official Journal of the Human Biology Association* **13(5)**: 626-634.

Bidmos, M.A., Gibbon, V.E. and Strkalj, G., 2010. Recent advances in sex identification of human skeletal remains in South Africa. *South African Journal of Science* **106(11)**: 1-6.

Biehler-Gomez, L., Tritella, S., Martino, F., Campobasso, C.P., Franchi, A., Spairani, R., Sardanelli, F. and Cattaneo, C. (2019). The synergy between radiographic and macroscopic observation of skeletal lesions on dry bone. *International Journal of Legal Medicine* **133(5)**: 611-1628.

Bierry, G., Le Minor, J.M. and Schmittbuhl, M. (2010). Oval in males and triangular in females? A quantitative evaluation of sexual dimorphism in the human obturator foramen shape. *American Journal of Physical Anthropology: The Official Publication of the American Association of Physical Anthropologists* **141(4)**: 626-631.

Blanchard, B.K. (2010). *A study of the accuracy and reliability of sex estimation methods of the human pelvis* (Masters Thesis: California State University, Chico). Retrieved from The California State University at ScholarWorks.

Boese, C.K., Dargel, J., Oppermann, J., Eysel, P., Scheyerer, M.J., Bredow, J. and Lechler, P. (2016). The femoral neck-shaft angle on plain radiographs: a systematic review. *Skeletal Radiology* **45**:19-28.

Boffard, K.D., Goosen, J., Plani, F., Degiannis, E. and Potgieter, H. (2006). The use of low dosage X-ray (Lodox/Statscan) in major trauma: comparison between low dose X-ray and conventional X-ray techniques. J*ournal of Trauma and Acute Care Surgery* **60(6)**: 1175-1183.

Braun, S., Ridel, A.F., l'Abbé, E.N., Theye, C.E. and Oettlé, A.C. (2022). Repeatability of a morphoscopic sex estimation technique for the mental eminence on micro-focus X-ray computed tomography models. *Forensic Imaging* **28**: 200500 https://doi.org/10.1016/j.fri.2022.200500.

Braun, S., Schwendener, N., Kanz, F., Lösch, S. and Milella, M. (2023). What we see is what we touch? Sex estimation on the pelvis in virtual anthropology. *International Journal of Legal Medicine* **137(6)**:1839-1852.

Brits, D.M., Bidmos, M.A. and Manger, P.R. (2017). Stature estimation from the femur and tibia in Black South African sub-adults. *Forensic Science International* **270**: 277-e1-277.e10.

Brits, D.M., Manger, P.R. and Bidmos, M.A. (2018). Assessing the use of the anatomical method for the estimation of sub-adult stature in Black South Africans. *Forensic Science International* **283**: 221.e1-221.e9.

Brits, D.M., Billings, B.K., Krämer, B. and Hutchinson, E.F. (2020). The altered profile of a donated cadaver population: challenges for teaching and research? *European Journal of Anatomy* **24(6)**: 475-483.

Bruzek, J. (2002). A method for visual determination of sex, using the human hip bone. *American Journal of Physical Anthropology: The Official Publication of the American Association of Physical Anthropologists* **117(2)**: 157-168.

Buikstra, J.E and Ubelaker, D.H. (eds) (1994). *Standards for Data Collection from Human Skeletal Remains: proceedings of a seminar at the Field Museum of Natural History, organized by Jonathan Haas*, Arkansas: Arkansas Archaeological Survey Research Series.

Carneiro, C., Curate, F., Borralho, P. and Cunha, E. (2013). Radiographic fetal osteometry: approach on age estimation for the Portuguese population. *Forensic Science International* **231(1-3)**: 397-e1-397.e5.

Chen, R.J., Fu, C.Y., Wu, S.C., Wang, Y.C., Chung, P.K., Huang, H.C., Huang, J.C. and Lu, C.W., (2010). Diagnostic accuracy, biohazard safety, and cost effectiveness—the Lodox/Statscan provides a beneficial alternative for the primary evaluation of patients with multiple injuries. *Journal of Trauma and Acute Care Surgery* **69(4)**: 826-830.

Chimhundu, C., Smit, J., Sivarasu, S. and Douglas, T.S. (2014). Inter-landmark Measurements from Lodox Statscan Images. *Journal of Medical Devices* **8(3)**: 30908-1-30908.3.

Christensen, A.M., Passalacqua, N.V. and Bartelink, E.J. (2014a). "Chapter 4 – Medicolegal Significance", in *Forensic Anthropology: current methods and practice,* London: Academic Press, 91-117.

Christensen, A.M., Passalacqua, N.V. and Bartelink, E.J. (2014b). "Chapter 5 – Forensic Taphonomy", in *Forensic Anthropology: current methods and practice,* London: Academic Press, 199-222.

Christensen, A.M., Passalacqua, N.V. and Bartelink, E.J. (2014c). "Chapter 8 – Sex Estimation", in *Forensic Anthropology: current methods and practice,* London: Academic Press, 199-222.

Christensen, A.M., Passalacqua, N.V. and Bartelink, E.J. (2014d). "Chapter 2 – Human osteology and Odontology", in *Forensic Anthropology: current methods and practice,* London: Academic Press, 19-53.

Clark, J.L., Wadhwani, C.P., Abramovitch, K., Rice, D.D. and Kattadiyil, M.T. (2018). Effect of image sharpening on radiographic image quality. *The Journal of Prosthetic Dentistry* **120(6)**: 927-933.

Cleary, M.K. (2012). *Sex estimation from the clavicle: A discriminant function analysis* (Masters Thesis: University of California). Retrieved from Southern Illinois University at Carbondale ProQuest Dissertation & Theses (1514206).

Cohen, J. (1960). A coefficient of agreement for nominal scales. *Educational and Psychological Measurement* **20(1)**:37-46.

Colman, K.L., van der Merwe, A.E., Stull, K.E., Dobbe, J.G., Streekstra, G.J., van Rijn, R.R., Oostra, R.J. and de Boer, H.H. (2019). The accuracy of 3D virtual bone models of the pelvis for morphological sex estimation. *International Journal of Legal Medicine* **133**:1853-1860.

Cox, S.L. (2021). A geometric morphometric assessment of shape variation in adult pelvic morphology. *American Journal of Physical Anthropology* **176(4)**: 652-671.

Curate, F., Alves, I., Rodrigues, T. and Garcia, S.J. (2024). Assigned sex estimation with the clavicle and scapula: A study in a Portuguese reference sample. *Medicine, Science and the Law* **64(1)**: 15-22.

Damiata, B.N., Steinberg, J.M., Bolender, D.J. and Zoëga, G. (2013). Imaging skeletal remains with ground-penetrating radar: comparative results over two graves from Viking Age and Medieval churchyards on the Stóra-Seyla farm, northern Iceland. *Journal of Archaeological Science* **40(1)**: 268-278.

de Villiers, H. (1968). Sexual dimorphism of the skull of the South African Banu-speaking Negro. *South African Journal of Science* **64(2)**: 118-124.

Decker, S.J., Davy-Jow, S.L., Ford, J.M. and Hilbelink, D.R. (2011). Virtual determination of sex: metric and nonmetric traits of the adult pelvis from 3D computed tomography models. *Journal of Forensic Sciences* **56(5)**: 1107-1114.

DeMaio, D.N., Herrmann, T., Noble, L.B., Orth, D., Peterson, P., Young, J. and Odle, T.G. (2019). Best practices in digital radiography. *Radiologic Technology* **91(2)**: 198-201.

Demir, U., Etli, Y., Hekimoglu, Y., Kartal, E., Keskin, S., Yavuz, A. and Asirdizer, M. (2022). Sex estimation from the clavicle using 3D reconstruction, discriminant analyses, and neural networks in an Eastern Turkish population. *Legal Medicine* **56**: 102043 https://doi.org/10.1016/j.legalmed.2022.102043.

Dempers, J.J., Burger, E.H., Du Toit-Prinsloo, L. and Verster, J. (2018). "A South African Perspective", in Duncan, J.R. and Roger W Byard (ed), R.W., *SIDS Sudden Infant and Early Childhood Death: the past, the present and the future*, University of Adelaide Press: Adelaide (AU).

Dereli, A.K., Zeybek, V., Sagtas, E., Senol, H., Ozgul, H.A. and Acar, K. (2018). Sex determination with morphological characteristics of the skull by using 3D modeling techniques in computerized tomography. *Forensic Science, Medicine and Pathology* **14**: 450-459.

Dettori, J.R. and Norvell, D.C. (2020). Kappa and beyond: is there agreement?. *Global Spine Journal* **10(4)**: 499-501.

Deyle, S., Brehmer, T., Evangelopoulos, D.S., Krause, F., Benneker, L.M., Zimmermann, H. and Exadaktylos, A.K. (2010). Review of Lodox Statscan in the detection of peripheral skeletal fractures in multiple injury patients. *Injury* **41(8)**: 818-822.

Dillon, A. (2014). *Cranial sexual dimorphism and the population specificity of anthropological standards* (Masters Thesis: The University of Western Australia). Retrieved from The University of Western Australia Profiles and Research Repository.

Djorojevic, M., Roldán, C., García-Parra, P., Alemán, I. and Botella, M. (2014). Morphometric sex estimation from 3D computed tomography os coxae model and its validation in skeletal remains. *International Journal of Legal Medicine* **128**: 879-888.

Dorion, R.B. (1983). Photographic superimposition. *Journal of Forensic Sciences* **28(3)**:724-734.

du Plessis, M., Date-Chong, M. and Liebenberg, L. (2020). Lodox®: the invaluable radiographic solution in the forensic setting. *International Journal of Legal Medicine* **134**: 655-662.

Elbuken, F., Baykara, M. and Ozturk, C. (2012). Standardisation of the neck-shaft angle and measurement of age-, gender-and BMI-related changes in the femoral neck using DXA. *Singapore Medical Journal* **53(9)**: 587–590.

Elifritz, J. M., Nolte, K. B., Hatch, G. M., Adolphi, N. L., and Gerrard, C. (2014). "Forensic Radiology" in McManus, L.M. and Mitchell, R.N. (editors) *Pathobiology of Human Disease: a dynamic encyclopaedia of disease mechanisms,* Albuquerque: Elsevier Inc., 3448–3458.

Elkeles, A. (1966). Sex differences in the calcification of the costal cartilages. *Journal of the American Geriatrics Society* **14(5)**: 456-462.

Evangelopoulos, D.S., Deyle, S., Zimmermann, H. and Exadaktylos, A.K. (2009). Personal experience with whole-body, low-dosage, digital X-ray scanning (LODOX-Statscan) in trauma. *Scandinavian Journal of Trauma, Resuscitation and Emergency Medicine* **17**: 1-5.

Fahrni, S., Campana, L., Dominguez, A., Uldin, T., Dedouit, F., Delémont, O. and Grabherr, S. (2017). CT-scan vs. 3D surface scanning of a skull: first considerations regarding reproducibility issues. *Forensic Sciences Research* **2(2)**: 93-99.

Falys, C.G., Schutkowski, H. and Weston, D.A. (2005). The distal humerus-a blind test of Rogers' sexing technique using a documented skeletal collection. *Journal of Forensic Sciences* **50(6)**: 1-5.

Fischer, C.S., Kühn, J.P., Völzke, H., Ittermann, T., Gümbel, D., Kasch, R., Haralambiev, L., Laqua, R., Hinz, P. and Lange, J. (2020). The neck–shaft angle: an update on reference values and associated factors. *Acta Orthopaedica*, **91(1)**: 53-57.

Franklin, D., Cardini, A., Flavel, A. and Marks, M.K. (2014). Morphometric analysis of pelvic sexual dimorphism in a contemporary Western Australian population. *International Journal of Legal Medicine* **128**: 861-872.

Franklin, D., Swift, L. and Flavel, A. (2016). 'Virtual anthropology' and radiographic imaging in the Forensic Medical Sciences. *Egyptian Journal of Forensic Sciences* **6(2)**: 31-43.

Frayer, D.W. and Wolpoff, M.H. (1985). Sexual dimorphism. *Annual Review of Anthropology* **14(1)**: 429-473.

Gant, H., Ghimire, N., Min, K., Musa, I., Ashraf, M. and Lawan, A. (2024). Impact of the quadriceps angle on health and injury risk in female athletes. *International Journal of Environmental Research and Public Health* **21(12)**: 1547 https://doi.org/10.3390/ijerph21121547.

Garnett, E.M. and Lewis, M.E. (2022). The potential for over diagnosis of Paget's disease of bone using macroscopic analysis. *International Journal of Paleopathology* **38**:55-63.

Garofalo, E.M. and Garvin, H.M. (2020). "The confusion between biological sex and gender and potential implications of misinterpretations" in Klales, A.R. (ed), *Sex estimation of the human skeleton: history, methods, and emerging techniques,* London: Academic Press, 35-52.

Garvin, H.M. (2020). "Adult sex estimation from cranial morphological traits", in Klales, A.R. (ed), *Sex estimation of the human skeleton: history, methods, and emerging techniques,* London: Academic Press, 95-112.

Garvin, H.M. and Stock, M.K. (2016). The utility of advanced imaging in forensic anthropology. *Academic Forensic Pathology* **6(3)**: 499-516.

Garvin, H.M., Stock, M.K., Marciniec, K.A., Mohamed, M.M., Ternent, E., Cirillo, L.E. and Stull, K.E., 2021. Sex estimation of the subadult ilium prior to acetabular fusion. *Journal of Forensic Sciences* **66(6)**: 2113-2125.

Gillet, C., Costa-Mendes, L., Rérolle, C., Telmon, N., Maret, D. and Savall, F. (2020). Sex estimation in the cranium and mandible: a multislice computed tomography (MSCT) study using anthropometric and geometric morphometry methods. *International Journal of Legal Medicine* **134**: 823-832.

Gilligan, I., Chandraphak, S. and Mahakkanukrauh, P. (2013). Femoral neck-shaft angle in humans: variation relating to climate, clothing, lifestyle, sex, age and side. *Journal of Anatomy* **223(2)**: 133-151.

Giurazza, F., Schena, E., Del Vescovo, R., Cazzato, R.L., Mortato, L., Saccomandi, P., Paternostro, F., Onofri, L. and Zobel, B.B., 2013. "Sex determination from scapular length measurements by CT scans images in a Caucasian population", in *35th Annual International Conference of the IEEE Engineering in Medicine and Biology Society (EMBC)*, 1632-1635.

Gómez-Valdés, J.A., Quinto-Sánchez, M., Garmendia, A.M., Veleminska, J., Sánchez-Mejorada, G. and Bruzek, J. (2012). Comparison of methods to determine sex by evaluating the greater sciatic notch: visual, angular and geometric morphometrics. *Forensic Science International* **221(1-3)**: 156.e1-156.e7.

González-Colmenares, G., Medina, C.S., Rojas-Sánchez, M.P., León, K. and Malpud, A. (2019). Sex estimation from skull base radiographs in a contemporary Colombian population. *Journal of Forensic and Legal Medicine* **62**: 77-81.

Gonzalez, P.N., Bernal, V. and Perez, S.I. (2009). Geometric morphometric approach to sex estimation of human pelvis. *Forensic Science International* **189(1-3)**: 68-74.

Grabherr, S., Egger, C., Vilarino, R., Campana, L., Jotterand, M. and Dedouit, F. (2017). Modern post-mortem imaging: an update on recent developments. *Forensic Sciences Research* **2(2)**: 52-64.

Gupta, A., Billings, B.K., Hummel, S. and Grosskopf, B. (2022). Evaluating morphological methods for sex estimation on isolated human skeletal materials: comparisons of accuracies between German and South African skeletal collections. *Forensic Sciences*, **2(3)**: 574-584.

Haddad, B., Hamdan, M., Al Nawaiseh, M., Aldowekat, O., Alshrouf, M.A., Karam, A.M., Azzam, M.I., Ar Altamimi, A. and Abu Shokor, M. (2022). Femoral neck shaft angle measurement on plain radiography: is standing or supine radiograph a reliable template for the contralateral femur?. *BMC Musculoskeletal Disorders* **23(1)**: 1092-1101.

Hammer, Ø., Harper, D.A., Ryan, P.D. (2001). Past: paleontological statistics software package for education and data analysis. *Palaeontologia Electronica* **4(1)**: 1-7.

Hishmat, A.M., Michiue, T., Sogawa, N., Oritani, S., Ishikawa, T., Fawzy, I.A., Hashem, M.A.M. and Maeda, H. (2015). Virtual CT morphometry of lower limb long bones for estimation of the sex and stature using postmortem Japanese adult data in forensic identification. *International Journal of Legal Medicine* **129**: 1173-1182.

Horton, M.G. and Hall, T.L. (1989). Quadriceps femoris muscle angle: normal values and relationships with gender and selected skeletal measures. *Physical Therapy* **69(11)**: 897-901.

Huda, W. and Abrahams, R.B. (2015). X-ray-based medical imaging and resolution. *American Journal of Roentgenology* **204(4)**: W393-W397.

Hutchinson, E. F., Kramer, B., Billings, B. K., Brits, D. M., & Pather, N. (2020). The law, ethics and body donation: a tale of two bequeathal programs. *Anatomical Sciences Education* **13(4)** 512-519.

IBM Corporation (2023). IBM SPSS Statistics for Windows, Version 29.0.2.0 Armonk, NY: IBM Corp.

Indra, L. and Lösch, S. (2021). Forensic anthropology casework from Switzerland (Bern): taphonomic implications for the future. *Forensic Science International: Reports* **4**: 100222 https://doi.org/10.1016/j.fsir.2021.100222

Inskip, S., Scheib, C.L., Wohns, A.W., Ge, X., Kivisild, T. and Robb, J. (2019). Evaluating macroscopic sex estimation methods using genetically sexed archaeological material: the medieval skeletal collection from St John's Divinity School, Cambridge. *American Journal of Physical Anthropology* **168(2)**: 340-351.

İşcan, M.Y. and Steyn, M. (2013). "Sex", in İşcan, M.Y., Krogman, W.M. and Steyn, M., *The Human Skeleton in Forensic Medicine* (3rd edition), Springfield: Charles C Thomas Publisher, 143-193.

Ishwarkumar, S., Pillay, P., Haffajee, M.R. and Rennie, C. (2016). Sex determination using morphometric and morphological dimensions of the clavicle within the KwaZulu-Natal population. *International Journal of Morphology* **34(1)**: 244-451.

Ives, G., Johns, S.E. and Deter, C. (2024). Sexual dimorphism of pelvic scarring: a new method of adult biological sex estimation. *Journal of Forensic Sciences* **69(6)**: 1959-1971.

Jager, V.R. and Eliopoulos, C. (2023). Sex assessment from the pelvis: a test of the Phenice (1969) and Klales *et al*. (2012) methods. *Forensic Science, Medicine and Pathology* **20(3)**:778-784.

Jerković, I., Bašić, Ž., Anđelinović, Š. and Kružić, I. (2020). Adjusting posterior probabilities to meet predefined accuracy criteria: a proposal for a novel approach to osteometric sex estimation. *Forensic Science International* **311**: 110273. https://doi.org/10.1016/j.forsciint.2020.110273.

Jilala, W., Ng'walali, P., Russa, D. and Bushozi, P. (2021). Sexing contemporary Tanzanian skeletonised remains using skull morphology: a test of the walker sex assessment method. *Forensic Science International: Reports* **3**: 100195 https://doi.org/10.1016/j.fsir.2021.100195

Jit, I. and Kaur, H. (1986). Rhomboid fossa in the clavicles of North Indians. *American Journal of Physical Anthropology* **70(1)**: 97-103.

Johnstone-Belford, E., Flavel, A. and Franklin, D. (2018). Morphoscopic observations in clinical pelvic MDCT scans: assessing the accuracy of the Phenice traits for sex estimation in a Western Australian population. *Journal of Forensic Radiology and Imaging* **12**:5-10.

Joon, V. and Rohatgi, R. (2021). Sex Determination by Pelvis: A Mini Literature. *International Journal for Research in Applied Science and Engineering Technology* **10(X)**: 1-12.

Kelley, S.R. (2022). *Incorporating metrics and nonmetrics in the development of a population-inclusive sex estimation model using volume rendered CT images of the skull* (Masters Thesis: Boston University). Retrieved from Boston University ProQuest Dissertations Publishing. (28865727).

Kenyhercz, M.W. (2012). Sex estimation using pubic bone morphology in a modern South African sample: a test of the Klales *et al*. method. *American Journal of Physical Anthropology* **147(54)**: 179-179.

Kenyhercz, M.W., Klales, A.R., Stull, K.E., McCormick, K.A. and Cole, S.J. (2017). Worldwide population variation in pelvic sexual dimorphism: a validation and recalibration of the Klales et al. method. *Forensic Science International* **277**: 259.e1-259.e8.

Keyes, C.A., Myburgh, J. and Brits, D. (2021). Scavenger activity in a peri-urban agricultural setting in the Highveld of South Africa. *International Journal of Legal Medicine* **135**: 979-991.

Khasawneh, R.R., Allouh, M.Z. and Abu-El-Rub, E. (2019). Measurement of the quadriceps (Q) angle with respect to various body parameters in young Arab population. *PloS One* **14(6)**: e0218387.1-e0218387.13.

Khosla, S., Melton, L.J., Riggs, B.L. and Melton 3rd, L.J. (2001). Estrogens and bone health in men. *Calcified Tissue International* **69(4)**: 189-192.

Klales, A.R. (2013). Current practices in physical anthropology for sex estimation in unidentified, adult individuals. *American Journal of Physical Anthropology* **150**: 168-168.

Klales, A.R. (2020a). "MorphoPASSE: morphological pelvis and skull sex estimation program", in *Sex estimation of the human skeleton: history, methods, and emerging techniques*, London: Academic Press, 271-278.

Klales, A.R. (2020b). "Sex estimation using pelvis morphology", in *Sex estimation of the human skeleton: history, methods, and emerging techniques*, London: Academic Press, 74-92.

Klales, A.R. (2021). Current State of Sex Estimation in Forensic Anthropology. *Forensic Anthropology* **4(2)**: 118-135.

Klales, A.R. and Cole, S.J. (2018). MorphoPASSE: The morphological pelvis and skull sex estimation database manual. *Washburn University, Topeka*. Available at:

klales_nij_database_manual_v1_03.29.19_on_website.pdf (morphopasse.com) (Accessed: 14 April 2024).

Klales, A.R., Ousley, S.D. and Passalacqua, N.V. (2020). "Statistical approaches to sex estimation", in *Sex estimation of the human skeleton: history, methods, and emerging techniques*, London: Academic Press, 203-207.

Klales, A.R., Ousley, S.D. and Vollner, J.M. (2012). A revised method of sexing the human innominate using Phenice's nonmetric traits and statistical methods. *American Journal of Physical Anthropology* **149(1)**:104-114.

Knobel, G.J., Flash, G. and Bowie, G.F. (2006). Lodox Statscan proves to be invaluable in forensic medicine: forensic files. *South African Medical Journal* **96(7)**: 593-594.

Koukiasa, A.E., Eliopoulos, C. and Manolis, S.K. (2017). Biometric sex estimation using the scapula and clavicle in a modern Greek population. *Anthropologischer Anzeiger* **74(3)**: 241-246.

Krishan, K., Chatterjee, P.M., Kanchan, T., Kaur, S., Baryah, N. and Singh, R.K. (2016). A review of sex estimation techniques during examination of skeletal remains in forensic anthropology casework. *Forensic Science International* **261**: 165.e1-165.e8.

Krogman, W.M. and İşcan, M.Y. (1962). "Sexing skeletal remains", in *The Human Skeleton in Forensic Medicine*, Springfield: Charles C Thomas Publisher, 112-152.

Krüger, G.C., L'Abbé, E.N., Stull, K.E. and Kenyhercz, M.W. (2015). Sexual dimorphism in cranial morphology among modern South Africans. *International Journal of Legal Medicine* **129**: 869-875.

Lakha, K.N. (2015). *Standards for epiphyseal union in South African children between the ages of 6 to 24 years using low dose X-ray (lodox)* (Doctoral Thesis: University of Cape Town). Retrieved from the University of Cape Town OpenUCT Doctoral Collections.

Langley, N.R., Jantz, L.M., Ousley, S.D., Jantz, R.L. and Milner, G. (2016). Data collection procedures for forensic skeletal material 2.0. *University of Tennessee and Lincoln Memorial University.*

Lembert, P.M. and Walker, P.L. (2019). "Bioarchaeological Ethics: a historical perspective on the value of human remains", in Katzenberg, M.A., and Saunders, S.R. (eds), *Biological Anthropology of the Human Skeleton*, (3rd edition), Hoboken, New Jersey: John Wiley & Sons, 1-42.

Leong, A. (2006). Sexual dimorphism of the pelvic architecture: a struggling response to destructive and parsimonious forces by natural & mate selection. *McGill Journal of Medicine: MJM* ***9*****(1)**: 61-66.

Lesciotto, K. M. and Doershuk, L. J. (2017). Accuracy and Reliability of the Klales *et al.* (2012) Morphoscopic Pelvic Sexing Method. *Journal of Forensic Sciences* **63(1)**: 214–220.

Leskovar, T., Mlinšek, T., Počivavšek, T. and Zupanič Pajnič, I. (2023). Comparison of morphological sex assessment and genetic sex determination on adult and sub-adult 17th–19th century skeletal remains. *Genes* **14(8)**: 1561-1574.

Lewis, C.J. and Garvin, H.M. (2016). Reliability of the Walker cranial nonmetric method and implications for sex estimation. *Journal of Forensic Sciences* **61(3)**: 743-751.

Listi, G.A. and Elizabeth Bassett, H. (2006). Test of an alternative method for determining sex from the os coxae: applications for modern Americans. *Journal of Forensic Sciences* **51(2)**: 248-252.

Livingston, L.A. (1998). The quadriceps angle: a review of the literature. *Journal of Orthopaedic & Sports Physical Therapy* **28(2)**: 105-109.

LODOX® (2023a). About us. Available at: About Us –Lodox Systems (Accessed: 08 December 2023).

LODOX® (2023b). Case Studies; Projectiles from a head shot found in the abdomen: A case study from the Tygerberg Forensic Pathology Services Laboratory, Cape Town, South Africa. Available at: Lodox Forensic Imaging System – The eXero-dr – Lodox Systems (Accessed: 08 December 2023).

LODOX® (2024). Lodox World. Available at: Lodox World - Lodox Systems (Accessed: 30 May 2024).

López-Lázaro, S., Pérez-Fernández, A., Alemán, I. and Viciano, J. (2020). Sex estimation of the humerus: a geometric morphometric analysis in an adult sample. *Legal Medicine* **47**: 101773 https://doi.org/10.1016/j.legalmed.2020.101773

Macaluso Jr, P.J. and Lucena, J. (2014a). Morphological variations of the anterior thoracic skeleton and their forensic significance: radiographic findings in a Spanish autopsy sample. *Forensic Science International* **241**: 220.e1-220.e7.

Macaluso Jr, P.J. and Lucena, J. (2014b). Stature estimation from radiographic sternum length in a contemporary Spanish population. *International Journal of Legal Medicine* **128(5)**: 845-851.

Maijanen, H., Junno, J.A., Keisu, A., Niinimäki, J., Lehenkari, P. and Oura, P. (2021). Sex estimation from knee breadth dimensions in a Finnish population. *Legal Medicine* **51**: 101873.1-101873.5.

Maijanen, H., Lynch, J., Junno, J.A. and Niinimäki, J. (2024). Sex estimation from humeral and femoral head diameters using CT-scans of living Finns. *Legal Medicine* **69**: 102341 https://doi.org/10.1016/j.legalmed.2023.102341.

Malek, S., Sealy, J.C. and Gibbon, V.E. (2023). Assessment and improvement of sex estimation standards for application in Holocene San and Khoekhoe populations. *International Journal of Osteoarchaeology* **33(3)**: 489-505.

Mamabolo, B., Alblas, A. and Brits, D.M. (2020). Modern imaging modalities in forensic anthropology and the potential of low-dose X-rays. *Forensic Imaging* **23**: 200406 https://doi.org/10.1016/j.fri.2020.200406

Maranho, R., Ferreira, M.T. and Curate, F. (2022). Sexual dimorphism of the human scapula: a geometric morphometrics study in two Portuguese reference skeletal samples. *Forensic Sciences* **2(4)**: 780-794.

Maranho, R., Ferreira, M.T. and Curate, F. (2023). Secular Trends in the Size and Shape of the Scapula among the Portuguese between the 19th and the 21st Centuries. *Biology* **12(7)**: 928-943.

Mays, S. (2022). "The macroscopic study of human skeletal paleopathology", in Grauer, A.L. (ed) *The Routledge Handbook of Paleopathology*, (1st edition), New York: Routledge, 19-42.

McCormick, W.F. and Stewart, J.H. (1983). Ossification patterns of costal cartilages as an indicator of sex. *Archives of Pathology & Laboratory Medicine* **107(4)**: 206-210.

McCormick, W.F., Stewart, J.H. and Langford, L.A. (1985). Sex determination from chest plate roentgenograms. *American Journal of Physical Anthropology* **68(2)**: 173-195.

McHugh, M.L. (2012). Interrater reliability: the Kappa statistic. *Biochemia Medica* **22(3)**: 276-282.

McKeown, A.H. and Schmidt, R.W. (2013). "Chapter 13: Geomtric Morphometrics", in DiGangi, E.A. and Moore, M.K. (eds), *Research methods in human skeletal biology,* Amsterdam: Academic Press, 325-359.

Mehta, M., Saini, V., Nath, S. and Menon, S.K. (2015). CT scan images for sex discrimination–a preliminary study on Gujarati population. *Journal of Forensic Radiology and Imaging* **3(1)**: 43-48.

Mello-Gentil, T. and Souza-Mello, V. (2022). Contributions of anatomy to forensic sex estimation: focus on head and neck bones. *Forensic Sciences Research* **7(1)**: 11-23.

Meral, O., Meydan, R., Toklu, B.B., Kaya, A., Karadayi, B. and Acar, T. (2022). Estimation of sex from computed tomography images of skull measurements in an adult Turkish population. *Acta Radiologica* **63(11)**: 1513-1521.

Microsoft Corporation (2024). Microsoft Excel. Available at: https://www.microsoft.com/en-za/microsoft-365/excel (Accessed: 18 October 2024).

Mitteroecker, P. and Gunz, P. (2009). Advances in geometric morphometrics. *Evolutionary Biology* **36**: 235-247.

Morele, B.M., Hill, L. and Keyes, C.A. (2024). An Overview of digital X-ray (LODOX StatScan) usage in a South African medico-legal mortuary. *Forensic Imaging* **36**: 200581 https://doi.org/10.1016/j.fri.2024.200581.

Muehleman, C., Li, J., Zhong, Z., Brankov, J.G. and Wernick, M.N. (2006). Multiple-image radiography for human soft tissue. *Journal of Anatomy* **208(1)**:115-124.

Nakashima, J. and Duong, H. (2020). "Radiology, Image Production and Evaluation" in *StatPearls [Internet]*. Treasure Island (FL): StatPearls Publishing, Available at: https://www.ncbi.nlm.nih.gov/books/NBK553145/ (Accessed 25 February 2025).

Obertová, Z., Adalian, P., Baccino, E., Cunha, E., De Boer, H.H., Fracasso, T., Kranioti, E., Lefévre, P., Lynnerup, N., Petaros, A. and Ross, A. (2019). The status of forensic anthropology in Europe and South Africa: Results of the 2016 FASE questionnaire on forensic anthropology. *Journal of Forensic Sciences* **64(4)**: 1017-1025.

Oliveira Costa, A.C., de Albuquerque, P.P.F., de Albuquerque, P.V., de Oliveira, B.D.R., de Albuquerque, Y.M.L. and Caiaffo, V. (2016). Morphometric analysis of the scapula and their differences between females and males. *International Journal of Morphology* **34(3)**: 1164-1168.

Omololu, B.B., Ogunlade, O.S. and Gopaldasani, V.K. (2009). Normal Q-angle in an adult Nigerian population. *Clinical Orthopaedics and Related Research®* **467(8)**: 2073-2076.

Ontell, F.K., Moore, E.H., Shepard, J.A. and Shelton, D.K. (1997). The costal cartilages in health and disease. *Radiographics* **17(3)**: 571-577.

Ou, X., Chen, X., Xu, X., Xie, L., Chen, X., Hong, Z., Bai, H., Liu, X., Chen, Q., Li, L. and Yang, H. (2021). Recent development in x-ray imaging technology: future and challenges. *Research* **2021**: 98292152 https://doi.org/10.34133/2021/9892152

Ousley, S.D. and Jantz, R.L. (2012). "Fordisc 3 and statistical methods for estimating sex and ancestry", in Dirkmaat, D.C. (ed), *A companion to forensic anthropology*, Malden: Wiley-Blackwell, 311-329.

Park, E., Chang, J. and Park, J., 2023. Facial soft tissue thickness differences among three skeletal classes in Korean population using CBCT. *International Journal of Environmental Research and Public Health* **20(3)**: 2658.1-2658.8.

Patriquin, M.L., Loth, S.R. and Steyn, M. (2003). Sexually dimorphic pelvic morphology in South African whites and blacks. *Homo* **53(3)**: 255-262.

Patyal, S. and Bhatia, T. (2022). Evaluating costal cartilage for sex and age estimation from PA chest radiographs of North Indian population: a retrospective study. *Egyptian Journal of Forensic Sciences* **12(1)**: 41-51.

Pauwels, R., Araki, K., Siewerdsen, J.H. and Thongvigitmanee, S.S. (2015). Technical aspects of dental CBCT: state of the art. *Dentomaxillofacial Radiology* **44(1)**: 1-20.

Phenice, T.W. (1969). A newly developed visual method of sexing the os pubis. *American Journal of Physical Anthropology* **30(2)**: 297-301.

Pilli, E., Palamenghi, A., Marino, A., Staiti, N., Alladio, E., Morelli, S., Cherubini, A., Mazzarelli, D., Caccia, G., Gibelli, D. and Cattaneo, C. (2023). Comparing genetic and physical anthropological analyses for the biological profile of unidentified and identified bodies in Milan. *Genes* **14(5)**: 1064-1078.

Pilmann Kotěrová, A., Santos, F., Bejdová, Š., Rmoutilová, R., Attia, M.H., Habiba, A., Velemínská, J. and Brůžek, J. (2024). Prioritizing a high posterior probability threshold leading to low error rate over high classification accuracy: the validity of MorphoPASSE software for cranial morphological sex estimation in a contemporary population. *International Journal of Legal Medicine* **138(4)**:1759-1768.

Pitcher, R.D., van As, A.B., Sanders, V., Douglas, T.S., Wieselthaler, N., Vlok, A., Paverd, S., Kilborn, T., Rode, H., Potgieter, H. and Beningfield, S.J. (2008). A pilot study evaluating the "STATSCAN" digital X-ray machine in paediatric polytrauma. *Emergency Radiology* **15**: 35-42.

Pomeroy, E., Mushrif-Tripathy, V., Wells, J.C., Kulkarni, B., Kinra, S. and Stock, J.T. (2018). Stature estimation equations for South Asian skeletons based on DXA scans of contemporary adults. *American Journal of Physical Anthropology* **167(1)**: 20-31.

Poongodi, V., Kanmani, R., Anandi, M.S., Krithika, C.L., Kannan, A. and Raghuram, P.H. (2015). Prediction of age and gender using digital radiographic method: A retrospective study. *Journal of Pharmacy and BioAllied Sciences* **7(Suppl 2)**: S504-S508.

Popović, Z.B. and Thomas, J.D. (2017). Assessing observer variability: a user's guide. *Cardiovascular Diagnosis and Therapy* **7(3)**: 317-333.

Prado, F.B., de Mello Santos, L.S., Caria, P.H.F., Kawaguchi, J.T., Preza, A.D.O., Jnr, E.D., da Silva, R.F. and Daruge, E. (2009). Incidence of clavicular rhomboid fossa (impression for costoclavicular ligament) in the Brazilian population: forensic application. *The Journal of Forensic Odonto-Stomatology-JFOS* **27(1)**: 12-16.

Purkait, R. (2001). Measurements of ulna—a new method for determination of sex. *Journal of Forensic Sciences* **46(4)**: 924-927.

Quarrie, K.C. (2015). *Correlation of post mortem LODOX digital radiological images with histopathological findings at autopsy: a prospective autopsy study at the Tygerberg Forensic Pathology Service Facility* (Masters Thesis:Stellenbosch University). Retrieved from Masters Degrees (Forensic Sciences) Collections.

Ramsthaler, F., Kettner, M., Gehl, A. and Verhoff, M.A. (2010). Digital forensic osteology: morphological sexing of skeletal remains using volume-rendered cranial CT scans. *Forensic Science International* **195(1-3)**: 148-152.

Raveendranath, R., Nachiket, S., Sujatha, N., Priya, R. and Rema, D. (2011). Bilateral variability of the quadriceps angle (Q angle) in an adult Indian population. *Iranian Journal of Basic Medical Sciences* **14(5)**: 465-471.

Raveendranath, V., Nachiket, S., Sujatha, N., Priya, R. and Rema, D. (2009). The Quadriceps angle (Q angle) in Indian men and women. *European Journal of Anatomy* **13(3)**: 105-109.

Reid, K.M., Martin, J.L. and Heathfield, L.J. (2020). Bodies without names: A retrospective review of unidentified decedents at Salt River Mortuary, Cape Town, South Africa, 2010-2017. *South African Medical Journal* **110(3)**: 223-228.

Rejtarová, O., Slízová, D., Smoranc, P., Rejtar, P. and Bukac, J. (2004). Costal cartilages—a clue for determination of sex. *Biomed Pap Med Fac Univ Palacky Olomouc Czech Repub* **148(2)**: 241-243.

Richtsmeier, J.T., Paik, C.H., Elfert, P.C., Cole, T.M. and Dahlman, H.R. (1995). Precision, repeatability, and validation of the localization of cranial landmarks using computed tomography scans. *The Cleft Palate-Craniofacial Journal* **32(3)**: 217-227.

Rogers, L.M., Halcrow, S.E., Kleffmann, T. and King, C.L. (2024). Comparing Walker's (2008) skull trait sex estimation standard to proteomic sex estimation for a group of South Asian individuals. *Forensic Science International: Synergy* **8**: 1004580 https://doi.org/10.1016/j.fsisyn.2023.100450

Rogers, M.J., King, T.L., Kim, J., Adeyemi, T.F., Higgins, T.F. and Maak, T.G. (2021). Femoral neck shaft angle and management of proximal femur fractures: Is the contralateral femur a reliable template? *Journal of Orthopaedic Trauma* **35(10)**: 529-534.

Rogers, N.L., Flournoy, L.E. and McCormick, W.F. (2000). The rhomboid fossa of the clavicle as a sex and age estimator. *Journal of Forensic Sciences* **45(1)**: 61-67.

Rogers, T.L. (1999). A visual method of determining the sex of skeletal remains using the distal humerus. *Journal of Forensic Sciences* **44(1)**: 57-60.

Rogers, T. and Saunders, S. (1994). Accuracy of sex determination using morphological traits of the human pelvis. *Journal of Forensic Sciences* **39(4)**:1047-1056.

Rohatgi, R. and Kapoor, A.K. (2014). Importance of still photography at scene of crime: A forensic vs. judicial perspective. *Journal of Harmonized Research in Applied Science* **2**: 271-274.

Rojas González, N., Obertová, Z. and Franklin, D. (2024). Accuracy of the Phenice (1969) and Klales *et al.* (2012) sex estimation methods in a Chilean population. *Australian Journal of Forensic Sciences* **56(sup1)**: 30-32.

Rowbotham, S. K. (2016). "Anthropological estimation of sex", in Blau, S. and Ubelaker, D. (eds.), *Handbook of forensic anthropology and archaeology* (2nd ed), New York: Routledge, 261–272.

Rowbotham, S.K. and Blau, S. (2020). “The application of medical imaging to the anthropological estimation of sex", in Klales, A.R. (ed), *Sex estimation of the human skeleton: history, methods, and emerging techniques,* London: Academic Press, 351-369.

Safety, P. (2012). Radiation dose in x-ray and CT exams. American College of Radiology and Radiological Society of North America. Available at: http://brookeimaging.ca/sfty_xray.pdf (Accessed: 20 January 2025).

Safir, O., Lin, C., Kosashvili, Y., Mayne, I.P., Gross, A.E. and Backstein, D., (2012). Limitations of conventional radiographs in the assessment of acetabular defects following total hip arthroplasty. *Canadian Journal of Surgery* **55(6)**: 401-407.

Saitou, N., Kimura, R., Fukase, H., Yogi, A., Murayama, S. and Ishida, H. (2011). Advanced CT images reveal nonmetric cranial variations in living humans. *Anthropological Science* **119(3)**: 231-237.

Salim, Z. (2012). *Accuracy and reliability in sex determination using the os coxa: A comparison of metric vs. Phenice method* (Masters Thesis: The University of Houston).

Sangvichien, S., Boonkaew, K., Chuncharunee, A., Komoltri, C., Udom, C. and Chandee, T. (2008). Accuracy of cranial and mandible morphological traits for sex determination in Thais. *Siriraj Medical Journal* **60(5)**: 240-243.

Schneider, T., Huisman, T.A.G.M., Fiehler, J., Savic, L.J. and Yousem, D.M. (2015). Differences in neuroradiology training programs around the world. *American Journal of Neuroradiology* **36(3)**: 440-444.

Scholtz, Y., Steyn, M. and Pretorius, E. (2010). A geometric morphometric study into the sexual dimorphism of the human scapula. *Homo* **61(4)**: 253-270.

Scott, S., Peckmann, T.R. and Alblas, M. (2018). The influence of biological affinity and sex on morphometric parameters of the clavicle in a South African sample. *American Journal of Human Biology* **30(5)**: 1-11.

Segar, S. (2023) *Tales from the autopsy table — top forensic pathologist on his career and the critical need for DNA collection*. Available at: https://www.up.ac.za/faculty-of-health-sciences/news/post_3165494-tales-from-the-autopsy-table-top-forensic-pathologist-on-his-career-and-the-critical-need-for-dna-collection (Accessed: 9 September 2025).

Setiawati, R., Rahardjo, P., Ruriana, I. and Guglielmi, G. (2023). Anthropometric study using three-dimensional pelvic CT scan in sex determination among adult Indonesian population. *Forensic Science, Medicine and Pathology* **19(1)**: 24-33.

Shantanu, K., Singh, S., Kumar, D., Singh, A., Tewari, P.G., Gupta, P. and Tewari, P. (2023). Anatomical variation in quadriceps angle with regard to different anthropometric parameters in a tertiary care centre in Northern India: a descriptive study. *Cureus* **15(1)**: e34224.1-e34224.10.

Sim, J. and Wright, C.C. (2005). The Kappa statistic in reliability studies: use, interpretation, and sample size requirements. *Physical Therapy* **85(3)**: 257-268.

Singh, J. and Singh, D. (2009). Rhomboid fossa of clavicle: Is it a reliable estimator of gender and age of northwest Indian subjects of Chandigarh zone. *Indian Journals* **9(2)**: 58-65.

Skouras, A.Z., Kanellopoulos, A.K., Stasi, S., Triantafyllou, A., Koulouvaris, P., Papagiannis, G. and Papathanasiou, G. (2022). Clinical significance of the static and dynamic q-angle. *Cureus* **14(5)**: 24911 https://doi.org/10.7759/cureus.24911.

Smal, S.A. (2020). *Assessing the sexual dimorphism of the upper limb in a Free State skeletal population using univariate measurements* (Masters Thesis: University of the Free State). Retrieved from University of the Free State All Electronic Theses and Dissertations Collections.

Small, C., Brits, D.M. and Hemingway, J. (2012). Quantification of the subpubic angle in South Africans. *Forensic Science International* **222(1-3)**: 395-e1-395e6.

Snow, F.J. (2004). *Geometric morphometry analysis of the scapula: Implications for the determination of sex and ancestry* (Doctoral dissertation: The University of Tennessee, Knoxvile). Retrieved from The University of Tennessee ProQuest Dissertations & Theses (3130182).

Spies, A.J., Steyn, M., Prince, D.N. and Brits, D. (2021). Can forensic anthropologists accurately detect skeletal trauma using radiological imaging?. *Forensic Imaging* **24**: 200424 https://doi.org/10.1016/j.fri.2020.200424.

Spradley, M.K. and Jantz, R.L. (2011). Sex estimation in forensic anthropology: skull versus postcranial elements. *Journal of Forensic Sciences* **56(2)**: 289-296.

Stock, M.K. (2020). "Analyses of the postcranial skeleton for sex estimation", in Klales, A.R. (ed), *Sex estimation of the human skeleton: history, methods, and emerging techniques,* London: Academic Press, 113-130.

Stull, K.E. and Armelli, K. (2020). Combining variables to improve subadult age estimation. *Forensic Anthropology (University of Florida)* **3(4)**: 203-213.

Stull, K.E., Cirillo, L.E., Cole, S.J. and Hulse, C.N. (2020). "Subadult sex estimation and KidStats" in *Sex estimation of the human skeleton: history, methods, and emerging techniques,* London: Academic Press, 219-242.

Stull, K.E., L'Abbé, E.N. and Ousley, S.D. (2017). Subadult sex estimation from diaphyseal dimensions. *American Journal of Physical Anthropology* **163(1)**: 64-74.

Stull, K.E., Tise, M.L., Ali, Z. and Fowler, D.R. (2014). Accuracy and reliability of measurements obtained from computed tomography 3D volume rendered images. *Forensic Science International* **238**:133-140.

Stull, K.E., Kenyhercz, M.W. and L'Abbe, E.N. (2013a). Non-metric cranial and pelvic traits as a measure of sexual dimorphism in a modern South African population. *American Journal of Physical Anthropology* **150(S56)**: 266-266.

Stull, K.E., L'abbé, E.N. and Steiner, S. 2013b). Measuring distortion of skeletal elements in Lodox Statscan-generated images. *Clinical Anatomy* **26(6)**: 780-786.

Tallman, S.D. and Blanton, A.I. (2020). Distal humerus morphological variation and sex estimation in modern Thai individuals. *Journal of Forensic Sciences* **65(2)**: 361-371.

Teodoru-Raghina, D., Perlea, P. and Marinescu, M. (2017). Forensic anthropology from skeletal remains to CT scans: a review on sexual dimorphism of human skull. *Romanian Journal of Legal Medicine* **25(3)**: 287-292.

Thambura, M.J. (2023). An investigation into the use of Full-body Low Dose X-rays Imaging system in South Africa: Radiographer's perspective. *African Journal of Emergency Medicine* **13(3)**: 166-170.

Thrall, D.E., 2012. *Textbook of veterinary diagnostic radiology sixth edition-E-book*. Elsevier Health Sciences: Saunders.

Toneva, D.H., Nikolova, S.Y., Fileva, N.F. and Zlatareva, D.K. (2023). Size and shape of human mandible: Sex differences and influence of age on sex estimation accuracy. *Legal Medicine* **65**: 102322 https://doi.org/10.1016/j.legalmed.2023.102322.

Triaca, A., Mahon, T.J. and Myburgh, J. (2022). A comparison of different maceration techniques on burnt remains. *Journal of Forensic Sciences* **67(2)**: 676-682.

Ubelaker, D.H. and Volk, C.G. (2002). A test of the Phenice method for the estimation of sex. *Journal of Forensic Sciences* **47(1)**: 19-24.

Uy, J. and Laudicina, N.M. (2021). Assessing the role of the pelvic canal in supporting the gut in humans. *Plos One* **16(10)**: 0258341 https://doi.org/10.1371/journal.pone.0258341.

Vance, V.L. and Steyn, M. (2013). Geometric morphometric assessment of sexually dimorphic characteristics of the distal humerus. *Homo* **64(5)**: 329-340.

Vance, V.L., Steyn, M. and L'Abbé, E.N. (2011). Nonmetric sex determination from the distal and posterior humerus in black and white South Africans. *Journal of Forensic Sciences* **56(3)**: 710-714.

Varzandeh, M., Akhlaghi, M., Farahani, M.V., Mousavi, F., Jashni, S.K. and Yousefinejad, V. (2019). The diagnostic value of anthropometric characteristics of ilium for sex estimation using pelvic radiographs. *International Journal of Medical Toxicology and Forensic Medicine* **9(1)**: 1-10.

Vellema, J. (2014). "LODOX statscan operation procedures" in *Vellema J Johannesburg Forensic Pathology Services (FPS) Standard Operating Procedures*, Gauteng Province.

Venketsamy, Y. (2022). *A pilot study on stature estimation of the South African male population using the post mortem Lodox® Xmplar-dr imaging device at the Salt River Forensic Medico-Legal Laboratory* (Masters Thesis: University of Cape Town). Retrieved from the University of Cape Town OpenUCT Masters Collections.

Viera, A.J. and Garrett, J.M. (2005). Understanding interobserver agreement: the Kappa statistic. *Family Medicine* **37(5)**: 360-363.

Viner, M. (2018). "Overview of Advances in Forensic Radiological Methods of Human Identification" in Latham, K.E., Bartelink, E.J. and Finnegan, M. (eds) *New Perspectives in Forensic Human Skeletal Identification*, London: Academic Press, 217-226.

Walker, P.L. (2008). Sexing skulls using discriminant function analysis of visually assessed traits. *American Journal of Physical Anthropology: The Official Publication of the American Association of Physical Anthropologists* **136(1)**: 39-50.

Walker, P.L. (2005). Greater sciatic notch morphology: sex, age, and population differences. *American Journal of Physical Anthropology: The Official Publication of the American Association of Physical Anthropologists* **127(4)**: 385-391.

Washburn, S.L. (1960). Tools and human evolution. *Scientific American* **203(3)**: 62-75.

White, T.D., Black, M.T. and Folkens, P.A. (2011). *Human Osteology,* (3rd edition). Burlington: Academic Press.

Williams, B.A. and Rogers, T.L. (2006). Evaluating the accuracy and precision of cranial morphological traits for sex determination. *Journal of Forensic Sciences* **51(4)**: 729-735.

Williams, M.B., Krupinski, E.A., Strauss, K.J., Breeden III, W.K., Rzeszotarski, M.S., Applegate, K., Wyatt, M., Bjork, S. and Seibert, J.A. (2007). Digital radiography image quality: Image acquisition. *Journal of the American College of Radiology* **4(6)**: 371-388.

Wilson, L.A., MacLeod, N. and Humphrey, L.T. (2008). Morphometric criteria for sexing juvenile human skeletons using the ilium. *Journal of Forensic Sciences* **53(2)**: 269-278.

Zhang, M. (2022). Forensic imaging: a powerful tool in modern forensic investigation. *Forensic Sciences Research* **7(3)**: 385-392.

Zhang, M. (2024). The Application of forensic imaging to sex estimation: Focus on skull and pelvic structures. *Perspectives in Legal and Forensic Sciences* **1(1)**: 10005 https://doi.org/10.35534/plfs.2024.10005.

APPENDICES

Appendix 1: Ethical clearance for Cadaveric Collection of the Department of Anatomical Sciences, School of Biomedical Sciences, University of the Witwatersrand, Johannesburg.

UNIVERSITY OF THE WITWATERSRAND, JOHANNESBURG | FACULTY OF HEALTH SCIENCES | Anatomical Sciences

SCHOOL OF ANATOMICAL SCIENCES ETHICS WAIVER CLEARANCE LETTER

Faculty of Health Sciences
School of Anatomical Sciences
University of the Witwatersrand
Johannesburg

Re: In terms of Chapter 8, sections 62-64 of the National Health Act No 61 of 2003 donated bodies and their tissues may be used for, among other purposes, health, and research. Use of such Material is subject only to permission from the responsible person in the School of Anatomical Sciences – the Head or person designated by the Head of School.

Human Research Ethics Committee (Medical) Clearance Certificate:

W-CBP-220504-01

This letter serves to confirm that the Head of School, based in the School of Anatomical Sciences, Faculty of Health Sciences, has reviewed the research proposal entitled:

TITLE: MORPHOLOGICAL SEX ESTIMATION FROM LOW DOSE X-RAY SCANS – AN EXPLORATIVE STUDY

by principal investigator: Mr Boikano Morele

and supervisor/collaborators: Mr Boikano Morele, Associate Professor Desiré Brits, Ms. Tamara Lottering

and has granted approval for the ethics waiver to conduct the above-mentioned research study.

Professor Amadi O Ihunwo
Head, School of Anatomical Sciences
Faculty of Health Sciences

5 August 2024
Dated

School of Anatomical Sciences
7 York Rd, Parktown, 2193, South Africa, Private Bag 3, WITS 2050
Tel: +27 11 717 2405/2305 | www.wits.ac.za/anatomicalsciences/

Appendix 2: Declaration on plagiarism and research misconduct

UNIVERSITY OF THE WITWATERSRAND, JOHANNESBURG | FACULTY OF HEALTH SCIENCES | Anatomical Sciences

UNIVERSITY OF THE WITWATERSRAND, JOHANNESBURG
DEPARTMENT OF ANATOMICAL SCIENCES

DECLARATION ON PLAGIARISM AND RESEARCH MISCONDUCT

Research misconduct is defined as the fabrication, falsification, or plagiarism in the proposing, performing, reviewing or reporting of research, where:
Fabrication is making up data or results and recording or reporting them;
Falsification is manipulating research materials, equipment, or processes, or changing or omitting data or results such that the research is not accurately represented; and
Plagiarism is the appropriation of another person's ideas, processes, results, or words without giving appropriate credit.

I, the undersigned, declare that this work (1) is my own. It is being submitted for, or in contribution to, the fulfilment of the requirements of the Master of Science in Medicine degree in the Faculty of Health Sciences at the University of the Witwatersrand, Johannesburg.

I have read and understood the School's/University's definition of plagiarism. I understand that plagiarism in any form is a serious offence that among other actions may lead to a mark of zero and/or expulsion from the University.

The research presented here is an accurate account and there has been not attempt to fabricate, falsify or misrepresent data or results. In addition, this work has not been submitted before for, or as a part of, any degree or examination in any other course in this or another Academic Institution.

I certify that the studies contained herein were approved by the Animal Ethics Committee and/or the Human Ethics Screening Committee of the University of the Witwatersrand, as appropriate.
Tick where applicable: Yes..✓..... No…… Not applicable……..

1. Nature of the work:
a. Essay .....
b. Project .....
c. Dissertation .....✓.....
d. Thesis .....
e. Other written work .....

Name: Boikano Molalelo Morele Date: 30 March 2025

Student Registration Number: 1656836
Class/Degree: Master of Science in Medicine (Research)
Program: Anatomical Sciences

Signature: .....

A copy of this form MUST be completed and included with all work handed in for assessment. No work will be marked without it.

Appendix 3: Turn-it-in Report

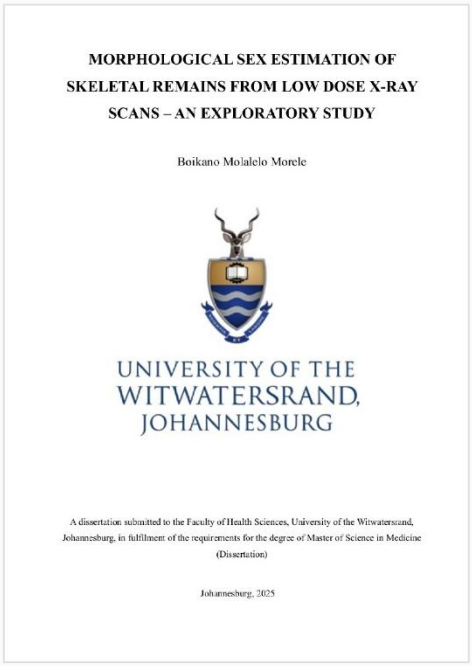
turnitin

Digital Receipt

This receipt acknowledges that Turnitin received your paper. Below you will find the receipt information regarding your submission.

The first page of your submissions is displayed below.

Submission author:	Boikano Morele
Assignment title:	Final submission (all, regardless of course/programme)
Submission title:	MSc Med (Disssertation) -1.pdf
File name:	MSc_Med_28Disssertation_29_.pdf
File size:	3.51M
Page count:	149
Word count:	46,913
Character count:	279,384
Submission date:	29-Mar-2025 10:23AM (UTC+0200)
Submission ID:	2628688824



MORPHOLOGICAL SEX ESTIMATION OF SKELETAL REMAINS FROM LOW DOSE X-RAY SCANS – AN EXPLORATORY STUDY

Boikano Molalelo Morele

UNIVERSITY OF THE WITWATERSRAND, JOHANNESBURG

A dissertation submitted to the Faculty of Health Sciences, University of the Witwatersrand, Johannesburg, in fulfilment of the requirements for the degree of Master of Science in Medicine (Dissertation)

Johannesburg, 2025

Copyright 2025 Turnitin. All rights reserved.

MSc Med (Disssertation) -1.pdf

ORIGINALITY REPORT

13%	9%	10%	5%
SIMILARITY INDEX	INTERNET SOURCES	PUBLICATIONS	STUDENT PAPERS

PRIMARY SOURCES

1	Submitted to CSU, Los Angeles Student Paper	1%
2	www.morphopasse.com Internet Source	1%
3	wiredspace.wits.ac.za Internet Source	1%
4	Sean D. Tallman, Amelia I. Blanton. "Distal Humerus Morphological Variation and Sex Estimation in Modern Thai Individuals,", Journal of Forensic Sciences, 2019 Publication	1%
5	hdl.handle.net Internet Source	<1%
6	repository.up.ac.za Internet Source	<1%
7	open.uct.ac.za Internet Source	<1%
8	es.scribd.com Internet Source	<1%
9	Submitted to University of Witwatersrand Student Paper	<1%
10	pure.manchester.ac.uk Internet Source	<1%
11	discovery.ucl.ac.uk Internet Source	<1%
	pure.uva.nl	

12	Internet Source	<1%
13	library2.smu.ca Internet Source	<1%
14	mspace.lib.umanitoba.ca Internet Source	<1%
15	Submitted to University College London Student Paper	<1%
16	Jagesur, Suvasha. "Variations in Pelvic Canal and Skull Dimensions in South Africans Considering Possible Relationships and Implications", University of Pretoria (South Africa), 2023 Publication	<1%
17	etheses.dur.ac.uk Internet Source	<1%
18	eurjanat.com Internet Source	<1%
19	www.researchgate.net Internet Source	<1%
20	repository.nwu.ac.za Internet Source	<1%
21	upetd.up.ac.za Internet Source	<1%
22	Submitted to University of Dundee Student Paper	<1%
23	Submitted to Universidad de Cádiz Student Paper	<1%
24	open.bu.edu Internet Source	<1%
25	www.frontiersin.org Internet Source	<1%